



VCU

Virginia Commonwealth University
VCU Scholars Compass

Theses and Dissertations

Graduate School

2021

CK2 phosphorylation of human papillomavirus 16 E2 on serine 23 promotes interaction with TopBP1 and is critical for E2 plasmid retention function

Apurva Tadimari Prabhakar
Virginia Commonwealth University

Follow this and additional works at: <https://scholarscompass.vcu.edu/etd>



Part of the [Oral Biology and Oral Pathology Commons](#)

© Apurva Tadimari Prabhakar

Downloaded from

<https://scholarscompass.vcu.edu/etd/6553>

This Dissertation is brought to you for free and open access by the Graduate School at VCU Scholars Compass. It has been accepted for inclusion in Theses and Dissertations by an authorized administrator of VCU Scholars Compass. For more information, please contact libcompass@vcu.edu.

© Apurva Tadimari Prabhakar 2021

All Rights Reserved

**CK2 PHOSPHORYLATION OF HUMAN PAPILLOMAVIRUS 16 E2 ON
SERINE 23 PROMOTES INTERACTION WITH TOPBP1 AND IS CRITICAL
FOR E2 PLASMID RETENTION FUNCTION**

A dissertation submitted in partial fulfillment of the requirements for the degree of
Doctor of Philosophy at Virginia Commonwealth University.

by

Apurva Tadimari Prabhakar

Bachelor of Dental Surgery, M. S. Ramaiah Dental College and Hospital (India), 2012
Master of Science in Oral Biology, University of Louisville, 2016

Director: **Iain M Morgan, Ph.D.**

Edmund G. Brodie Professor

Director, VCU Philips Institute for Oral Health Research
Chair, Oral and Craniofacial Molecular Biology
VCU School of Dentistry

Virginia Commonwealth University
Richmond, Virginia
April 2021

Dedication

This dissertation is dedicated to my parents

Mr. Prabhakar Tadimari

and

Mrs. Sarvamangala Tadimari

who have been my pillars of strength and are my biggest source of inspiration, love, and motivation. Thank you for believing in me, for teaching me to be honest and to always strive for the best. Thank you for encouraging me to go on every adventure, especially this one.

Acknowledgments

I am using this opportunity to express my sincere gratitude to everyone who supported me throughout this challenging yet most rewarding journey.

First and foremost, I want to thank my advisor Dr. Iain Morgan. I am immensely indebted to Dr. Morgan for all the knowledge and confidence he has instilled in me during my time as a Ph.D. student. He has always been nothing but a positive force and voice of encouragement all the way through. He embodies the definition of a mentor and he adds a component of compassion, which fostered an excellent learning environment for me.

I am extremely thankful to Dr. Oonagh Loughran, the best program director anyone could ever ask for. Her utmost support, guidance and encouragement has been extremely valuable to me.

I would like to thank my committee members, Dr. Michael McVoy, Dr. Larisa Litovchick, Dr. Oonagh Loughran, Dr. Renfeng Li and Dr. Molly Bristol. Their collective knowledge, guidance and setting the direction for the project is highly appreciated.

I am also grateful to all the past and present members of the Morgan lab who have been the best colleagues to work with especially Dr. Claire James, for her mentoring and for oh-so patiently teaching me everything I know about cell culture today. Christian Fontan, for being my sounding board, and for making my time in the lab a lot more enjoyable. Xu Wang and Raymonde Otoa for all their help. I would want to thank all my other fellow Ph.D. students in the program, especially Dr. Tanya Puccio, Dr. Erin Mooney and Chris Pham, for their friendship and reinforcement. A special thanks to Dung Pham and all the members of the Philips Institute.

Finally, it will be incomplete if I do not mention all the love and care from my family and friends, which has been the driving force for me to succeed.

Table of Contents

Acknowledgements	iii
List of Figures	ix
List of Tables	xiv
List of Abbreviations	xv
Abstract	xx
Chapter 1- Introduction	1- 28
1.1 Head and neck squamous cell carcinoma	1
1.2 Human papillomaviruses (HPV).....	4
1.3 Genome organization of high-risk HPV	6
1.4 Genomic status of HPV16 and its significance in HNSCC	11
1.5 HPV lifecycle	14
1.6 E2 protein	16
1.7 Essential roles of E2 protein in HPV16 lifecycle	18
1.7.1 Viral DNA replication initiation	18
1.7.2 Transcription	19
1.7.3 Genome segregation	20
1.8 Importance of viral genome segregation	20
1.9 HPV16 E2 and host cellular proteins interaction	23
1.9.1 Role of Brd4 association with E2Transcription	23

1.9.2	E2- TopBP1 interaction	25
1.10	Purpose of the study	28
Chapter 2- Materials and methods		29- 42
2.1	Generation of stable cell lines	29
2.2	Western blotting	30
2.3	<i>In vivo</i> immunoprecipitation	31
2.4	Immunofluorescence	32
2.5	Cell synchronization and FACS analysis	33
2.6	Transient transcription activation and repression assays	34
2.7	Plasmid retention assay	35
2.8	Small interfering RNA (siRNA) and segregation assay	36
2.9	Production of bacterial recombinant protein	37
2.10	<i>In vitro</i> GST pull-down assays	38
2.11	<i>In vitro</i> kinase assay with or without lambda phosphatase	38
2.12	Growth assay	39
2.13	CK2 inhibitor treatment	39
2.14	Organotypic raft culture	39
2.15	Immortalization of human foreskin keratinocytes (HFK)	40
2.16	Southern blotting	40
2.17	Exonuclease V assay	41
2.18	Statistical analysis	42

Chapter 3- Results43- 102

3.1 E2 serine 23 is critical for TopBP1 interaction *in vivo* and the E2 S23A mutation disrupts E2 plasmid retention function43

3.1.1 S23 is highly conserved in HR-HPV E2 proteins with no known function43

3.1.2 E2 interacts with TopBP1 via serine 2344

3.1.3 E2-WT and E2-S23A have similar transcriptional activation/repression and replication properties45

3.1.4 E2-S23A has compromised interaction with mitotic chromatin45

3.1.5 E2-WT levels are elevated during mitosis, while E2-S23A levels are not46

3.1.6 E2-WT has a plasmid retention function lost by E2-S23A47

3.1.7 E2-WT loses its ability to segregate after TopBP1 knockdown48

3.1 Summary64

3.2 CK2 phosphorylation of E2 promotes interaction with TopBP1 *in vitro* and *in vivo*66

3.2.1 Recombinant E2-S23D forms a direct complex with TopBP1, *in vitro*66

3.2.2	CK2 mediates the interaction between recombinant E2-WT and TopBP1, <i>in vitro</i>	67
3.2.3	CK2 promotes interaction with TopBP1 <i>in vivo</i>	67
3.2.4	siRNA knock down of CK2 diminishes E2-WT retention of ptk6E2 plasmid	68
3.2.5	CK2 phosphorylates E2 on serine 23 <i>in vivo</i> , and CK2 inhibitors disrupt the E2-TopBP1 complex	69
3.2.6	E2 is phosphorylated on serine 23 during mitosis	70
3.2	Summary	84
3.3	E2 serine 23 phosphorylation by CK2 is needed for E2-TopBP1 complex formation in human keratinocytes	85
3.3.1	E2-S23A mutation abolishes TopBP1 interaction and E2 plasmid retention function in N/Tert-1 cells	85
3.3.2	CK2 phosphorylates E2 on serine 23 <i>in vivo</i> , and CK2 inhibitors disrupt the E2-TopBP1 complex in N/Tert-1 cells	86
3.3	Summary	90
3.4	E2 serine 23 and the HPV16 lifecycle	91
3.4.1	E2-TopBP1 interaction is required for the HPV16 lifecycle	91
3.4.2	S23A mutation in the HPV16 genome resulted in delayed immortalization of human foreskin keratinocytes and higher episomal viral genome copy number	93
3.4	Summary	102

Chapter 4- Discussion	103- 110
Chapter 5- Conclusions and future directions	111- 119
References	120- 156
Vita	157

List of Figures

Figure 1: Schematic illustration of anatomical regions where HNSCC can occur	2
Figure 2: Incidence of HPV positive and HPV negative tonsillar HNSCC over years	3
Figure 3: Average annual numbers of HPV-associated cancers based on the anatomical sites and gender	5
Figure 4: Schematic representation of the HPV16 genome organization	9
Figure 5: Schematic representation of the proposed three main HPV16 genomic status in HNSCC	13
Figure 6: HPV lifecycle is dependent on epithelial differentiation	15
Figure 7: Schematic of HPV E2 protein with its functional domains	17
Figure 8: The E2 protein functions are mediated through multiple E2 binding sites in the viral genome	21
Figure 9: Illustration depicting the HPV genome segregation mediated by E2 protein	22
Figure 10: TopBP1 BRCT domain structure	27

Figure 11: Motif analysis of the E2 serine 23 residue region	49
Figure 12: The growth rates of the indicated cell lines	50
Figure 13: A system to study E2 –TopBP1 interaction	51
Figure 14: Transcriptional activation/repression and replication properties of E2-WT and E2-S23A	52
Figure 15: Representative immunofluorescence images depicting the mitotic staining for E2 and TopBP1	53
Figure 16: Cell synchronization and western blot analysis on U2OS E2 cell lines	54
Figure 17: Quantitation of repeat experiments shown in Figure 16	55
Figure 18: Flow cytometry data for U2OS pCDNA-Vec, E2-WT and E2-S23A...	56
Figure 19: Assay to study segregation	57
Figure 20: Quantitation of transcriptional activation potential of E2-WT and E2-S23A at day 3 of plasmid retention assay	58
Figure 21: Quantitation of results from plasmid retention assay in U2OS cells	59
Figure 22: Western blot analysis to confirm siRNA knockdown of TopBP1 throughout the plasmid retention assay	60

Figure 23: The growth rates of the indicated cell lines following siRNA knockdown of TopBP1	61
Figure 24: Quantitation of results from plasmid retention assay in U2OS cells followed by siRNA knockdown of TopBP1	62
Figure 25: Quantitation of results from plasmid retention assay in U2OS cells followed by knockdown of TopBP1 with two additional siRNA	63
Figure 26: A summary of section 3:1	64
Figure 27: Western blot analysis to confirm and demonstrate purity of recombinant proteins	71
Figure 28: GST pull-down assay followed by western blot analysis using recombinant proteins	72
Figure 29: GST pull-down assay followed by western blot analysis using recombinant proteins with CK2 enzyme	73
Figure 30: Western blot analysis to demonstrate loss of CK2 mediated E2-WT- TopBP1 interaction in the presence of λ phosphatase after GST pull-down	74
Figure 31: Western blot analysis to demonstrate CK2 α knockdown disrupts E2-TopBP1 interaction	75
Figure 32: Quantitation of repeat experiments from Figure 31	76

Figure 33: Western blot analysis to demonstrate CK2 α ' knockdown disrupts E2-TopBP1 interaction	77
Figure 34: Quantitation of repeat experiments from Figure 33	78
Figure 35: Quantitation of results from plasmid retention assay in U2OS cells followed by siRNA knockdown of CK2 α or CK2 α '	79
Figure 36: Western blot analysis to confirm siRNA knockdown of CK2 α or CK2 α ' throughout the plasmid retention assay	80
Figure 37: E2 S23 is phosphorylated <i>in vivo</i> by CK2	81
Figure 38: Western blot analysis to demonstrate the effect of CK2 inhibitor on E2-TopBP1 interaction	82
Figure 39: Representative immunofluorescence images of interphase and mitotic cells stained with pS23-Ab	83
Figure 40: E2-TopBP1 interaction in N/Tert-1	87
Figure 41: Quantitation of results from plasmid retention assay in N/Tert-1 cells	88
Figure 42: Western blot analysis depicting E2 S23 is phosphorylated <i>in vivo</i> by CK2 in N/Tert-1 cell lines	89
Figure 43: E2-TopBP1 mutation disrupts the HPV16 lifecycle	96
Figure 44: Detection of E2 S23 phosphorylation in HPV16 lifecycle models	97

Figure 45: HPV16 S23A has diminished immortalization properties	98
Figure 46: The growth rates of the indicated cell lines following immortalization	99
Figure 47: Southern blot analysis to determine the status of the HPV16 genomes in the immortalized cells	100
Figure 48: Quantitation of result from the TV exonuclease assay	101
Figure 49: A schematic model depicting a summary of the results deduced from this study	111
Figure 50: A schematic depicting a potential impact E2-TopBP1 interaction could have with regards to a direct therapeutic relevance	112
Figure 51: A proposed model and roles of a potential TopBP1-Brd4- E2 complex	115
Figure 52: Western blot analysis to demonstrate E2-TopBP1 interaction in E2-R37A mutant	116
Figure 53: Western blot analysis to demonstrate E2-Brd4 interaction	117
Figure 54: Cell synchronization and western blot analysis on U2OS E2 cell lines	118
Figure 55: The E2 pS23 peptide does not interact with well characterized phospho- peptide binding domains of TopBP1.....	119

List of Tables

Table 1: Proteins expressed by high-risk HPV and their major functions	10
Table 2: List of siRNA used in the study	36
Table 3: List of primers used in section 2.16	42

List of Abbreviations

A

ATM	Ataxia telangiectasia mutated
ATP	Adenosine triphosphate
ATR	ATM- and Rad3-related
ATRIP	ATR interacting protein

B

BD	Bromodomains
Bp	Base pair
BPV	Bovine papillomavirus
BRCA	Breast cancer susceptibility gene
BRCT	BRCA C-Terminus
BRD	Bromodomain
Brd4	Bromodomain 4
BrdU	Bromodeoxyuridine

C

CaPo4	Calcium phosphate
CDC	Centre for Disease Control
CK2	Casein kinase 2
CX-4945	Silmitasertib

D

DAPI	4',6-diamidino-2-phenylindole
DBD	DNA binding domain
DMEM	Dulbecco's modified eagle's medium
DMSO	Dimethyl sulfoxide
DNA	Deoxyribonucleic acid
DREAM	Dimerization partner, RB-like, E2F and MuvB
dsDNA	Double stranded DNA
DTB	Double Thymidine Block
DTT	Dithiothreitol

E

E	Early
<i>E. coli</i>	<i>Escherichia coli</i>
EDTA	Ethylenediamine tetraacetic acid
EGF	Epidermal growth factor

F

FACS	Fluorescence-Activated Cell Sorting
FBS	Fetal bovine serum
FCS	Fetal calf serum

G

G418	Geneticin
GAPDH	Glyceraldehyde 3-phosphate dehydrogenase
GST	Glutathione S-transferases

H

HA	Human influenza hemagglutinin
H&E	Hematoxylin and Eosin
HFk	Human foreskin keratinocytes
His	Histidine
HNSCC	Head and neck squamous cell carcinoma
HPV	Human papillomavirus
HR- HPV	High-risk Human papillomavirus
HSV	Herpes Simplex Virus

I

IRDye	Infrared Fluorescent Dyes
IP	Immunoprecipitation

K

Kb	Kilobase
KSFM	Keratinocyte serum-free medium

L

L	Late
LB	Lysogeny broth
LCR	Long control region
LR-HPV	Low-risk Human papillomavirus
LSM	Laser scanning microscope

M

mAB	Monoclonal antibody
MgCl₂	Magnesium chloride
mg	Milligram
ml	Milliliter

N

NaCl	Sodium
NEB	New England Biolabs
NIH	National Institutes of Health
Ni-NTA	Nickel-nitrilotriacetic acid
nM	Nanomolar
NP40	Nonylphenoxypolyethoxyethanol
N/Tert-1	TERT immortalized foreskin keratinocytes

O

OD	Optical density
ORF	Open reading frame
OSCC	Oropharyngeal squamous cell carcinoma

P

PAGE	Polyacrylamide gel electrophoresis
PBS	Phosphate buffered saline
pCDNA	Plasmid cloning DNA.
PCR	Polymerase chain reaction
PDEF	Platelet-derived growth factor
pTEFb	Positive transcription elongation factor
PV	Papillomavirus

R

Rb	Retinoblastoma
Rcf	Relative centrifugal force
RNA	Ribonucleic acid
RPA	Replication protein A

S

Scr	Scramble
SDS	Sodium dodecyl sulfate
siRNA	Small interfering RNA
SV	Simian virus

T

TAD	Transactivation domain
TCGA	The Cancer Genome Atlas
TE	Tris-EDTA
TF	Transcription factor
tk	Thymidine kinase
TopBP1	Topoisomerase Binding Protein 1
TV Exonuclease	T5 Exonuclease

U

URR	Upstream Regulatory Region
U2OS	Human bone osteosarcoma epithelial cells

V

Vec	Vector
vol/vol	Volume/Volume

W

WGS	Whole Genome Sequencing
WT	Wild type

Symbols

α	Alpha
β	Beta

Symbols Continued

λ	Lambda
%	Percent
$^{\circ}\text{C}$	Degree Celsius
μg	Microgram
μM	Micromolar

Abstract

CK2 PHOSPHORYLATION OF HUMAN PAPILLOMAVIRUS 16 E2 ON SERINE 23 PROMOTES INTERACTION WITH TOPBP1 AND IS CRITICAL FOR E2 PLASMID RETENTION FUNCTION

By Apurva Tadimari Prabhakar, Ph.D.

A dissertation submitted in partial fulfillment of the requirements for the degree of Doctor of Philosophy at Virginia Commonwealth University.

Virginia Commonwealth University, 2021

Major Director: Iain M Morgan, Ph.D.

Edmund G. Brodie Professor

Director, VCU Philips Institute for Oral Health Research

Chair, Oral and Craniofacial Molecular Biology

VCU School of Dentistry

Human papillomaviruses (HPVs) are the causative agents in most cervical cancers and have been implicated in a rising number of oropharyngeal cancers. HPV positive oropharyngeal cancers have increased significantly over the last two decades with no specific anti-viral therapeutic options for the treatment of HPV diseases. During its lifecycle, HPV16 encoded E2 protein interacts with host cellular factors to regulate viral transcription, replication and genome segregation/retention. Our understanding of the cellular partner proteins that E2 uses to mediate its functions remains incomplete.

Previously, an interaction between E2 and the host protein TopBP1 was identified. In earlier studies, it was also demonstrated that E2 and TopBP1 co-locate to late telophase chromatin, and that TopBP1 regulates the interaction of E2 with interphase chromatin, suggesting that TopBP1 may be the chromatin receptor protein mediating E2 segregation function.

In this study, we sought a more mechanistic understanding of the E2-TopBP1 interaction. We demonstrate that CK2 phosphorylation of E2 on serine 23 promotes interaction with TopBP1 *in vitro* and *in vivo*, and that E2 is phosphorylated on this residue during the HPV16 lifecycle. We further investigated the consequences of mutating serine 23 on E2 functions. E2-S23A activates and represses transcription identically to E2-WT (wild-type), and in transient replication assays, E2-S23A is as efficient as E2-WT. However, E2-S23A has compromised interaction with mitotic chromatin when compared with E2-WT. In E2-WT cells, both E2 and TopBP1 levels increase during mitosis when compared with vector control cells. In E2-S23A cells, neither E2 nor TopBP1 levels increase during mitosis. We additionally tested whether this difference in E2-S23A levels during mitosis disrupts E2 plasmid retention function. We developed a novel plasmid retention assay and demonstrate that E2-S23A is deficient in plasmid retention when compared with E2-WT. siRNA targeted knockdown of TopBP1 abrogates E2-WT plasmid retention function.

Introduction of the S23A mutation into the HPV16 genome ensued delayed immortalization of human foreskin keratinocytes (HFK) and higher episomal viral genome copy number in resulting established HFK. Furthermore, S23A mutation results in an

aberrant lifecycle; there is an increase in koilocytes (indicative of a more transformed keratinocyte), a failure of E2 to be stabilized in differentiating epithelium, and a failure to amplify the viral genome in the epithelium. Overall, our results reveal that CK2 phosphorylation of E2 on serine 23 promotes interaction with TopBP1, which is critical for E2 plasmid retention function and in HPV16 immortalization of keratinocytes. Moreover, we demonstrate that TopBP1 regulation of E2 function is required for an optimum HPV lifecycle. These results will enhance the molecular understanding of the HPV16 lifecycle in order to identify potential anti-viral targets against HPV.

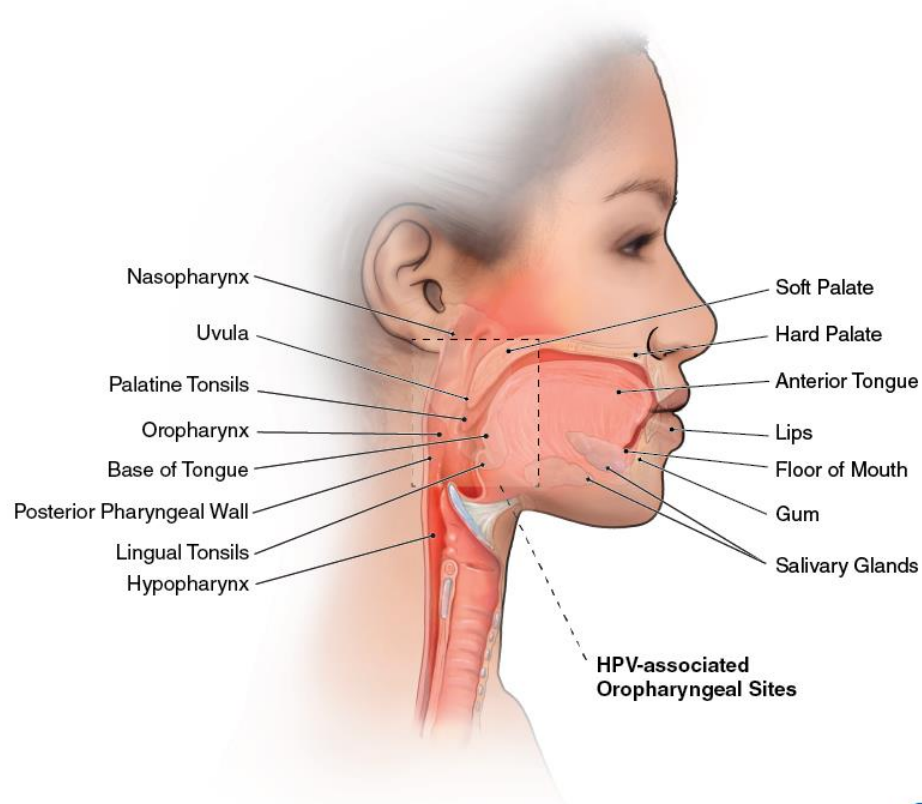
CHAPTER 1

Introduction

1.1 Head and neck squamous cell carcinoma

Head and neck squamous cell carcinoma (HNSCC) consist of a diverse group of squamous epithelial malignancies that occurs in the upper aerodigestive tract (**Figure 1**) that includes the nasal cavity and paranasal sinuses, nasopharynx, the hypopharynx, larynx, and trachea, and the oral cavity and oropharynx (1). The incidence of HNSCC is growing. Worldwide, it constitutes 10% or more of all cancers and is the fifth leading cause of cancer, with over 680,000 estimated cases diagnosed annually (2). Further, it accounts for approximately 4% of all cancers in the United States (3). About twice as many men as women develop HNSCC and it occurs usually in the age group of 50 years and older (4, 5).

Traditionally, tobacco use and alcohol consumption are considered the two most important risk factors contributing to the development of HNSCC (6). Over the past decade, HNSCC has become apparent in a cohort of nonsmokers/ minimal smokers who are human papillomavirus (HPV) positive (**Figure 2**). These HPV positive patients tend to develop oropharyngeal cancers, a subset of HNSCC (7, 8). Studies have suggested that there is an increase in incidence of oropharyngeal cancers caused by a slow epidemic of HPV infection (9).



1. Salivary glands are located throughout the oral cavity. These are identified for illustrative purposes only.
2. Not all sites, such as cheek, are included in this figure.



Figure 1. Schematic illustration of anatomical regions where HNSCC can occur. HNSCC is classified by its location: it can occur in the oral cavity, nasal cavity and paranasal sinuses, the upper part of the throat near the nasal cavity (nasopharynx), larynx, or the lower part of the throat near the larynx (hypopharynx). The majority of the HPV positive HNSCC are found in the region back of the tongue and throat called the oropharynx. Image was obtained from the CDC website (10).

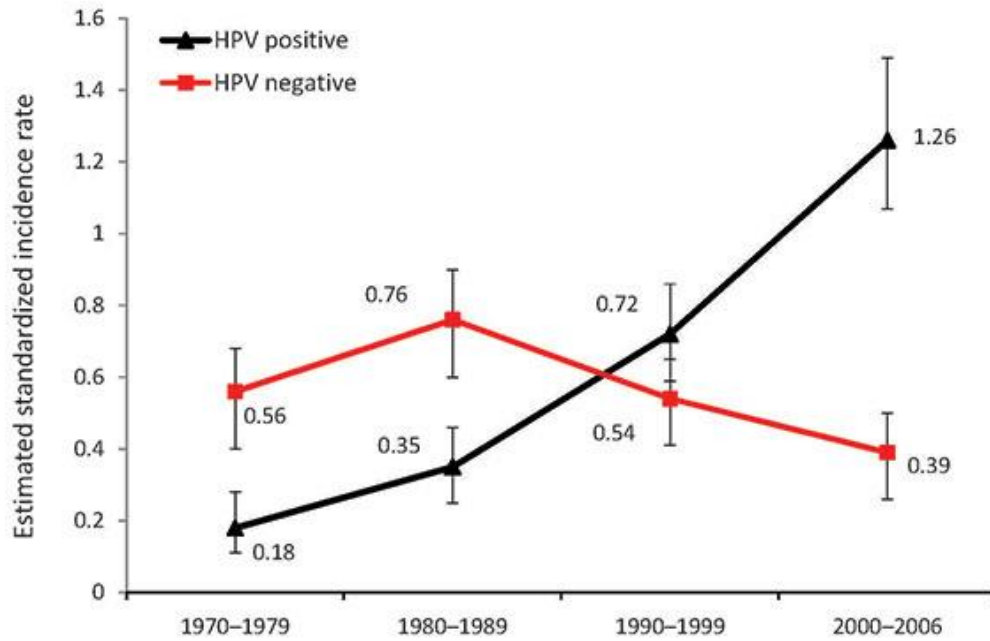


Figure 2. Incidence of HPV positive and HPV negative tonsillar HNSCC over years. Over the past decades, despite reduced smoking rates, cases of HNSCC have increased due to the rise in HPV positive oropharyngeal cancers. Image obtained from CDC website, based on the study by Ramqvist *et al.*, 2010 (7).

1.2 Human papillomaviruses (HPVs)

HPVs are DNA viruses that infect both cutaneous and mucosal epithelium (11). Viral infections are responsible for causing 15% of all human cancers (12) and HPV accounts for more than 600,000 new cases of cancer worldwide annually (13). These cancers caused by HPV in women mainly include cervical cancers, vaginal and vulvar cancers. In men, HPV infection can cause predominantly ano-genital as well as oropharyngeal cancers (14) (15) (**Figure 3**). The high-risk HPV (HR-HPV) genotypes, including HPV 16, 18, 31, are responsible for causing cancers (16). Whereas the low-risk HPVs, such as HPV 6 and 11, can cause genital warts (17). Research has shown a strong association between oropharyngeal cancers and HPV, with 95% of HPV positive cases primarily caused by HPV16 (18-20).

Compared to HPV negative HNSCC, HPV positive cancers possess distinct demographic, molecular, and clinical characteristics such as a male predominance, younger age at the time of diagnosis, lower exposure to the classic risk factors such as smoking, difference in tumor pathways involved with somatic molecular alterations, and the location it occurs (21-23). Additionally, it has been reported that HPV positive cancer patients have a better prognosis than HPV negative patients (24-26). Regardless, currently the treatment for head and neck cancers are not dependent on HPV status. Many studies have proposed development of de-escalation protocols to maintain high survival rates and mitigate treatment-related side effects in HPV positive HNSCC (27). Furthermore, there is a dire necessity for targeted therapeutics to treat HPV positive cancers.

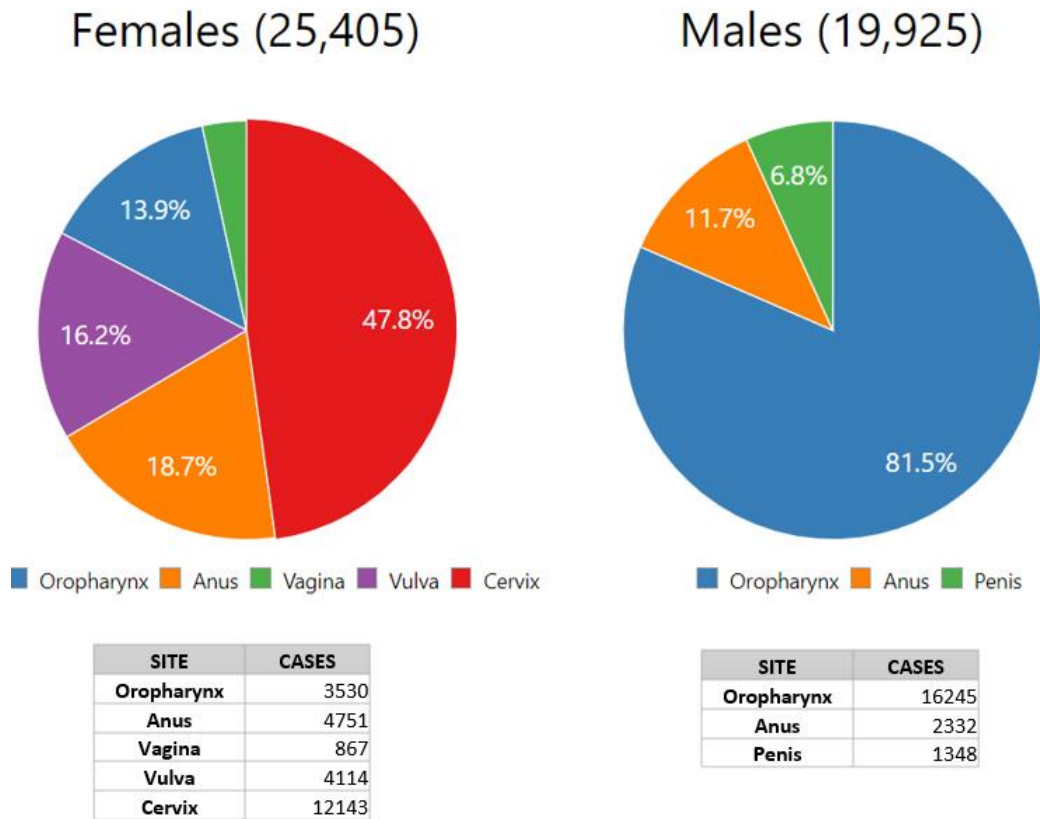


Figure 3. Average annual numbers of HPV-associated cancers based on the anatomical sites and gender. Cervical cancer among women and oropharyngeal cancers in men are the most common HPV-associated cancers. Based on data from 2013 to 2017, about 45,300 new cases of HPV-associated cancers occurred in the United States each year, including about 25,400 among women, and about 19,900 among men (14).

1.3 Genome organization of high-risk HPV

HPVs are small, circular, non-enveloped, double-stranded DNA viruses with a genome approximately eight kilobases in length (28). The genome contains approximately eight ORFs that are all transcribed from a single DNA strand (Figure 4). The ORF is divided into three functional parts (**Figure 4**). The early (E) region encodes proteins (E1, E2, E4–E7) that are essential for viral replication. Then there is the late (L) region that encodes the structural proteins (L1–L2), required for virion assembly. Also, it consists of the long control region (LCR), sometimes also referred to as upstream regulatory region (URR), essentially a non-coding part which consists of *cis*-elements that are needed for the replication and transcription of viral DNA (29) (**Figure 4**).

The early viral proteins, E1 and E2, together are responsible for initiation of the viral genome replication. E1 is the solo enzyme that HPV expresses which is an ATP-dependent helicase, essential for viral DNA replication (30, 31). E1 cannot initiate replication on its own; it requires E2 to function. E2 is a DNA binding protein that has versatile roles in viral replication, transcription, and cell cycle regulation among other functions (32). E2 protein, a DNA-binding protein in its homodimer form, can bind to a 12-bp palindromic sequence around the AT-rich origin of replication. E2 recruits E1 at the origin of replication via a protein-protein interaction, to initiate replication (33). The functions of E2 are further discussed in section 1.7.

E4 is expressed at later stages in HPV lifecycles as E1^{E4} fusion proteins (34, 35). Studies have indicated that this E1^{E4} protein has various functions such as its ability to

arrest cell cycle progression and reorganization of cytokeratin networks, to further facilitate the exit of the virus from the cell (36).

E5 plays a significant role in cell growth and can impair various cell signal transduction pathways (37-39). In Bovine papillomavirus (BPV), E5 can cause direct transmembrane activation of the platelet-derived growth factor (PDGF) β receptor, which can further result in recruitment and activation of cellular signaling proteins, resulting in mitogenesis (40, 41). HPV16 E5 has been shown to alter cell surface levels or activity of numerous different receptors, including those involved in cell proliferation, such as epidermal growth factor receptor (EGFR) (42, 43). E5 protein can further directly modulate the host immune response, which supports onset and persistence of infection (44, 45). Additionally, it can aid oncoproteins E6 and E7 in cellular transformation and cancer progression (37, 46).

E6 and E7 are the two main oncogenes of HPV (47,48). HR-HPV E6 protein binds to and degrades the p53 tumor suppressor (49-51). This is brought about by complexing with a ubiquitin ligase called E6-associated protein (E6-AP), which causes ubiquitination of p53 leading to p53 degradation and evasion of cellular apoptotic and growth arrest responses (52). E6 has also shown to target proteins like PDZ, which are implicated in cellular proliferation, signaling pathways, and in maintaining epithelial integrity, ultimately promoting cellular transformation (53).

E7 interacts with cellular proteins including p21 and pRb (54) which further causes the disruption of growth-suppressive pRB-E2F complexes, which can stimulate quiescent cells into a proliferating state, aiding viral replication to proceed efficiently (51, 55-57). Additionally, E7 has been shown to cause deregulation of several cell cycle genes that are

normally regulated by DREAM (Dimerization partner, RB-like, E2F and MuvB), which is a transcriptional repressor complex. DREAM complex was demonstrated as another important tumor suppressor which is disrupted by E7 protein that can play an important role in HR-HPV induced oncogenic transformation, independent of the pRb and p53 tumor suppressors (58). E7 disrupts the DREAM complex via competitive binding with p130 (a Rb family pocket protein), which further drives the cell cycle and cell proliferation (59, 60). Thus, in HR-HPV combination of E6 and E7 expression can ultimately promote cell immortalization and transformation.

The HPV viral genome is enveloped by an icosahedral capsid which is comprised of two proteins: L1, the major capsid protein, and L2, the minor capsid protein (61). The different functions of proteins expressed by high-risk HPV are summarized in **Table 1**.

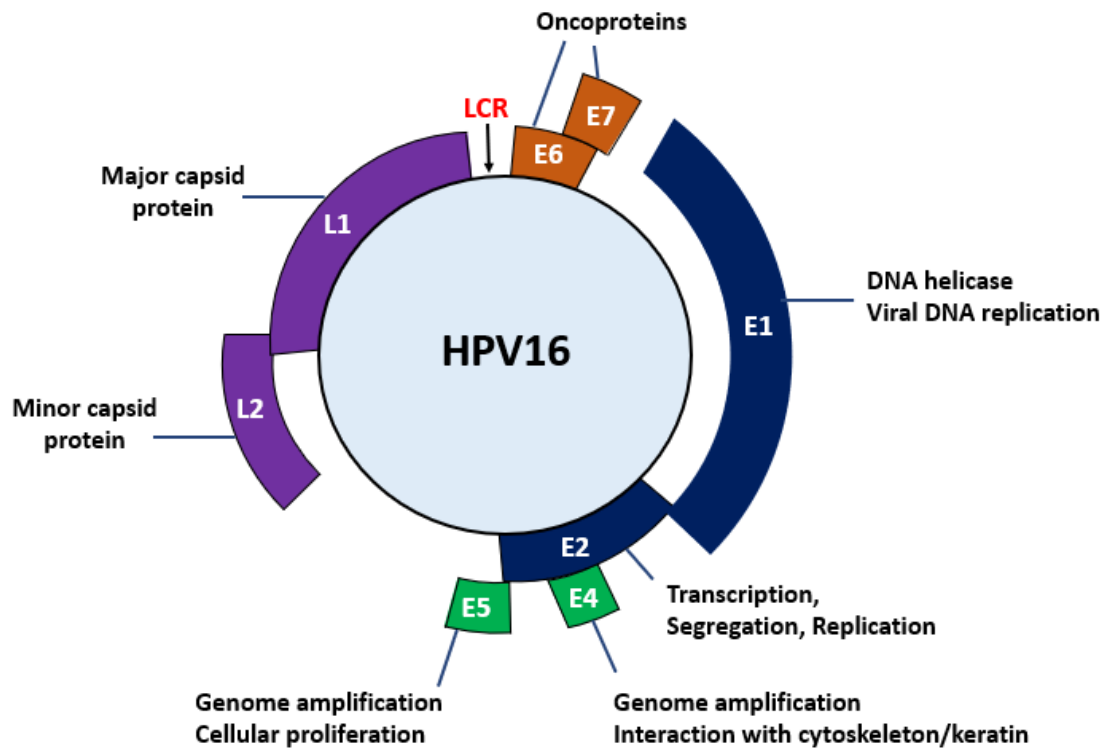


Figure 4. Schematic representation of the HPV16 genome organization. Full circular genome of HR-HPV16 displaying its 8 different genes and LCR region, whose functions are specified. Adapted from D'Abramo et al., 2011 (62).

Table 1. Proteins expressed by high-risk HPV and their major functions (63)

Protein	Role in the virus lifecycle
E1	ATP-dependent DNA helicase, initiates viral genome replication.
E2	Genome replication, transcription, segregation. Regulation of cellular gene expression. Cell cycle and apoptosis regulation.
E4	Cell cycle arrest, viral genome packaging.
E5	Control of cell growth and differentiation. Immune modulation, interacts with EGF-receptor.
E6	Major oncoprotein. Degradation of p53. Inhibits apoptosis and differentiation. Interacts with numerous host proteins.
E7	Major oncoprotein. Cell cycle control. Binds to pRB-105.
L1	Major capsid protein
L2	Minor capsid protein. Recruits L1. Virus assembly

1.4 Genomic status of HPV16 and its significance in HNSCC

The genomic status of HPV and its interaction with the host genome has been well-characterized in cervical cancer, but less is known with regards to the physical status of the viral genome in HPV positive HNSCC. A recent study proposed three main types of genomic status of HPV in HNSCC (**Figure 5**) based on head and neck cancer data from TCGA: an episomal state, an integrated state, and as a virus–human hybrid episomal state (64).

HPV16 typically exists as an episome where the viral DNA is in a circular form (65). When integrated, the HPV genome gets inserted into and is maintained in the human genome. This is a common finding in cervical cancers caused by HR-HPV (66-68). It has been proposed that during HPV integration, there is a loss of E2 expression which can lead to deregulated expression of E6 and E7, contributing to carcinogenic progression (69, 70). This can be a potential biomarker for disease progression. Apart from the viral E6 and E7 expression, it is possible that HPV could drive oncogenesis by modification of the host genomes at sites of integration. Integration can cause disruption of tumor suppressor genes, high-level DNA amplifications, and interchromosomal rearrangements (71, 72).

A study of TCGA Whole Genome Sequencing (WGS) data (73) suggested a third type of HPV16 genomic state, wherein the HPV genome is not integrated into that of the host genome and the HPV can replicate autonomously from its origin, as an independent viral–human hybrid episome (64). This was previously interpreted and characterized as being a combination of episomal and integrated viral genomes existing within the same tumor and was considered as the “mixed tumors” (74). But the evidence following analysis of TCGA

data suggested that the viral genome was in fact episomal and replicates joined to a segment of human DNA (64). This distinction of which patients truly have integrated tumors is crucial to identify HNSCC patients who are at increased risk. This further emphasizes the need to use appropriate techniques for categorizing the genomic status of HPV in head and neck cancer, which is currently lacking (75).

As mentioned in section 1.2, HPV positive HNSCC patients have higher survival rates than that of HPV negative HNSCC patients. Recent TCGA data has shown that the HPV positive HNSCC patients with integrated viral DNA fair clinically worse than those with tumors containing the virus as an episome (76). Identifying the genomic status in HPV positive HNSCC can aid as a potential biomarker and can help in development of a de-escalation treatment protocol for these patients who have a better prognosis and there are preliminary studies demonstrating the success of de-escalation in HPV positive HNSCC patients (77, 78).

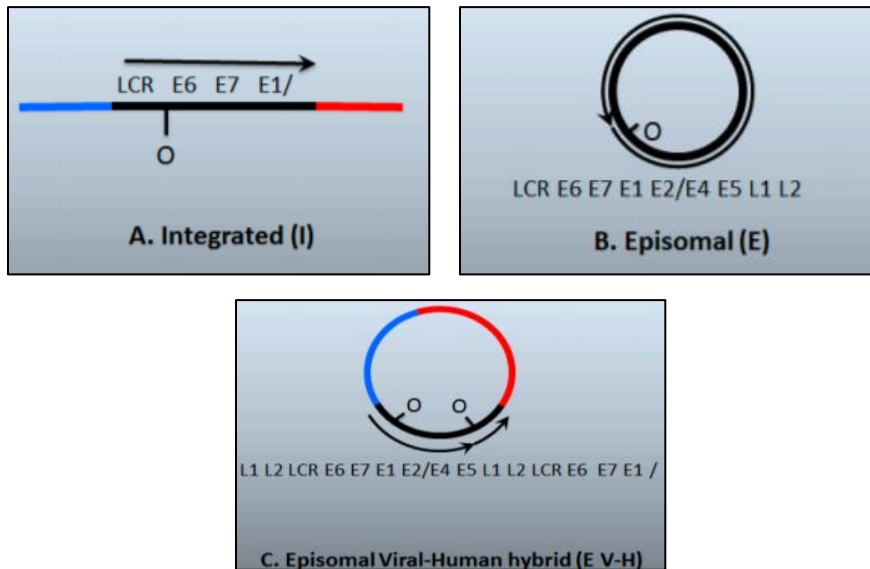


Figure 5. Schematic representation of the proposed three main types of HPV16 genomic status in HNSCC. (A) Integrated, where the HPV genome is inserted and maintained within the host genome; (B) Episomal, where the genome exists as a circular DNA; and (C) Episomal viral-human hybrid, in which the integrated HPV dimer or multimer gets excised along with human DNA and together ligated to form this hybrid episome. Image adapted from Morgan IM *et al.*, 2017 (75).

1.5 The HPV lifecycle

The HPV16 lifecycle depends on the differentiation process of the human epithelium it infects (79-80). The viral lifecycle occurs in four different phases (**Figure 6**). The first phase is called establishment. In this phase, the virus gains entry through micro-abrasions in the epithelium to infect the basal layer cells. After their successful establishment in the basal cells, the HPV is maintained in an episomal state at a copy number of about 50 to 100 copies per undifferentiated cell. Low level expression of viral early proteins such as E1, E2, E6 and E7 occurs in this phase, which helps in evasion of the host immune response to infection (81).

Following this, during the maintenance phase of viral lifecycle, the HPV infected basal cells undergo differentiation. HPV genomes are small and do not encode polymerases or other enzymes which are necessary for viral replication (82). HPVs rely on host cell replication proteins to facilitate viral DNA synthesis (83, 84). As the infected host cells migrate towards the upper layers, different viral proteins are expressed at high levels, and viral DNA is amplified. In this amplification phase, the number of copies can range up to thousands per cell. Subsequently, in the final stage the viral genome gets packed inside a capsid to form progeny virions. This shed virus can then initiate a new infection (85).

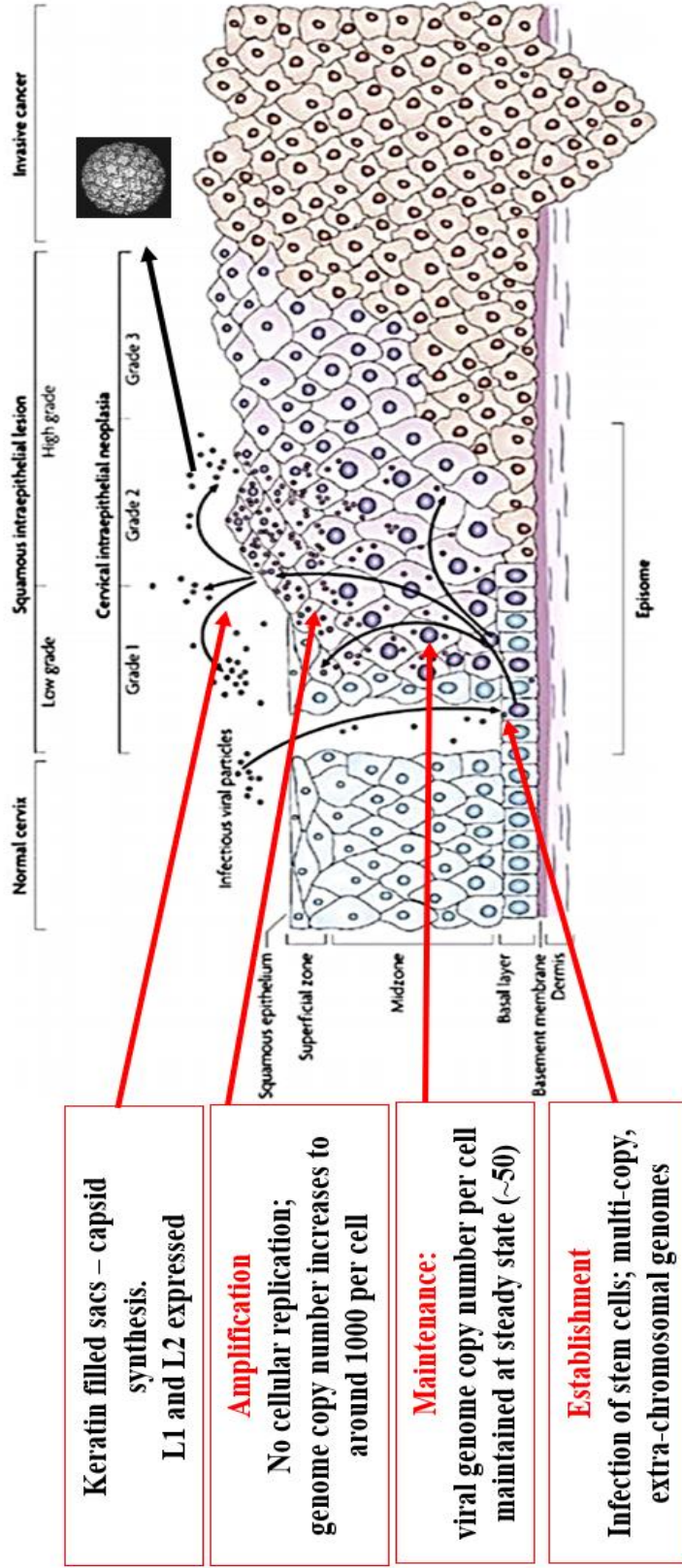


Figure 6. The HPV lifecycle is dependent on epithelial cell differentiation. HPV infects the basal layer of the stratified epithelium via microabrasions and HPV genomes are maintained as episomes in the nuclei of infected cells. The viral lifecycle is closely linked to the differentiation process of host cells. As the infected host cells differentiate and migrate upwards, viral proteins are expressed and viral DNA gets amplified. The later productive stage of the viral lifecycle occurs in the upper layers of the epithelium and followed by which the progenitor virions are released. Image adapted from Woodman *et al.*, (85).

1.6 E2 protein

The 43 kDa HPV16 E2 protein binds as a homodimer to a 12-bp palindromic DNA sequence, ACCGN₄CGGT, which is present in multiple copies within the LCR of the viral genome (86). The E2 protein has three domains: the amino terminal transactivation domain, which is about 200 amino acids; the carboxyl terminal DNA binding domain, which is about 100 amino acids; and the third domain called the hinge domain, which forms a flexible link between the other two domains (**Figure 7**) (87). The hinge domain has roles in chromatin binding and protein stability (88-90). The transactivation domain can bind via its one surface to the viral E1 helicase to initiate replication of HPV genomes (91). Additionally, it is required for transcriptional regulation, interaction with mitotic chromosomes, and association with numerous cellular proteins (92-95). The C-terminus of E2 protein comprises a DNA binding domain which can bind to specific consensus motifs located primarily in the LCR region of the viral genome (96, 97)

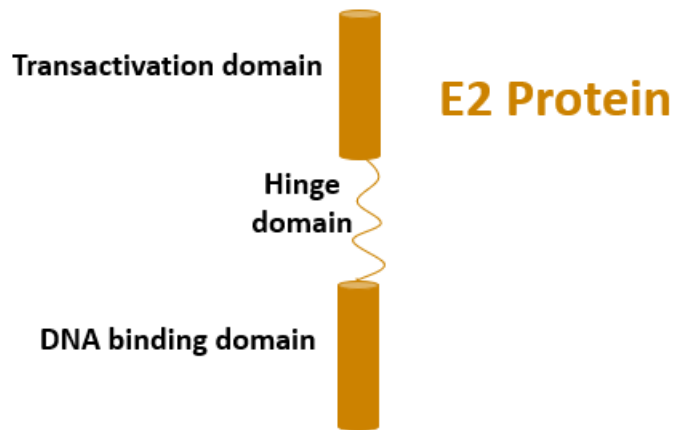


Figure 7. Schematic of HPV E2 protein with its functional domains. E2 is approximately 370 amino acids in length. Different functional domains of E2 protein are indicated. The N-terminal transactivation domain of approximately 200 amino acids is essential for transcription, replication, and viral DNA segregation. This is connected to the DNA binding domain via a flexible proline-rich hinge domain. E2 is a homodimer and that can bind to 12-bp palindromic sequences surrounding the A/T-rich origin of replication (87).

1.7 Essential roles of the E2 protein in the HPV16 lifecycle

HPV E2 is a regulatory protein which has several crucial functions during the viral lifecycle, including initiation of viral DNA replication, transcriptional regulation, and segregation of the viral genome. In addition, a role for E2 in cell cycle regulation, apoptosis, and senescence have also been demonstrated (98, 99).

1.7.1 Viral DNA replication initiation

HPV genome replication occurs inside nuclear foci and formation of these foci depends on the E2 protein as it recruits several viral and host cellular proteins needed to synthesize viral DNA (100-102). The first step in this replication process is that the early E2 protein binds the upstream regulatory region via its DNA binding domain (97, 103, 104). Following this, E2 recruits the helicase protein E1 to the HPV origin via a protein-protein interaction (**Figure 8A**) (105-107). E1 protein then forms a di-hexameric complex to interact with the host proteins including DNA polymerase, pol ϵ , replication protein A (RPA), and topoisomerase I (topoI) (108-111). This recruitment of cellular replication factors by E1 is needed to replicate the viral genomes (112, 113). E2 then gets displaced in an ATP-dependent manner, along with removal of nucleosomes from the origin of replication which reverses the repression, allowing the enhancer proteins to stimulate DNA replication (106, 114, 115). Although E1 is the primary replication protein, E2 is required to initiate replication (33, 116).

1.7.2 Transcription

E2 protein can either activate or repress transcription depending on the promoter or enhancer sequence context and the cellular factors with which it interacts (117, 118). E2 has been shown to activate transcription when E2 sites are present upstream from a heterologous promoter like the herpes simplex virus 1 (HSV1) thymidine kinase (tk) promoter (119, 120). Furthermore, overexpression of E2 can repress transcription from the viral LCR (121). E2 can also recruit several cellular factors via its transactivation domain to the viral genomes (**Figure 8B**), which can further influence viral transcription (122-124).

E2 protein regulates host gene transcription to alter cellular functions, promoting infection and facilitating the HPV lifecycle (125-128). This regulation can happen at multiple levels by controlling cellular gene expression as well as splicing of cellular transcripts, which are implicated in cancer and cell motility (125). Additionally, HPV E2 proteins can interact and regulate many cellular proteins involved in host transcriptional regulation, including SMCX, BRD4, topoisomerase I, BRCA1, chromatin remodeling components p/CAF, CBP, PARP (poly(ADP-ribose) polymerase 1), p300, Sp1, hSNF5, NAP1 and Mdm2 (122, 129-133). E2 also regulates immune response associated genes in keratinocytes, which would aid in persistence of viral infection, that can ultimately lead to cancer (126, 134).

1.7.3 Genome segregation

The viral genome is maintained as an episome inside the nuclei of the dividing epithelial cells. During cell division, the HPV genome segregates into daughter cells, which occurs by tethering to the host mitotic chromosomes to ensure that the viral DNA is maintained within the nuclei. E2 is important for this viral genome partitioning (135-137). Via its DNA binding domain, E2 homodimerizes and binds to 12-bp palindromic sequences in the viral control region, and simultaneously the E2 amino terminal domain complexes with host mitotic chromatin (**Figure 8C**) (138, 139). E2 acts as a bridge between the host chromosome and viral genome, via protein-protein interactions with cellular receptors on the host mitotic chromatin apparatus (140-144).

1.8 Importance of viral genome segregation

DNA partition or segregation is the process wherein the genetic material is accurately moved and positioned between the daughter cells during cell division by the formation of microtubule spindles, which pull chromosomes to opposite cell poles (145). Episomal viral genomes are retained in the nucleus of infected keratinocytes and are segregated between daughter cells during cell division via E2 as a bridge, which tethers viral DNA onto the mitotic chromosomes (93, 146, 147). This is an important step, and if it fails to occur the viral genome will not enter the nuclei and will be lost in the cytoplasm leading to loss of viral genomes from infected cells (**Figure 9**). So, this tethering and viral genome retention inside the nuclei is very important for the viral lifecycle (148, 149).

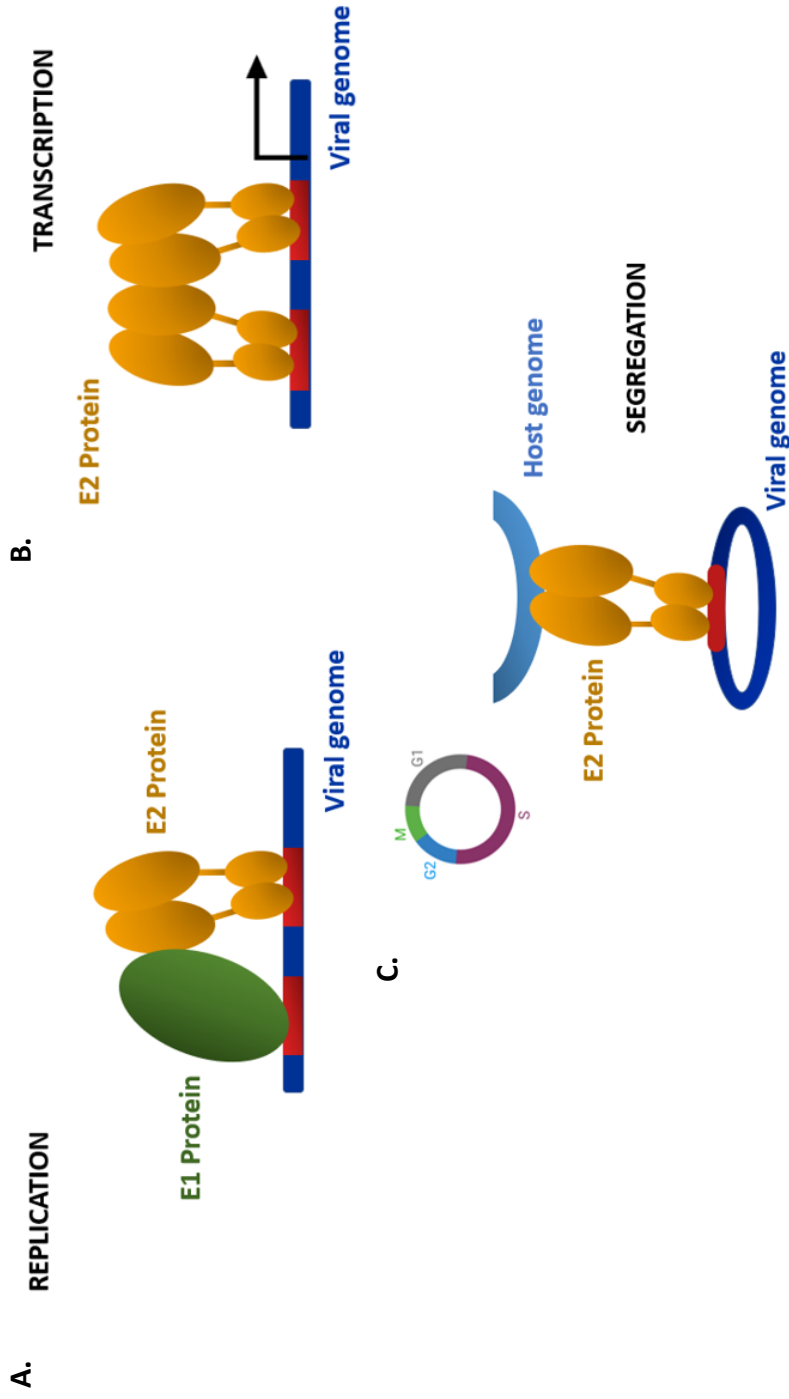


Figure 8. E2 protein functions are mediated through multiple E2 binding sites in the viral genome. The E2 DNA binding domain binds to sites located in transcriptional enhancers and in the replication origin. The dimeric DNA binding domain is linked to an N-terminal transactivation domain by a flexible, hinge region. The transactivation domain is required for transcriptional regulation (A); cooperative binding to the replication origin with the E1 protein (B); interaction with mitotic chromosomes (C), and association with numerous cellular proteins. Image adapted from McBride *et al.*, 2006 (140).

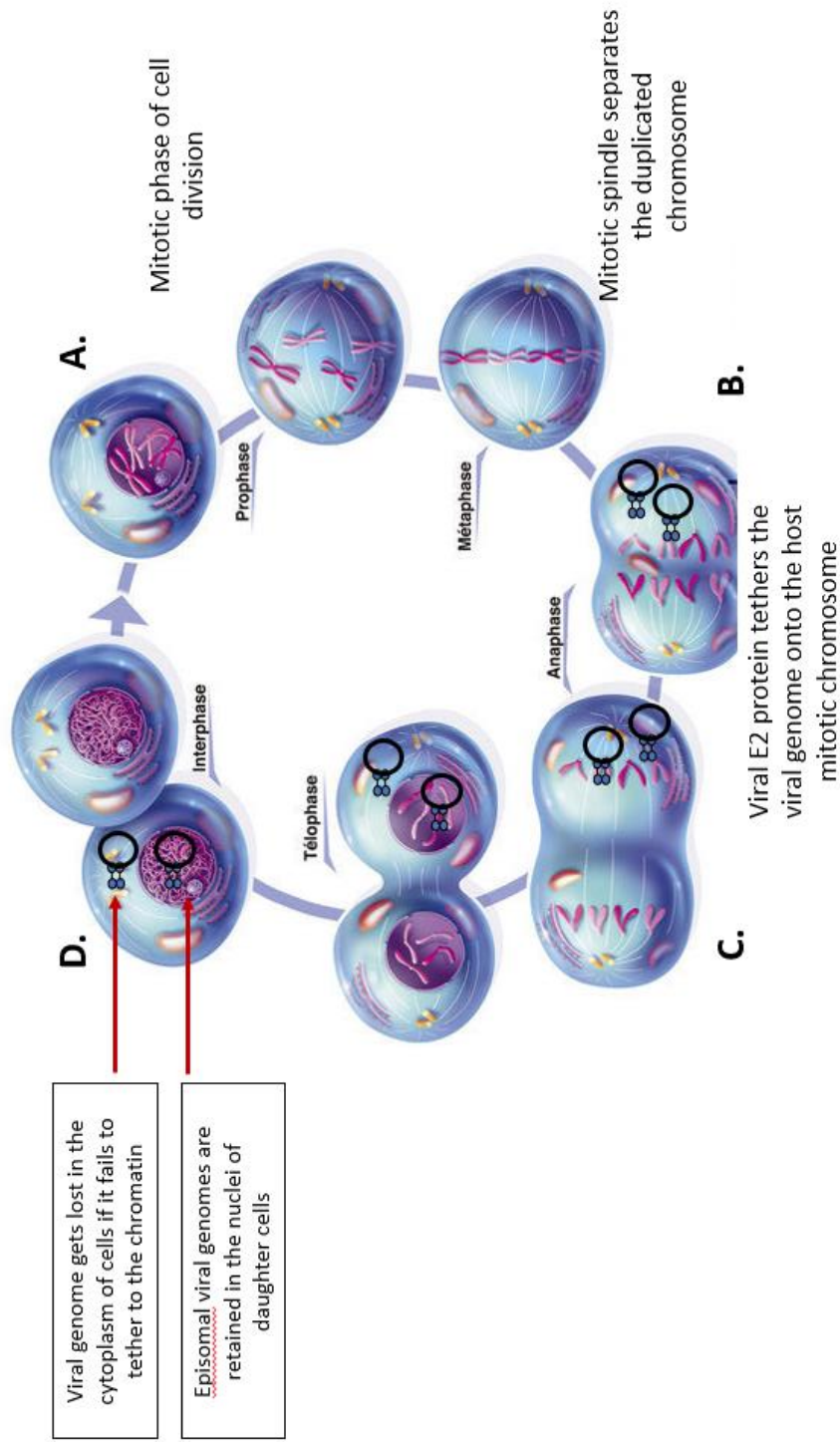


Figure 9. Illustration depicting HPV genome segregation mediated by E2 protein. During the mitotic phase of host cell division (A), the viral genomes are segregated between daughter cells (B). This occurs when the viral genome tethers onto the mitotic chromosomes and this is mediated by E2 protein (C). This is an important step, and if it fails to occur; the viral genome will not enter the nuclei and will be lost in the cytoplasm (D). Adapted from the original image obtained from the website of science photo library.

1.9 HPV16 E2 and host cellular protein interactions

E2 interacts with a number of cellular proteins to execute its different roles during the viral lifecycle. These proteins fall into several categories ranging from transcriptional regulation, RNA processing, apoptosis, cell cycle regulation, nuclear import, and protein degradation (150).

1.9.1 Role of Brd4 association with E2

The interaction between E2 and bromodomain-containing protein 4 (Brd4) is the best characterized E2-host protein interaction. Brd4 is a ubiquitous protein and is a component of both the transcriptional elongation complex pTEFb, to stimulate RNA polymerase II transcriptional elongation in general (151), and the Mediator complex (152). It is further characterized as a chromatin-binding adaptor which can recruit distinct transcriptional regulators to modulate promoter activity through cell cycle progression (153). Brd4 is also an essential gene that is crucial for G₁ transcription and progression into S phase (154, 155). Brd4 is potentially involved in the transcription of most cellular genes and has been implicated in many cancers (156). With regards to papillomavirus, Brd4 is involved in multiple processes critical to the viral lifecycle (157).

Brd4 primarily binds to the transactivation domain of the E2 proteins (148). Brd4 mediates E2's role in transcription modulation (123, 157-160). Studies which conducted mutational analysis identified two highly conserved residues in the transactivation domain of E2; R37 and I73 (159-161), which were demonstrated to be important for direct interaction with Brd4 (91, 162). When these residues were mutated, it abolished E2-mediated transactivation (163-168). Studies have additionally reported that Brd4 can also

be involved in E2-mediated transcriptional repression (95, 169-171). Also, it was shown that when the E2-Brd4 interaction was altered, it affected the ability of HPV16 E2 to regulate host genome expression and cellular movement (172).

Furthermore, studies have shown the role of E2-Brd4 interaction in the viral replication process. Although there have been contradictory reports on how Brd4 regulates E2-mediated viral genome replication (160, 168, 173-175), which seems to be cell type- and context-dependent, there is evidence to support that Brd4 has a functional role in viral replication initiation and that Brd4-E2 interaction is not required for continuing DNA replication (176).

E2 protein associates with host chromosomes to promote retention and partitioning of viral genome in dividing cells (177, 178). It was previously demonstrated that just the attachment of E2 protein to mitotic chromatin is not enough to mediate plasmid retention. E2 seems to form a complex via dual interactions with cellular proteins and two properties seem to be required for proper plasmid segregation (179). One property for BPV1 E2 is transcriptional activation (that is mediated by BRD4), and the other is yet to be known (further discussed in chapter 4). For BPV1 E2, Brd4 is also shown to be the host mitotic chromatin receptor of E2 for mediating the viral genome interaction (148, 174, 180). However, for HR-HPV, the E2 proteins do not co-localize with BRD4 on mitotic chromatin, indicating that BRD4 may not be the mitotic receptor for HR-HPV E2 proteins (158, 180, 181).

1.9.2 E2-TopBP1 interaction

Previous work from the Morgan lab

The Morgan lab aimed at identifying cellular partners that HPV16 E2 could interact with it to carry out different functions, with an aim to better understand the viral cycle. TopBP1 was identified as a functional interacting partner for HPV16 E2 (182). Previous work further demonstrated that TopBP1 interacted with E2 both *in vitro* and *in vivo* and regulate the DNA replication function of E2 (182-186). Additionally, TopBP1 and E2 co-localize on mitotic chromatin and TopBP1 regulates the interaction of E2 with host chromatin in interphase cells (187).

Structure and cellular functions of TopBP1

The 180 kDa topoisomerase II β binding protein 1 (TopBP1) is a key scaffold protein involved in various aspects of nucleic acid metabolism (188). TopBP1 has a transcriptional activation domain and two surrounding repressor domains and can regulate transcription (189). It contains 9 BRCT (BRCA1 carboxyl terminal) domains (**Figure 10**) which are hydrophobic pockets, some of which can potentially interact with phosphorylated motifs in other proteins, to regulate several cellular processes (190, 191). Interactions with cellular proteins can be mostly regulated through phosphorylation/dephosphorylation via the activity of specific kinases and phosphates (190, 192-195). TopBP1 is a multifunctional nuclear protein. Via its BRCT domains it mediates interactions with several cellular proteins that are phosphorylated following cell signaling events and further is involved in DNA replication, ATR checkpoint activation, DNA repair, mitosis, and transcriptional regulation, as explained below. TopBP1 is a part

of the replication complex in mammalian cells and is involved in replication initiation through its interaction with TICCR/Treslin (196-199). TopBP1 is implicated in DNA damage checkpoint, as TopBP1 is required for activation of ATR via interaction with ATRIP (ATR interacting protein), in response to replication stress (200, 201). TopBP1 is also a substrate for ATM. During the viral lifecycle, both ATM and ATR are activated in order to promote viral genome replication, therefore TopBP1 can be a vital mediator of the HPV16 lifecycle (202-206).

TopBP1 also has several roles during mitosis to prevent transmission of DNA damage (such as DNA double strand breaks and catenated DNA) to G1 daughter cells (207-210). During mitosis, TopBP1 forms a complex with MDC1 via CK2 phosphorylation of MDC1 on the mitotic chromatin, and this helps maintain chromosome stability when DNA double-strand breaks occur (211). Additionally, CK2 mediated phosphorylation of human Rad9 promotes the interaction between Rad9-Hus1-Rad1 (9-1-1) and TopBP1 and has an important role in ATR-dependent checkpoint (212). TopBP1 can directly interact with the transcription factor E2F1 and control its transcription and apoptotic functions (213). TopBP1 can regulate p53 target genes by a direct complex formation with p53 protein and can regulate properties of several mutant p53 proteins that can cause transformation (214).

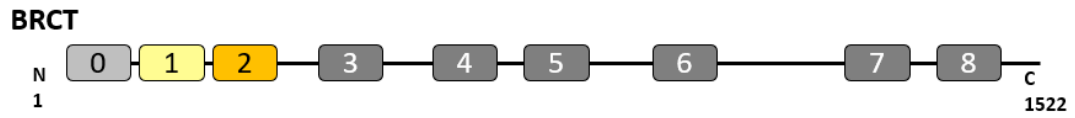


Figure 10. TopBP1 BRCT domain structure. TopBP1 can interact with various cellular and viral phosphorylated proteins through these BRCT domains (190).

1.10 Purpose of the study

E2 and TopBP1 are nuclear proteins and have overlapping functions including replication, transcription and chromatin interaction during mitosis (184-187). This suggested that TopBP1 may be the chromatin receptor protein mediating E2 segregation function. Previously, a structural mutant of E2 was identified that had a compromised interaction with TopBP1. This mutant also had a reduced replication function at low levels of E2 protein (185). In this mutant, asparagine 89 and glutamic acid 90 of E2 were mutated to tyrosine and valine, respectively (185). However, this is a structural mutant; the hydrophobic tyrosine and valine residues would potentially repel the interaction with hydrophobic TopBP1 BRCT domains. Therefore, in this thesis, we aimed at obtaining a more mechanistic understanding of the E2-TopBP1 interaction.

The hypothesis of this study was that HPV16 E2 mediates the segregation of viral genomes in host cells using TopBP1 as the mitotic chromatin receptor, which would keep the viral genome circular inside the nucleus. This study aimed at closing a gap in our understanding of E2 and host cellular protein interactions, which are needed for viral lifecycle progression. This could potentially aid in identifying therapeutic targets for the treatment of cancers caused by HPV16.

CHAPTER 2

Materials and methods

2.1 Generation of stable cell lines

Stable cell lines expressing wild type E2 (E2-WT), E2-S23A and E2-S23D (the aspartic acid mimics phosphorylation), along with pcDNA empty vector plasmid control were established both in U2OS and N/Tert-1 cell lines as previously described (125, 126). Low passage U2OS cells were seeded at 3×10^5 cells per 100-mm plate in Dulbecco's modified eagle medium (DMEM) with 10% Fetal Bovine Serum (Invitrogen) and 1% (v/v) penicillin/streptomycin mixture (Thermo Fisher Scientific) at 37 °C in a 5% CO₂/95% air atmosphere. The next day, the cells were transfected with 1 µg of E2-WT or E2-S23A or E2-S23D or pcDNA empty vector plasmid DNA containing a G418 resistance gene using the calcium phosphate method (215). After 48h of transfection, the cells were trypsinized with 0.5% trypsin EDTA (Invitrogen) and re-plated at 1:10 and 1:50 dilutions in DMEM media containing G418 (Thermo Fisher Scientific) at a concentration of 0.75 mg/ml.

N/Tert-1 cells were cultured in keratinocyte serum-free medium (K-SFM) (Invitrogen; catalog no. 37010022) supplemented with bovine pituitary extract, EGF (Invitrogen), 0.3 mM calcium chloride (Sigma; 21115) and 1% (v/v) of penicillin/ streptomycin mixture (Thermo Fisher Scientific) at 37 °C in a 5% CO₂/95% air atmosphere. Stable E2-WT, E2-S23A, E2-S23D and pcDNA empty vector containing a G418 resistance gene were generated utilizing Lipofectamine 2000 (according to the manufacturer's instructions, ThermoFisher Scientific). After 48h of transfection, the cells were trypsinized with 0.5% trypsin EDTA (Invitrogen) and re-plated at 1:10 and 1:50 dilutions in supplemented

K-SFM media containing G418 (Thermo Fisher Scientific) at a concentration of 0.75 mg/ml G418. Both cell types were closely monitored and re-fed with fresh G418-containing media every 3-4 days, for the next 14 days. Following this the cells growing in isolated colonies were observed which were trypsinized and re-plated onto 100-mm plates with G418 medium. E2 expression was confirmed using western blot analysis.

2.2 Western blotting

E2 stable cell lines generated above were trypsinized and washed with 1x phosphate-buffered saline (PBS). Protein from the cell pellets was extracted with 2x pellet volume of protein lysis buffer (0.5% Nonidet P-40, 50mM Tris [pH 7.8], and 150mM NaCl) supplemented with protease inhibitor (Roche Molecular Biochemicals) and phosphatase inhibitor cocktail (Sigma). The cells were lysed for 20 min on ice followed by centrifugation at 18,000 x g relative centrifugal force (rcf) for 20 min at 4°C to harvest the lysate. Bio-Rad protein estimation assay was used for protein concentration estimation. 50 µg of protein was combined with equal volume of 4X Laemmli sample buffer (Bio-Rad) then heat denatured using a heat block at 95°C. The samples were separated on a Novex™ WedgeWell™ 4 to 12% Tris-glycine gel (Invitrogen) and using the wet-blot method, transferred onto a nitrocellulose membrane (Bio-Rad) at 30 V overnight. The membrane was blocked with *Li-Cor* Odyssey® blocking buffer (PBS) diluted 1:1 with 1x PBS and then incubated with specified primary antibody in *Li-Cor* Odyssey® blocking buffer (PBS) diluted 1:1 with 1x PBS. Following this, the membrane was washed with 1 X PBS supplemented with 0.1% Tween and further probed with the Odyssey secondary antibodies (IRDye® 680RD Goat anti-Rabbit IgG (H + L), 0.1 mg or IRDye® 800CW Goat anti-

Mouse IgG (H + L), 0.1 mg) in *Li-Cor* Odyssey® blocking buffer (PBS) diluted 1:1 with 1x PBS at 1:10,000 for 1 h at room temperature. After washing with PBS-tween, the membrane was imaged using the Odyssey® CLx Imaging System and ImageJ was used for quantification. Primary antibodies used for western blotting studies are as follows: HPV16 E2 (TVG 261) at 1:500 dilution (Abcam; ab17185) monoclonal B9 1:500 (Abcam ab17185 for TVG261, (216) for monoclonal B9), TopBP1 at 1:1000 dilution (Bethyl; catalog no. A300-111A), GAPDH at 1:10,000 dilution (Santa Cruz; catalog no. sc-47724), Casein kinase II α (1AD9) at 1:500 dilution (Santa Cruz; catalog no. sc-12738), CKII alpha' Antibody at 1:1000 dilution (Bethyl; catalog no. A300-199A).

2.3 *In vivo* immunoprecipitation

Cell lysate was prepared as described above. 250 μ g of the lysate was incubated with lysis buffer (0.5% Nonidet P-40, 50mM Tris [pH 7.8], and 150mM NaCl) supplemented with protease inhibitor (Roche Molecular Biochemicals) and phosphatase inhibitor cocktail (Sigma) to a total volume of 500 μ l. Primary antibody of interest or a HA-tag antibody (used as a negative control) was added to this prepared lysate and rotated at 4°C overnight. The following day, 40 μ l of protein A beads per sample (Sigma, equilibrated to lysis buffer as mentioned in the manufacturer's protocol) was added to the above mixture and rotated for another 4 hours at 4°C. The samples were gently washed with 500 μ l lysis buffer by centrifugation at 1000 x g for 2-3 min. This wash was repeated for 4 times. The bead pellet was resuspended in 4X Laemmli sample buffer (Bio-Rad), heat denatured and centrifuged at 1000 x g for 2-3 min. The supernatant was gel electrophoresed using an SDS-PAGE system which was later transferred onto a nitrocellulose membrane using wet-blot transfer

method. The membrane was probed for the presence of E2 or TopBP1, as mentioned in the description of immunoblotting above.

2.4 Immunofluorescence

U2OS cells expressing stable E2-WT, E2-S23A and pcDNA empty vector plasmid control were plated on acid-washed, *poly-L-lysine*-coated coverslips in a 6-well plate at a density of 2×10^5 cells / well (5 ml DMEM + 10% FBS media). After 24 h, the cells were treated with 2 mM thymidine diluted in the supplemented DMEM media for 16 h. This was then washed 2 times with 1 X PBS and recovered in supplemented DMEM media. After 8 h, to block the cells at G1/S phase, a second dose of 2 mM thymidine was added and incubated for 17 h. The cells were then washed twice with 1 X PBS and recovered as before for 3 h. The cells were next treated with nocodazole (100 ng/ml) for 5 h and released for 2 h to enrich for mitotic cells. Following this, the cells were washed twice with 1 x PBS, fixed and stained as previously described (176).

The primary antibodies used are as follows: HPV16 E2 (TVG 261) 1:500 (Abcam; ab17185), HPV16 E2 B9 monoclonal antibody, 1:500 (216), TopBP1 1:1000 (Bethyl; catalog no. A300-111A), pS23-Ab 1:10,000 (Custom generated by GenScript; peptide sequence- CKILTHYENDS^PTDLR). For lifecycle studies, the antibodies used were as follows: BrdU, 1:500 (Cell Signaling Technology) and immune complexes were visualized using Alexa 488- or Alexa 595-labeled antispecies-specific antibody conjugates (Molecular Probes). The cells were thoroughly washed and incubated with secondary antibodies Alexa fluor 488 goat anti-mouse (Thermo fisher; catalog no. A-11001) or Alexa fluor 594 goat anti-rabbit (Thermo fisher; catalog no. A-11037) diluted at 1:1000. The

wash step was repeated as before, and the coverslips were mounted on a glass slide using Vectashield mounting medium containing 4',6-diamidino-2-phenylindole (DAPI). Images were captured with a Zeiss LSM700 laser scanning confocal microscope and analyzed using Zen LE software.

2.5 Cell synchronization and FACS analysis

U2OS cells expressing stable E2-WT, E2-S23A and pcDNA empty vector plasmid control were plated at 3×10^5 density onto 100-mm plates in DMEM + 10% FBS media. The cells were treated with 2 mM thymidine diluted in the supplemented DMEM media for 16 h. The cells were then washed 2 times with 1 X PBS and recovered in supplemented DMEM media. After 8 h, to block the cells at G1/S phase, a second dose of 2 mM thymidine was added and incubated for 17 h. The cells were then washed twice with 1 X PBS and recovered as before at different time points as follows: 0 h and 2 h (G1/S phase), 4 h and 6 h (S phase), 8 h (M1 phase), 10 h (M2 phase), and 12 h (the next G1 phase). The cell lysates were prepared using the harvested cells at different time points and immunoblotting was carried out as mentioned in the section above. Propidium iodide staining and FACS analysis with a FACSAria™ fusion SORP high-speed cell sorter (Becton Dickinson), using FlowJo software was used for the cell cycle phase analysis.

2.6 Transient transcription activation and repression assays

Parental U2OS cells were plated at a density of 1×10^5 cells per 60 mm plate. Next day, the cells were transiently transfected with plasmids mentioned below, using calcium phosphate transfection method. We measured the transcriptional activation potential of E2-WT and E2-S23A using our ptk6E2-luc system, a plasmid with 6 E2 sites located upstream from the HSV-1 tk promoter driving expression of luciferase. Plasmids used for transcription activation (119, 120): 1 μ g ptk6E2-luc + 1 μ g E2-WT, 1 μ g ptk6E2-luc + 1 μ g E2-S23A or 1 μ g ptk6E2-luc alone. Plasmids used for transcription repression (217): 1 μ g HPV16 LCR-luc + 1 μ g E2-WT, 1 μ g HPV16 LCR-luc + 1 μ g E2-S23A or 1 μ g HPV16 LCR-luc alone. pGL3control, containing the SV40 promoter and enhancer driving the expression of the luciferase gene, was included in each of the experimental setup to confirm similar levels of transfection efficiency between experiments. 24 h post transfection, cells were washed with 1 X PBS and re-fed with DMEM media + 10% FBS. After 48 h from initial transfection, the cells were washed twice with 1 X PBS and further lysed with 550 μ l of 1X reporter lysis buffer (Promega) at room temperature by rocking for 15 min. Lysates were then harvested by scraping and transferred into 1.5 ml microcentrifuge tubes. The tubes were then centrifuged at 4°C for 10 min at maximum speed to separate the supernatants. 80 μ l of this supernatants were used for luciferase activity analysis using the luciferase assay system (Promega). The Bio-Rad protein estimation assay was used for protein concentration estimation, to standardize for cell number. Relative fluorescence units were measured using the BioTek Synergy H1 hybrid reader. The activities shown are

expressed relative to the respective protein concentrations of the samples. The assays shown are representative of three independent experiments carried out in triplicates.

2.7 Plasmid retention assay

This assay is based upon the well-established fact that transfected DNA is lost from cells if there is no selective pressure put on them to retain the plasmid DNA; transfected DNA is quickly located to the cytoplasm and after day three the DNA is quickly lost (218). Two luciferase reporter plasmids were used for our novel assay; one containing the SV40 promoter and enhancer (pGL3 Control, Promega) which has no E2 DNA binding sites, the other with the HSV1 tk promoter driving expression of luciferase with 6-E2 target sites upstream. ptk6E2-luc plasmid has almost no activity in the absence of E2, therefore cannot be used to monitor for luciferase loss in non-E2 expressing U2OS cells. The pSV40-luc and the ptk6E2-luc were transiently transfected, separately into either E2-WT or E2-S23A cells. Three days post-transfection the cells were trypsinized and half re-plated and half harvested for luciferase assay (Promega). This luciferase activity was considered as the baseline activity. At day 6, the same process was repeated; half of the cells were harvested for luciferase assay and half re-plated. At day 9 all the cells were harvested for luciferase activity assays. The Bio-Rad protein estimation assay was used for protein concentration estimation, to standardize for cell number. Relative fluorescence units were measured using the BioTek Synergy H1 hybrid reader. The activities shown are expressed relative to the respective protein concentrations of the samples. The assays shown are representative of three independent experiments carried out in triplicates.

2.8 Small interfering RNA (siRNA) and segregation assay

U2OS parental cells were plated on a 100-mm plates. The next day, cells were transfected with 10 μ M of the following siRNA. Table 2 lists all the siRNAs used in the study sourced from Sigma-Aldrich. 10 μ M of **MISSION[®] siRNA Universal Negative Control (Sigma-Aldrich; catalog no. SIC001)** was used as a “non-targeting” control in our experiments. The Lipofectamine[™] RNAiMAX transfection (Invitrogen; catalog no. 13778-100) protocol was used in the siRNA knockdown. 48 h post transfection, the cells were harvested, and the knockdown was confirmed by immunoblotting for the protein of interest. The Segregation assay was performed as described before, after treating the cells with the siRNA of interest on day 3 of the protocol.

Table 2. List of siRNA used in the study

siRNA name	Target (sense) sequence (5' to 3')
TopBP1- A	CUCACCUUAUUGCAGGAGAdTdT
TopBP1- B	GUAAAUUAUCUGAAGCUGUAdTdT
TopBP1- C	ACAAAUACAUGGCUGGUUAdTdT
CK2 α	GGCUCGAAUGGGUUCAUCUtt
CK2 α'	CAGUCUGAGGAGCCGCGAGdTdT

2.9 Production of bacterial recombinant protein

E2-WT and E2-S23D (1-200 aa) were produced as fused proteins with His-tag and TopBP1 was produced as a fused protein with GST-tag (GST TopBP1 (aa 32- 1522) His from Addgene; plasmid # 20375). Expression was carried out by picking a single colony of BL21(DE3) Competent *E. coli* (NEB Inc.; catalog no. C2527) containing the plasmid of interest and growing it in LB media supplemented with 100 $\mu\text{g/ml}$ of respective antibiotics (kanamycin for His-tagged E2-WT and E2-S23D; ampicillin for GST-tagged TopBP1), grown overnight by shaking at a low speed at 37°C. The starter culture was then diluted 1:100 in fresh LB media with kanamycin, as mentioned above. The culture shaken as before at 37°C, until the optimal density of 0.6-0.8 at OD_{600nm} was achieved.

Following this, IPTG at final concentration of 1 mM was added to the culture for induction of protein expression with shaking at 16°C overnight. The His-tagged proteins were purified on Ni-NTA agarose (Qiagen; catalog no. 30761) and GST-tagged TopBP1 protein was purified on Glutathione Sepharose™ 4B (GE healthcare; catalog no. 17-0756), according to the batch purification method described in the manufacturer's manual, followed by size-exclusion chromatography. The purity of the recombinant protein was confirmed by SDS-PAGE analysis.

2.10 *In vitro* GST pull-down assays

Purified recombinant His-tagged E2-WT and E2-S23D protein and GST-tagged TopBP1 were used for the *In vitro* pull-down assays. GST-tagged NEDD4 E3 ligase was used as our GST-control. GST-TopBP1 and GST-control were kept stable at 0.65 pmol and 11 pmol of His-E2-WT and His-E2-S23D were used for the experiment. GST-TopBP1 and His-E2-WT or His-E2-S23D were immobilized on Glutathione Sepharose™ 4B (GE healthcare; catalog no. 17-0756), equilibrated to the GST lysis buffer (50 mM Tris-HCl, pH 8.0, 100 mM NaCl, 0.5 mM EDTA, 0.5 mM EGTA and 0.5% NP-40, 1 mM DTT plus protease inhibitors) at 4°C for 1 h with continual end-to-end rotation.

The protein-bound GST beads were washed 3 times in the GST lysis buffer by centrifugation at 1000 x g for 3 min and resuspended in 4X Laemmli sample buffer (Bio-Rad), heat denatured and centrifuged at 1000 x g for 2-3 min. The supernatant was gel electrophoresed using an SDS-PAGE system which was later transferred onto a nitrocellulose membrane using wet-blot transfer method. The membrane was probed for the presence of E2 or TopBP1, as mentioned in the description of immunoblotting above.

2.11 *In vitro* kinase assay with or without lambda phosphatase

Immunoprecipitated GST beads were prepared as mentioned above in the GST-pull down section. After 1 h incubation, the beads were incubated with 1 µl CK2 enzyme and 1 X CK2 reaction buffer (NEB Inc; catalog no. P6010S) supplemented with 200 µM ATP and 30 mM MgCl₂ and rotated for 1 h at 30°C. The beads were then incubated in presence or absence of lambda phosphatase (Santa Cruz; catalog no. sc-200312A) as mentioned in

the manufacturer's protocol. Following this, the beads were washed as before and analyzed by immunoblotting.

2.12 Growth assay

Cells were plated at 1×10^5 per 100-mm plate in their respective growth media. For siRNA studies, the cells were transfected with the respective siRNAs, the following day of plating. The cells were grown for 2 days and were trypsinized, then counted. A total of 1×10^5 cells per sample were further plated and allowed to grow for 2 more days. This procedure repeated for another 2 days. After a total of 6 days, the cells were counted, mean of the different replicates were calculated, analyzed and plotted on a log scale using Microsoft Excel.

2.13 CK2 inhibitor treatment

U2OS and N/Tert-1 cells were plated at a density of 2×10^5 in a 100-mm plate. The next day, the cells were treated with 10 μ M CK2 inhibitor, CX-4945 (Silmitasertib) from APEXIO (catalog no. A8330) or 10 μ M DMSO for 48 h. The cells were then harvested and processed for immunoprecipitation with pS23Ab as described in the section above.

2.14 Organotypic raft culture

N/Tert-1, N/Tert-1 HPV16, N/Tert-1 HPV16-S23A and N/Tert-1 HPV16-S23D cells were differentiated via organotypic raft culture, as described previously (219, 220). Briefly, cells were seeded onto type 1 collagen matrices containing J2 3T3 fibroblast feeder cells. Cells were then grown to confluence on top of the collagen matrices, which were then lifted onto wire grids and cultured in cell culture dishes at the air-liquid interface, with medium

replacement on alternate days. Following 13 days of culture, rafted samples were fixed with formaldehyde (4% [vol/vol]) and embedded in paraffin blocks. Multiple 4 μm sections were cut from each sample. Sections were stained with hematoxylin and eosin (H&E) and others were prepared for immunofluorescent staining, as described previously.

2.15 Immortalization of human foreskin keratinocytes (HFK)

HPV16 mutant genomes (S23A and S23D) were generated by Genscript. The HPV16 (WT, S23A, S23D) were removed from their parental plasmid using SphI, and the viral genomes isolated and then re-circularized using T4 ligase (NEB) and transfected into early passage HFK from three donor backgrounds (Lifeline technology), alongside a G418 resistance plasmid, pcDNA. Cells underwent selection in 200 $\mu\text{g}/\text{mL}$ G418 (Sigma-Aldrich) for 14 days and were cultured on a layer of J2 3T3 fibroblast feeders (NIH), which had been pre-treated with 8 $\mu\text{g}/\text{ml}$ mitomycin C (Roche). Throughout the immortalization process, HFK were cultured in Dermalife-K complete media (Lifeline Technology). In Figure 5A, transfected cells were stained with crystal violet 14 days following transfection and selection prior to passaging.

2.16 Southern blotting

Total cellular DNA was extracted by proteinase K-sodium dodecyl sulfate digestion followed by a phenol-chloroform extraction method. 5 μg of total cellular DNA was digested with either SphI (to linearize the HPV16 genome) or HindIII (which does not cut the HPV16 genome). All digests included DpnI to ensure that all input DNA was digested and not represented as replicating viral DNA. All restriction enzymes were purchased from

NEB and utilized as per manufacturer's instructions. Digested DNA was separated by electrophoresis of a 0.8% agarose gel, transferred to a nitrocellulose membrane, and probed with radiolabeled (32-P) HPV16 genome. This was then visualized by exposure to film for 1 to 24 hours. Images were captured from an overnight-exposed phosphor screen by GE Typhoon 9410 and quantified using ImageJ.

2.17 Exonuclease V assay

To examine whether viral genomes were maintained as episomes, we carried out an exonuclease V assay, as described by Bienkowska-Haba *et al.* 2018 (221), which determines the resistance of HPV16 genomes to exonuclease V. 20 ng genomic DNA was either treated with exonuclease V (RecBCD, NEB), in a total volume of 30 μ l, or left untreated for 1 hour at 37°C followed by heat inactivation at 95°C for 10 minutes. 2 ng of digested/undigested DNA was then quantified by real time PCR using a 7500 FAST Applied Biosystems thermocycler with SYBR Green PCR Master Mix (Applied Biosystems) and 100 nM of each primer in a 20 μ l reaction. Nuclease-free water was used in place of the template for a negative control. The following cycling conditions were used: 50°C for 2 minutes, 95°C for 10 minutes, 40 cycles at 95°C for 15 seconds, and a dissociation stage of 95°C for 15 seconds, 60°C for 1 minute, 95°C for 15 seconds, and 60°C for 15 seconds. Separate PCR reactions were performed to amplify HPV16 E6 genes. Table 3 lists the primers used for amplification.

Table 3. List of primers used in section 2.16

Primer used for the amplification	Sequence
HPV16 E6	F: 5'- TTGCTTTTCGGGATTTATGC-3' R: 5'- CAGGACACAGTGGCTTTTGA-3'
HPV16 E2	F: 5'- TGGAAGTGCAGTTTGATGGA-3' R: 5'- CCGCATGAACTTCCCATACT-3'
Human mitochondrial DNA	F: 5'- AGGAGTAGGAGAGAGGGAGGTAAG-3' R: 5'-TACCCATCATAATCGGAGGCTTTGG -3'
Human GAPDH DNA	F: 5'- GGAGCGAGATCCCTCCAAAAT-3' R: 5'- GGCTGTTGTCATACTTCTCATGG-3

2.18 Statistical analysis

All the data are represented as means \pm SE. Significance was determined using a student's *t* test and standard error was calculated from three independent experiments.

CHAPTER 3

Results

3.1 E2 serine 23 is critical for TopBP1 interaction *in vivo* and the E2 S23A mutation disrupts E2 plasmid retention function.

In a previous study by the Morgan lab, it was demonstrated that TopBP1 and E2 co-localize on mitotic chromatin and that TopBP1 regulates the interaction of E2 with host chromatin in interphase cells (187). Considering the important role of TopBP1 in regulating host functions during mitosis (192, 208-210), TopBP1's ability to regulate E2 interaction with interphase chromatin, and the co-localization of the two proteins during mitosis (187), we hypothesized that HPV16 E2 might mediate the segregation of viral genomes in the host cells using TopBP1 as a hook. Our primary aim in this section was to identify which residues of E2 mediate the interaction between E2 and TopBP1 and then dissect the functional aspect of this interaction.

3.1.1 S23 is highly conserved in HR-HPV E2 proteins with no known function.

An E2 mutant, N89Y E90V (aspartic acid 89 mutated to tyrosine, glutamic acid 90 mutated to valine), has compromised interaction with TopBP1 (185). This is a structural mutant where the hydrophobic residues potentially disrupt the interaction with hydrophobic TopBP1 BRCT domains. Therefore, we set out to gain a more mechanistic understanding of the E2-TopBP1 interaction. We tested potential phosphorylation sites on E2 that could mediate TopBP1 interaction, as TopBP1 can bind to a wide variety of

phosphorylated proteins via its BRCT domains. An E2 protein sequence analysis (Figure 11) showed that serine 23 is highly conserved in alpha-type HPV (which includes high-risk HPVs), without any known function.

3.1.2 E2 interacts with TopBP1 via serine 23.

To explore the interaction between E2 and TopBP1 via serine 23, U2OS cells stably expressing E2-WT (wildtype), E2-S23A (serine mutated to alanine) and E2-S23D (serine mutated to aspartic acid, which mimics the negative charge of phosphorylation) were generated, along with a pcDNA empty vector plasmid control. We used U2OS cells due to their excellent nuclear architecture for studying mitotic bodies, and it was previously demonstrated that E2 and TopBP1 co-localize during mitosis in U2OS cells (187). U2OS cells can also support HPV replication and the maintenance of episomal genomes (222). The growth rate of the mutants, U2OS E2-S23A and E2-S23D was no different from U2OS E2-WT (Figure 12). The successful generation of stable cell lines was confirmed by positive E2 expression, (Figure 13A).

Next, protein extracts from the stable U2OS cell lines (Figure 13A) were immunoprecipitated using a TopBP1 antibody, and TopBP1 and E2 detected using western blotting (Figure 13B). E2-WT co-precipitated with TopBP1 (lanes 4, Figure 13B), while E2-S23A did not (lane 3, Figure). The S23D mutant maintained this interaction (lanes 5, Figure 13B). This was repeated with three independent extracts and quantitated (Figure 13C).

3.1.3 E2-WT and E2-S23A have similar transcriptional activation/repression and replication properties.

Transient E2 transcriptional activation assays demonstrated that both E2-WT and E2-S23A are able to repress transcription from a pHPV16-LCR-luc reporter (Figure 14A). E2-WT and E2-S23A were also able to activate transcription from ptk6E2-luc reporter with no significant difference in activity (Figure 14B). Using a transient E1-E2 DNA replication assay (223), we demonstrated that both E2-WT and E2-S23A were able to activate replication with no significant difference between them (Figure 14C).

3.1.4 E2-S23A has compromised interaction with mitotic chromatin.

U2OS cells expressing E2-WT, E2-S23A and pCDNA-Vec control were synchronized to enrich for mitotic cells by double thymidine block. These cells were then fixed and stained with DAPI, E2 and TopBP1 antibodies. In our pCDNA-Vec control with no E2 expression, TopBP1 did not interact directly with the mitotic chromatin, but a punctate staining was detected as previously observed (211). E2-WT expressing cells had a strong interaction with mitotic chromatin, clearly co-localizing with TopBP1 during this process (Figure 15, middle panels). This was observed repeatedly and demonstrates that E2 recruits TopBP1 onto mitotic chromatin. E2-S23A had compromised interaction with the mitotic chromatin. It does co-localize with the chromatin, but the intensity of staining was less when compared with WT-E2. Although not obvious here, we also observed stronger TopBP1 staining in many of the E2-WT cells, but never in the E2-S23A cells.

3.1.5 E2-WT levels are elevated during mitosis, while E2-S23A levels are not.

The results from mitotic staining suggested that E2-WT levels are elevated at mitosis when compared with E2-S23A. We investigated this by double thymidine blocking of U2OS pCDNA-Vec, E2-WT and E2-S23A cells, arresting the majority of the cells at G1-S transition. The cells were then released and harvested at two-hour time points. Protein was extracted and used for western blot analysis for TopBP1 and E2 expression (Figure 16). As the cells move into S phase, the protein levels of both E2-WT and E2-S23A increase (compare the 4-hour time point for both with that of 0 hours). At the 8-hour time point, we observe a striking difference between E2-WT and E2-S23A. This is when the cells would complete the S phase following release from the block and enter G2/M. There was a large increase of E2-WT at this time point but not with that of E2-S23A, where the E2 levels remained constant. Another striking observation is that with E2-WT, TopBP1 levels are elevated at the 8-hour time point but not with E2-S23A. TopBP1 elevation was also not observed in pCDNA-Vec control cells. This increase in expression of E2-WT and TopBP1 at the 8-hour time point was reproducible, as was the clear difference with E2-S23A and the results were quantitated as shown in Figure 17. We confirmed the cell cycle status of these cells at different time points, by flow cytometry. We see that at the 8-hour time point, most of the cells would be completing S phase following release from the DTB and entering G2/M (Figure 18). We are currently investigating whether E2-WT is stabilized during mitosis when compared with E2-S23A.

3.1.6 E2-WT has a plasmid retention function lost by E2-S23A.

Next, we set out to investigate if the E2-TopBP1 interaction is functionally required for E2 plasmid retention function and if this is abolished in our E2-S23A mutant. There was no existing assay to measure E2 plasmid retention function, therefore, we developed an assay. The principal behind this assay is that, in transiently transfected cells, the transfected DNA is lost from the cell after 2-3 days unless a selective pressure is placed on the transfected cell to retain the plasmid (218). Figure 19 summarizes the flow of the plasmid retention assay. A crucial aspect of our assay is that we are measuring nuclear DNA because we are measuring transcription. If we followed DNA using PCR, all the DNA that is in the cytoplasm and which is stuck to the cells and cell culture dish would be detected. Hence, this luciferase-based assay allows us to monitor nuclear retention of plasmid DNA. It is also important that the ptk6E2-luc plasmid has almost no activity in the absence of E2, therefore luciferase cannot be used to monitor for plasmid loss in non-E2 expressing U2OS cells.

We confirmed that the transcription activity was comparable in both E2-WT and E2-S23A as shown in Figure 20. From the results, (Figure 21) we can see that the pSV40-luc plasmid activity is lost dramatically between day 3 and 6, reduced to almost zero at day 9. This was irrespective of which E2 protein was expressed. In contrast, ptk6E2-luc activity was significantly retained by E2-WT between day 3 and day 6 and this retention persists to day 9, when compared with E2-S23A. The differences between WT-E2 and E2-S23A were highly significant at days 6 and 9 (please note the log scale on both graphs). This experiment was repeated three times in triplicate. E2-S23D mutant was not used in these

assays as the mutant failed to activate transcription. We are currently probing the reasons for this.

3.1.7 E2-WT loses its ability to segregate after TopBP1 knockdown.

To further investigate the role of TopBP1 in E2 plasmid retention function, we used siRNA against TopBP1 at day 3 following transfection in our assay. We confirmed TopBP1 knockdown which persists till day 9 (Figure 22). We also confirmed that siRNA knockdown of TopBP1 did not affect the growth rate in our E2 cell lines (Figure 23). TopBP1 knockdown had no effect on pSV40-luc activity. But we see that E2-WT loses its ability to retain the ptk6E2 plasmid following TopBP1 knockdown (Figure 24). Using two additional siRNA against TopBP1, we were able to demonstrate the same results (Figure 25). Non-specific scrambled control siRNA (Scr) was used as a control for siRNA treatment. We were thus able to show that an E2-TopBP1 complex is required for E2-WT plasmid retention function.

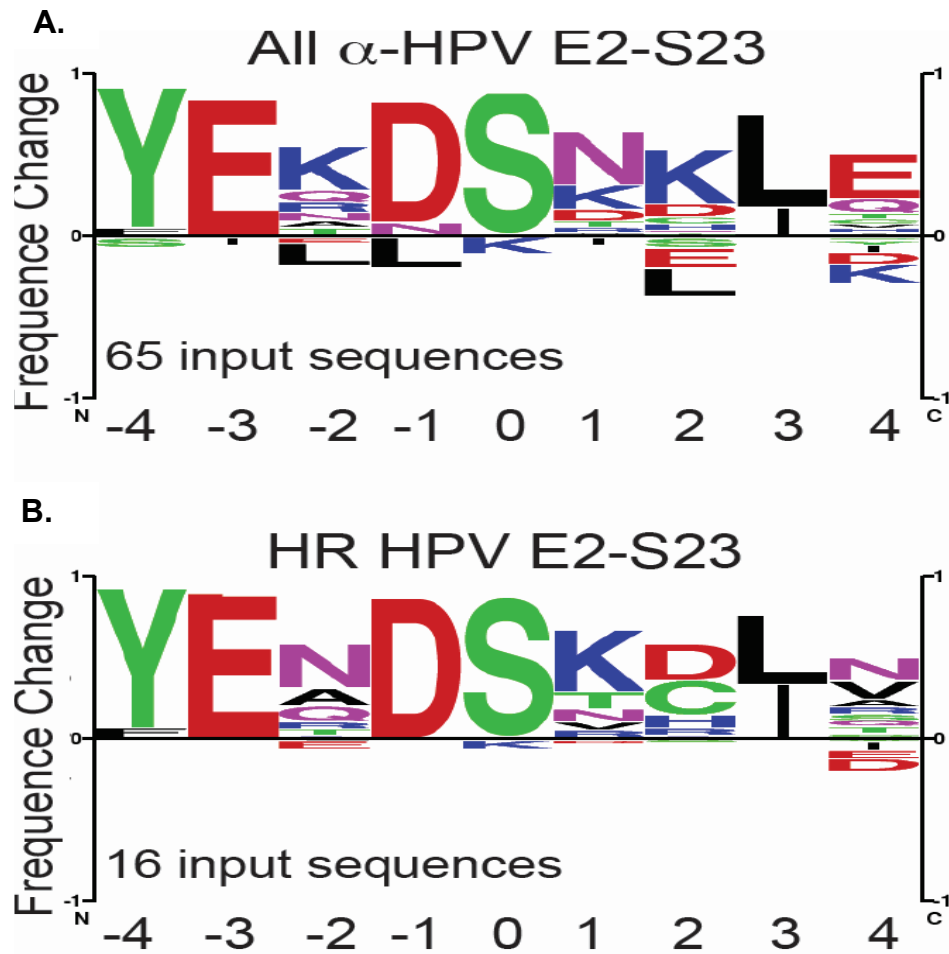


Figure 11. Motif analysis of the E2 serine 23 residue region. E2 protein sequence analysis indicated serine 23 to be highly conserved in most α -HPV (A) and high-risk (HR) HPVs, which are linked to causing cancer (B). The analysis was done by Dr. Renfeng Li.

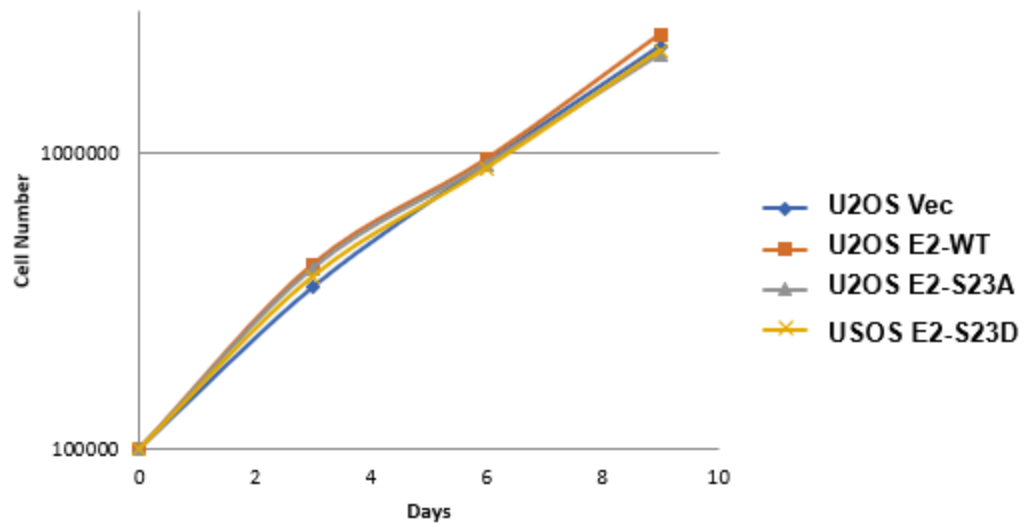


Figure 12. The growth rates of the indicated cell lines. A growth curve was carried out over 9 days and the accumulated number of cells is plotted on a log graph. The standard errors are so low and hence do not show on this log-scale graph. Cell numbers were not statistically significant at any point.

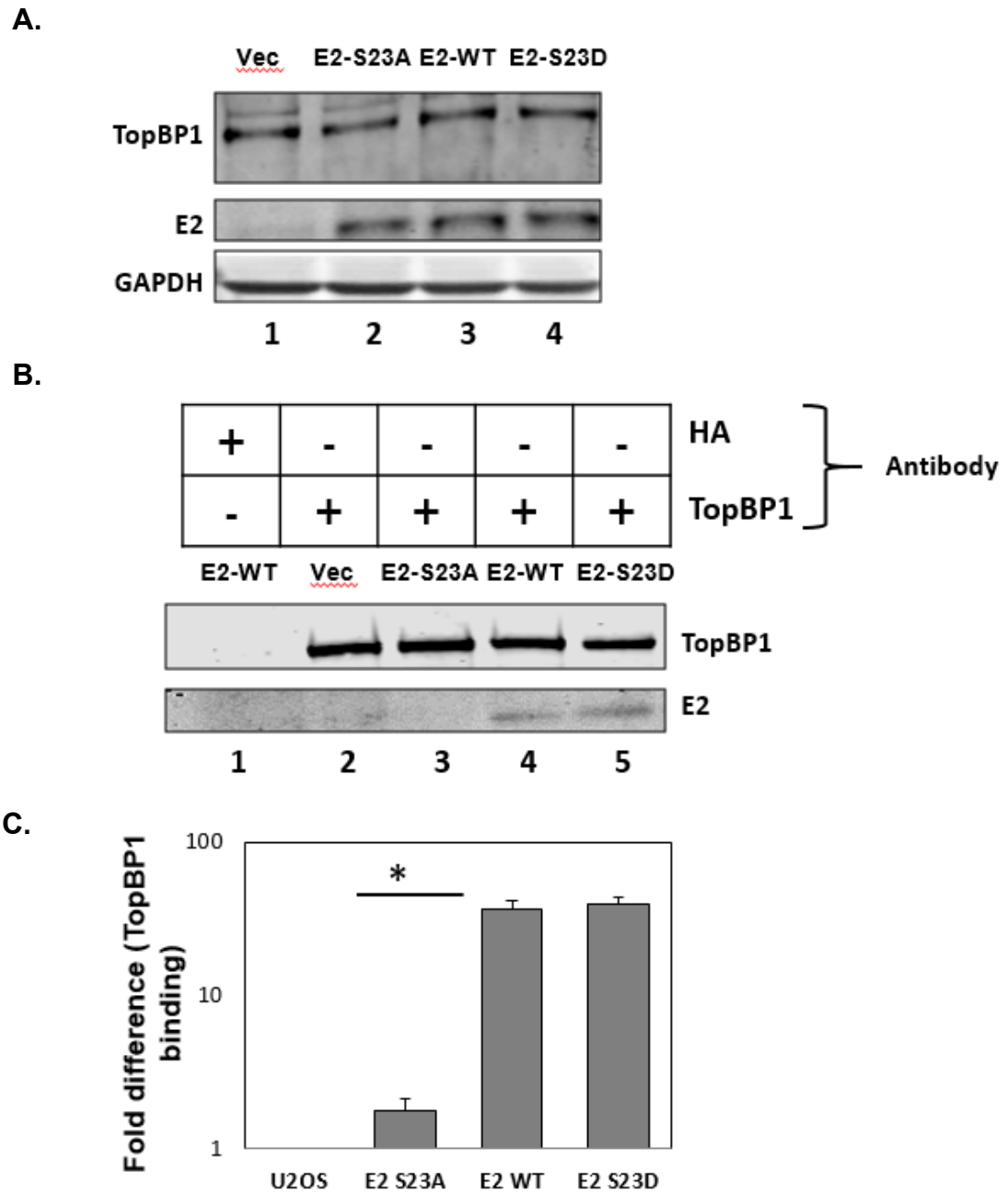


Figure 13. A system to study E2 –TopBP1 interaction. (A) Western blot showing the expression levels of indicated proteins in stable U2OS E2 cells. (B) Protein extracts were immunoprecipitated with HA (control) or TopBP1 antibodies followed by western blotting for TopBP1 or E2. (C) The experiment described for panel (B) was repeated and the results were quantitated. * indicates a significant decrease in E2-S3A interaction with TopBP1 when compared with E2-WT, p-value < 0.05. Significance was determined using a student's *t* test and standard error was calculated from three independent experiments.

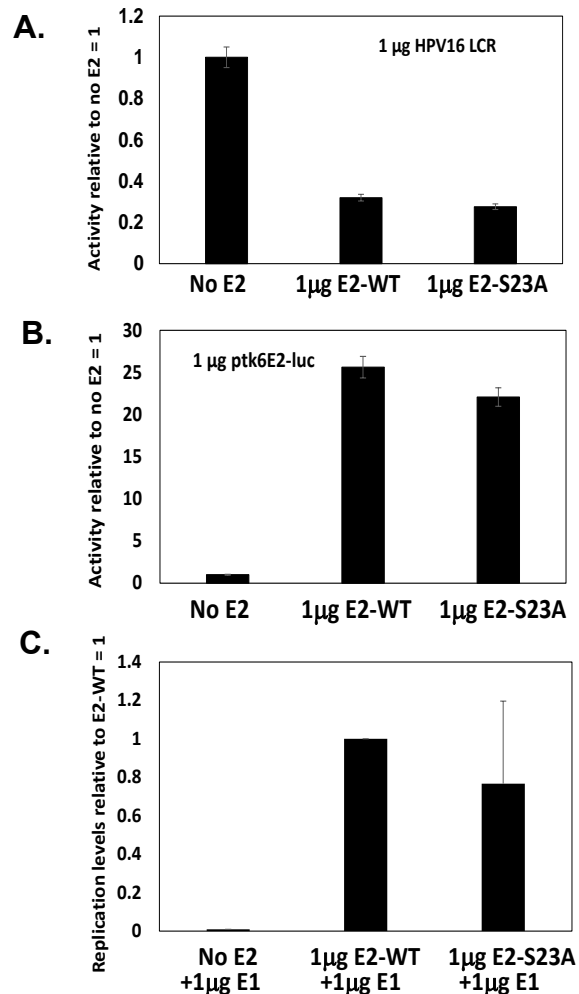


Figure 14. Transcriptional activation/repression and replication properties of E2-WT and E2-S23A. U2OS cells were transiently transfected with the indicated plasmids (no E2 indicates pcDNA-Vec control used to maintain identical DNA concentrations in all samples), and luciferase assays carried out on cell extracts from the transfected cells at day 3 post transfection. The luciferase activity was standardized to protein levels in the cell extract. Difference in activation (**A**) or repression properties (**B**) of E2-WT or E2-S23A, were not statistically significant. (**C**) E1-E2-mediated DNA replication assays were carried out in C33a after transiently transfection with the indicated plasmid. Low-molecular-weight DNA was harvested from the transfected cells after 48 hours and replication levels determined as described (223). There is no replication with E1 alone, E2 and E1 are required for replication in this assay. There was no statistically significant difference between the replication levels of E2-WT or E2-S23A. The figure represents a summary of three independent experiments carried out in duplicate. **Replication assay was performed by Dr. Molly Bristol.**

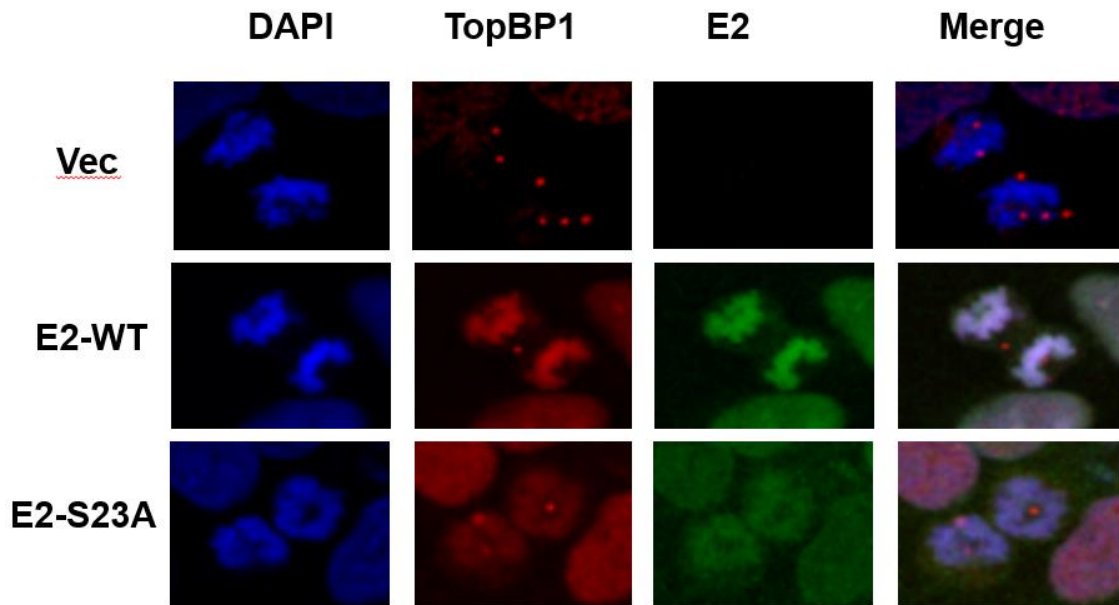


Figure 15. Representative immunofluorescence images depicting the mitotic staining for E2 and TopBP1. Mitotically enriched U2OS pCDNA-Vec (top panels), E2-WT (middle panels) and E2-S23A (bottom panels) were stained with DAPI, E2 and TopBP1. A merge of the two antibodies with DAPI staining is shown in the right-hand panels. The experiment was repeated multiple times and a similar phenotype was observed.

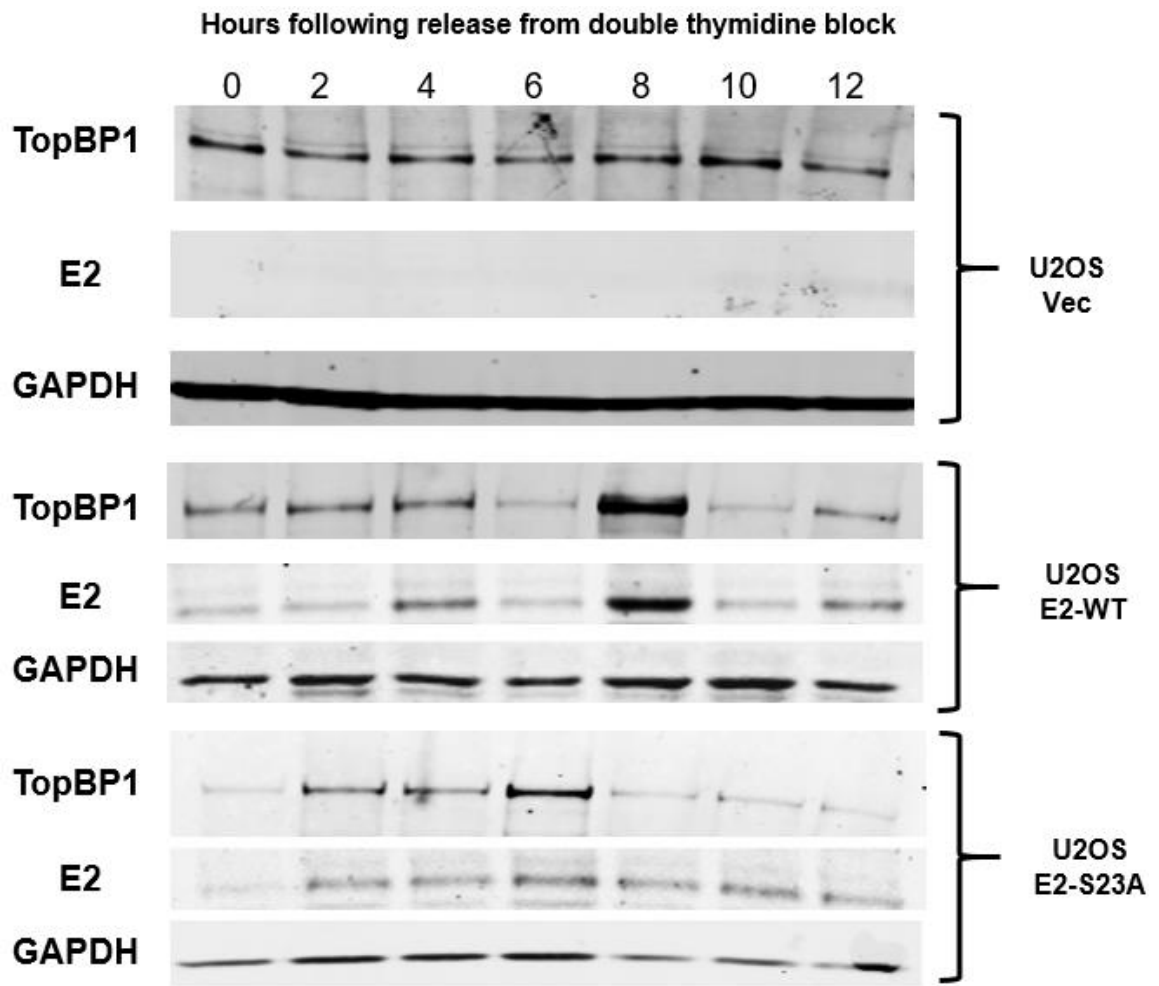


Figure 16. Cell synchronization and western blot analysis on U2OS E2 cell lines. U2OS lines as indicated, were double thymidine blocked to coordinate them in G1. The cells were then released for the time points shown, and protein extracts harvested and western blots carried out.

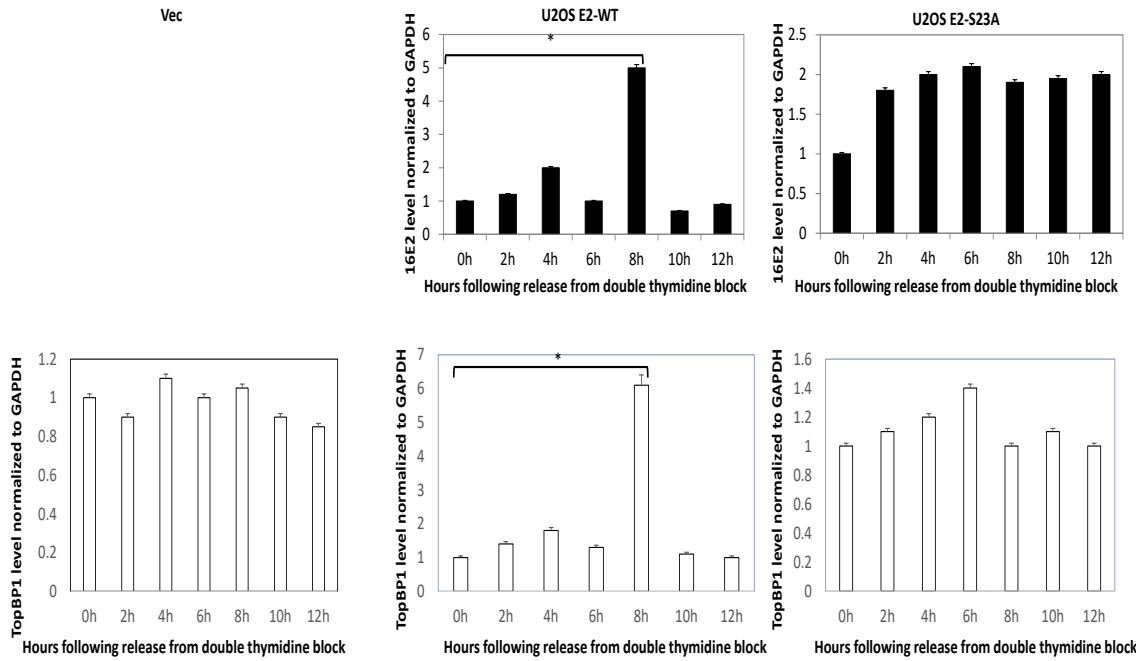


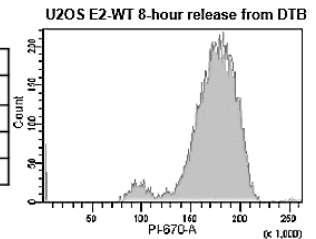
Figure 17. Quantitation of replicate experiments shown in Figure 16. The top panels show the levels of E2 relative to GAPDH at various times following release from double thymidine block, while the bottom panels show the levels of TopBP1 relative to GAPDH following release. * indicates a significant difference in protein levels between the 0- and 8-hour time points. Significance was determined using a student's *t* test and standard error was calculated from three independent experiments.

U2OS-Vec

Cell cycle stage	% of cell at different time point						
	0h	2h	4h	6h	8h	10h	12h
G0/G1	89.9	83.9	47.7	9.3	3.8	11.9	16.8
S	4.6	9.7	42.2	19.7	5	5.2	14
G2/M	5.5	6.3	10.1	70.9	91.2	82.8	69.1

U2OS E2-WT

Cell cycle stage	% of cell at different time point						
	0h	2h	4h	6h	8h	10h	12h
G0/G1	86.2	78.6	38.7	4.1	6.7	9.8	29
S	6.1	10.8	50.7	17.6	7.9	4.3	4.3
G2/M	4.1	10.6	10.3	78.2	88.1	85.6	66.5



U2OS E2-S23A

Cell cycle stage	% of cell at different time point						
	0h	2h	4h	6h	8h	10h	12h
G0/G1	89.3	87.7	31	8.6	3.5	10.2	28.7
S	4.5	6.3	60.5	14.3	11.3	7.4	5.2
G2/M	5.7	5.1	8.5	77.1	85.2	82.4	66.1

Figure 18. Flow cytometry data for U2OS pCDNA-Vec, E2-WT and E2-S23A. The cells were double thymidine blocked (DTB) as described in the Materials and Methods. Following release from the DTB, cells were harvested for flow cytometry analysis. Propidium iodide staining and flow cytometry analysis with a FACSaria™ fusion SORP high-speed cell sorter (Becton Dickinson), using FlowJo software, was used for the cell cycle phase analysis. The plot in the middle panel is a representation of enrichment for cells in mitosis which was seen in all cell lines, at 8-hour time point.

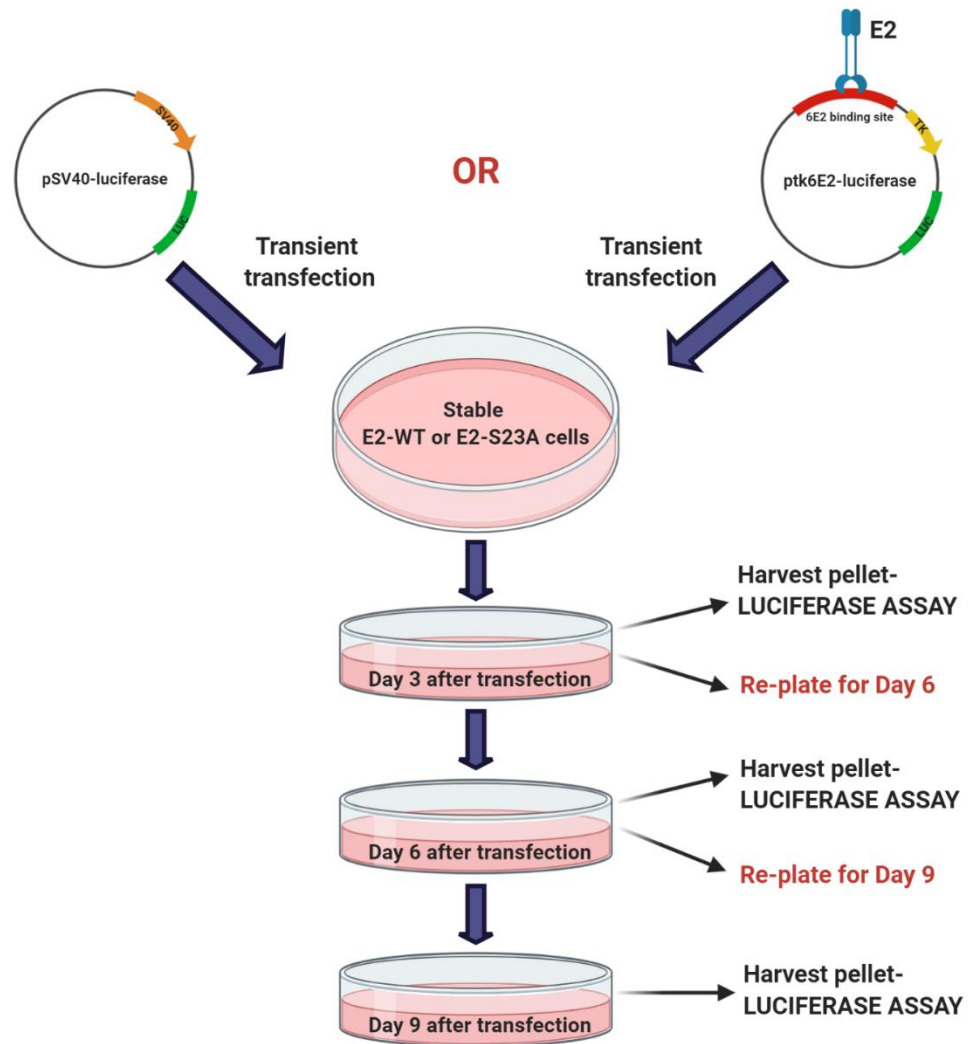


Figure 19. Assay to study plasmid retention. Summary of our novel plasmid retention assay, see section 2.7 for details.

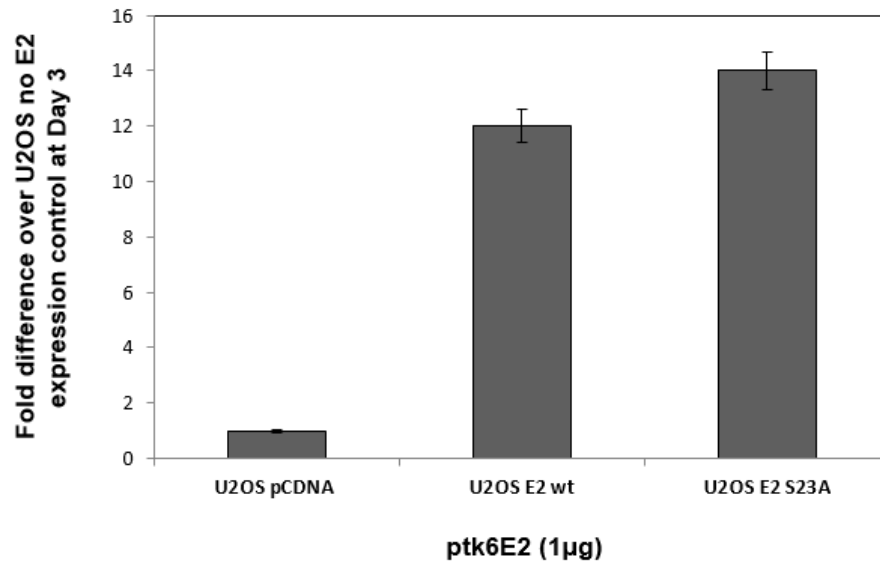


Figure 20. Quantitation of transcriptional activation by E2-WT and E2-S23A at day 3 of plasmid retention assay. Indicated stable U2OS cells were transiently transfected with 1µg ptk6E2 and the transcriptional activity at day 3 was measured and quantitated based on luciferase expression.

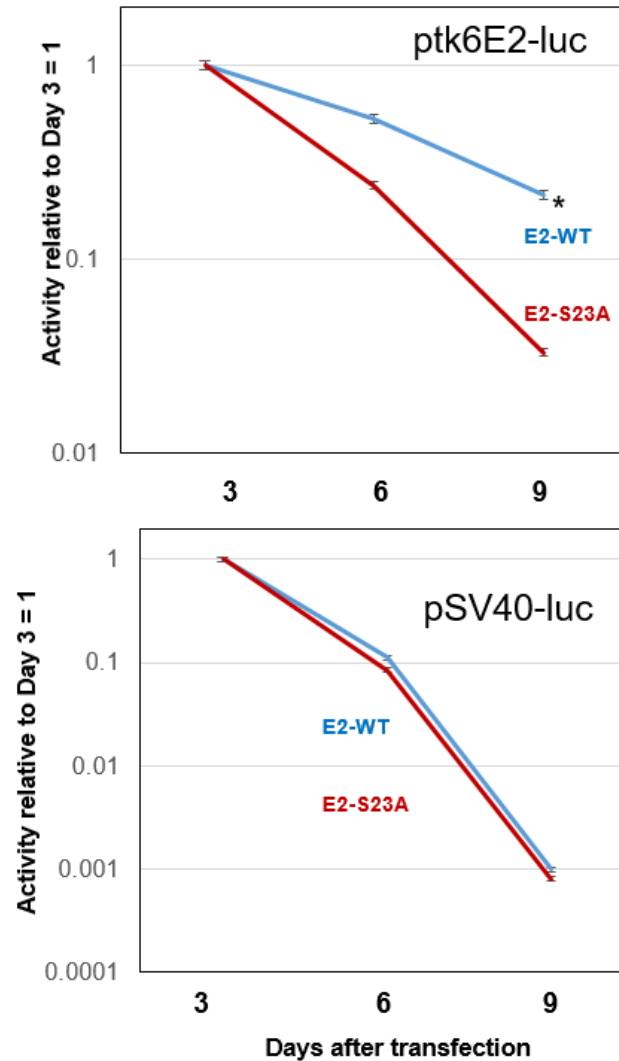


Figure 21. Quantitation of results from plasmid retention assay in U2OS cells. Graph depicting the luciferase expression of ptk6E2-luc (top panel) and of pSV40-luc (bottom panel) in E2-WT and E2-S23A cells. The experiment was repeated three times in duplicate. * indicates a significant difference between the E2-WT and E2-S23A luciferase activity at the day 6 and 9 time points, p-value < 0.05.

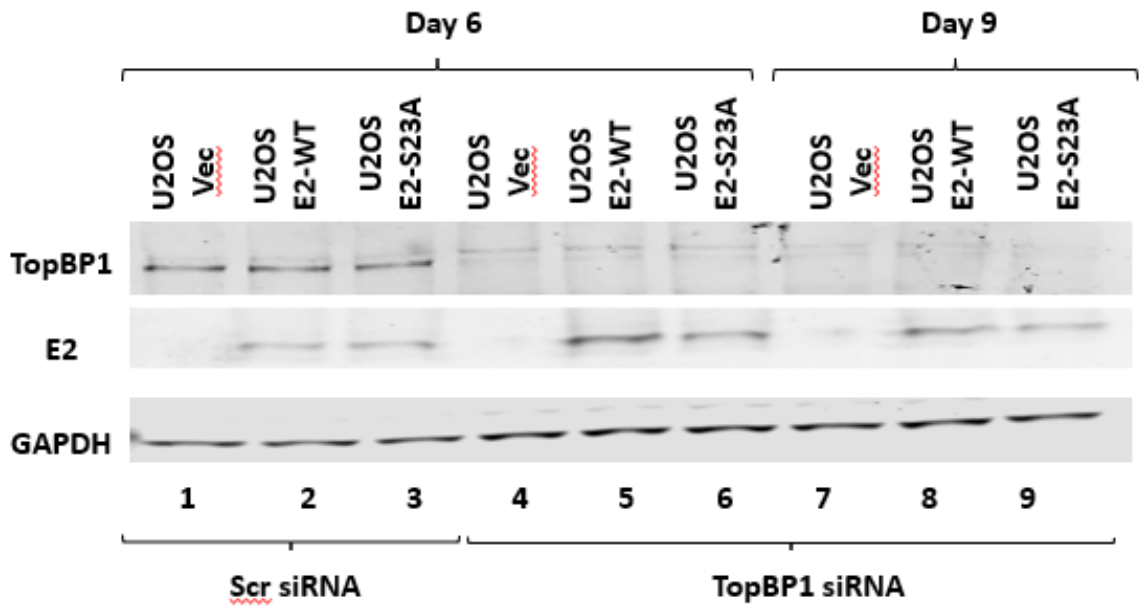


Figure 22. Western blot analysis to confirm siRNA knockdown of TopBP1 throughout the plasmid retention assay. The U2OS cells were treated with the indicated siRNAs. The lysates were probed in western blots using E2, TopBP1 or GAPDH antibodies.

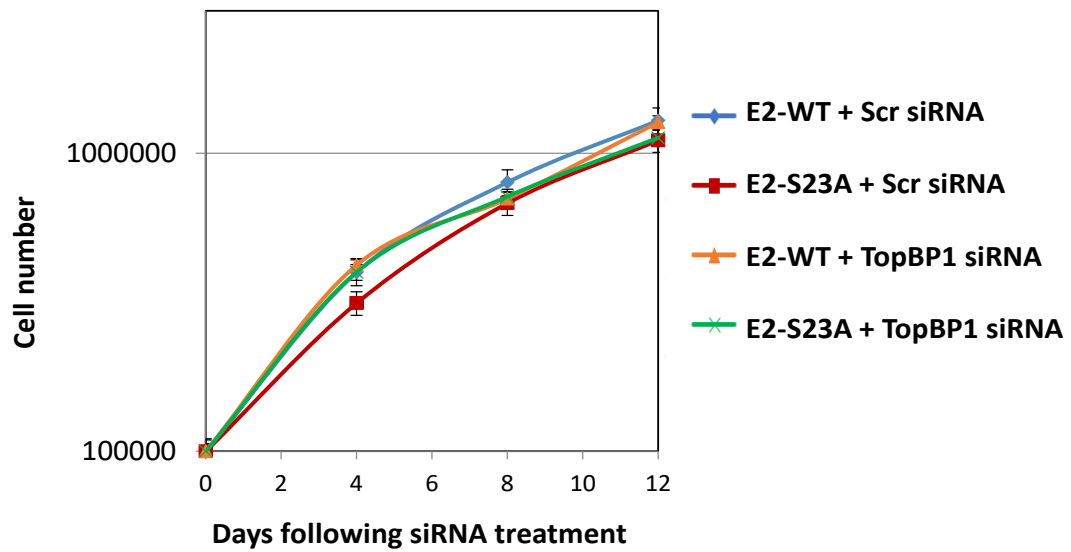


Figure 23. The growth rates of the indicated cell lines following siRNA knockdown of TopBP1. A growth curve was carried out over 12 days after addition of siRNA at day 3 and the accumulated number of cells is plotted on a log graph. Cell numbers were not statistically different at any time point.

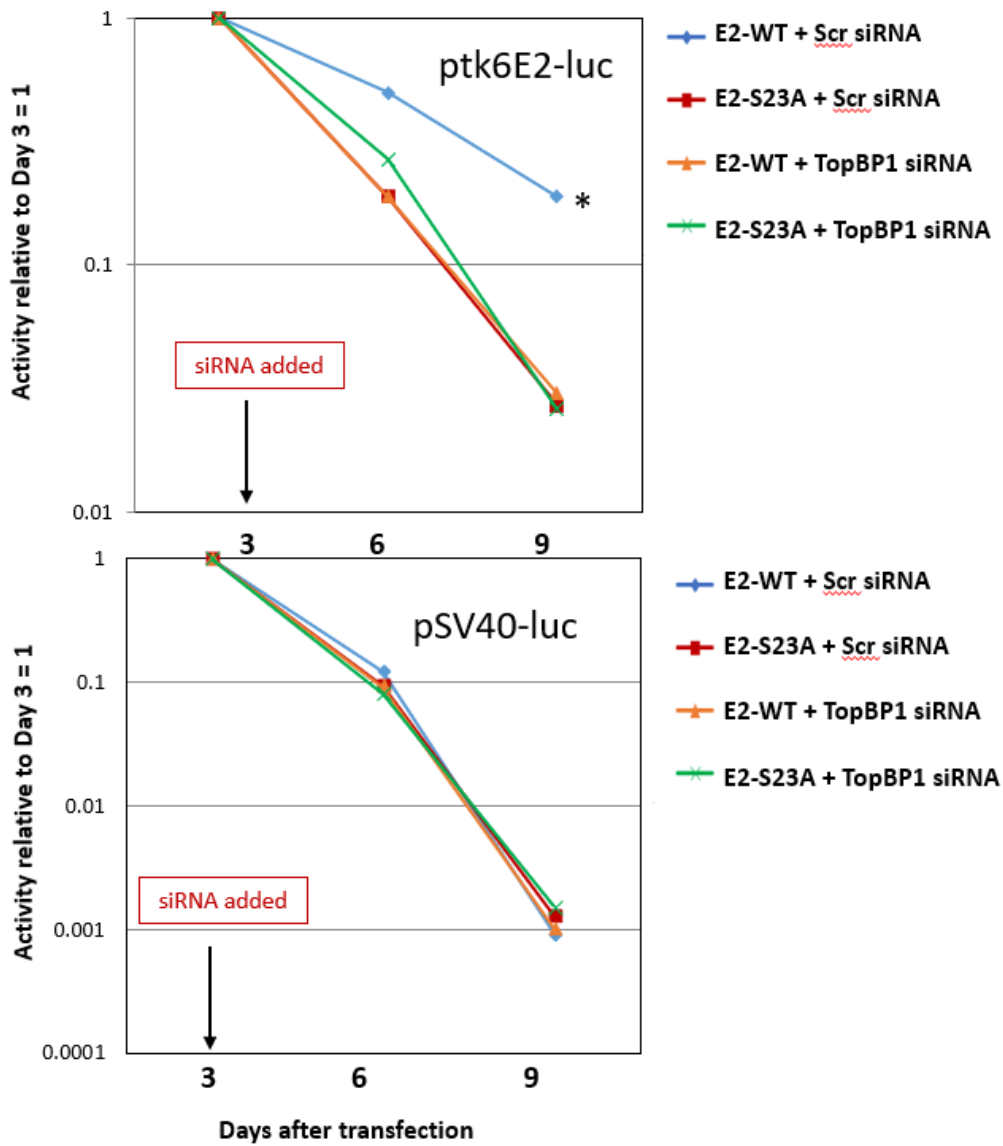


Figure 24. Quantitation of results from plasmid retention assay in U2OS cells followed by siRNA knockdown of TopBP1. This is a summary of three independent experiments carried out in duplicate. * indicates a significant difference in the luciferase activity at the day 6 and 9 time points between the Scr treated E2-WT and other indicated siRNA treated cell lines, p-value < 0.05.

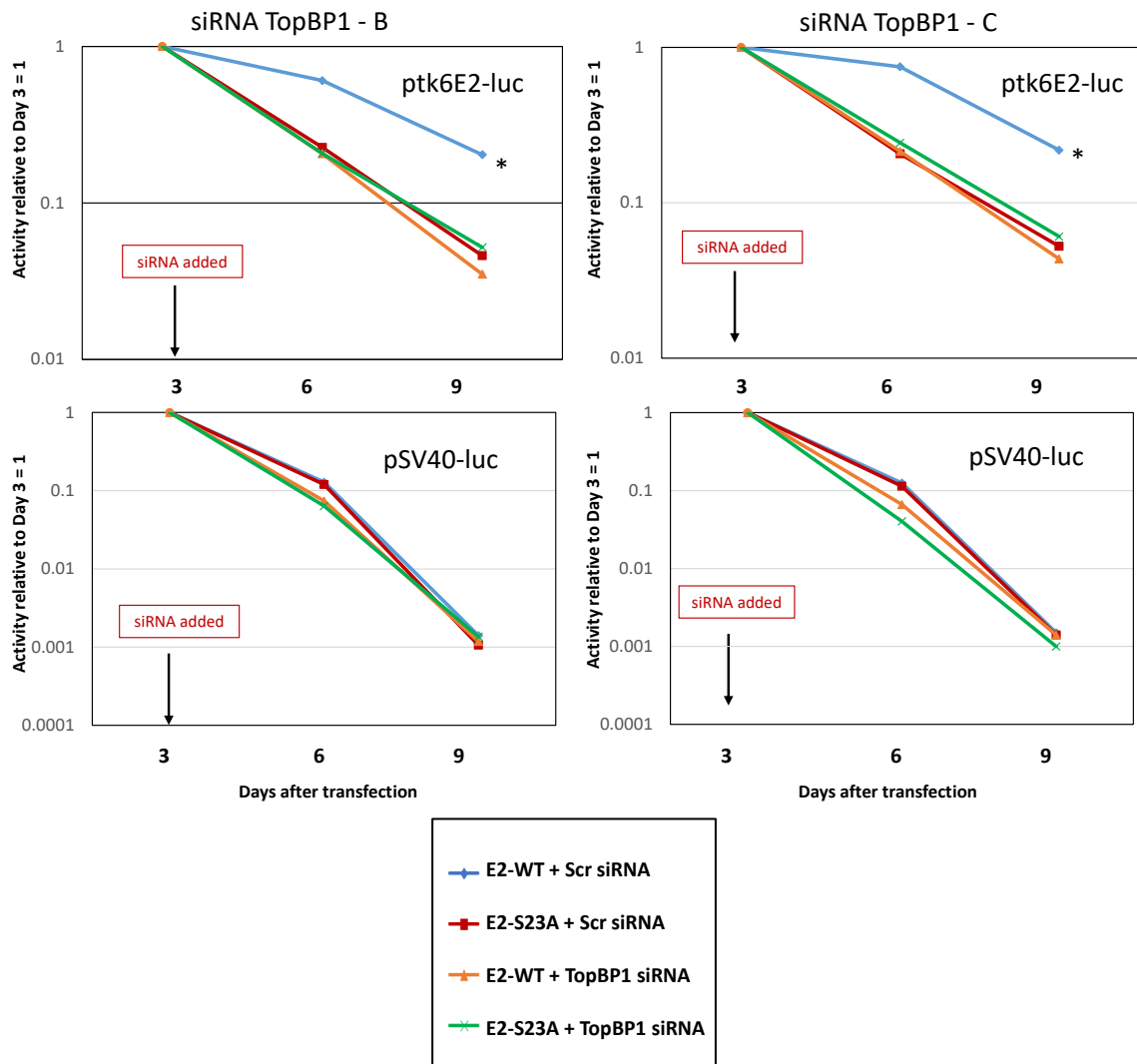


Figure 25. Quantitation of results from plasmid retention assay in U2OS cells followed by knockdown of TopBP1 with two additional siRNA. We repeated our previously described plasmid retention assay with two additional TopBP1 siRNAs. These experiments were carried out once in triplicate. * indicates a significant difference between E2-WT and all other conditions at the day 6 and 9 time points, p-value < 0.05.

3.1 Summary

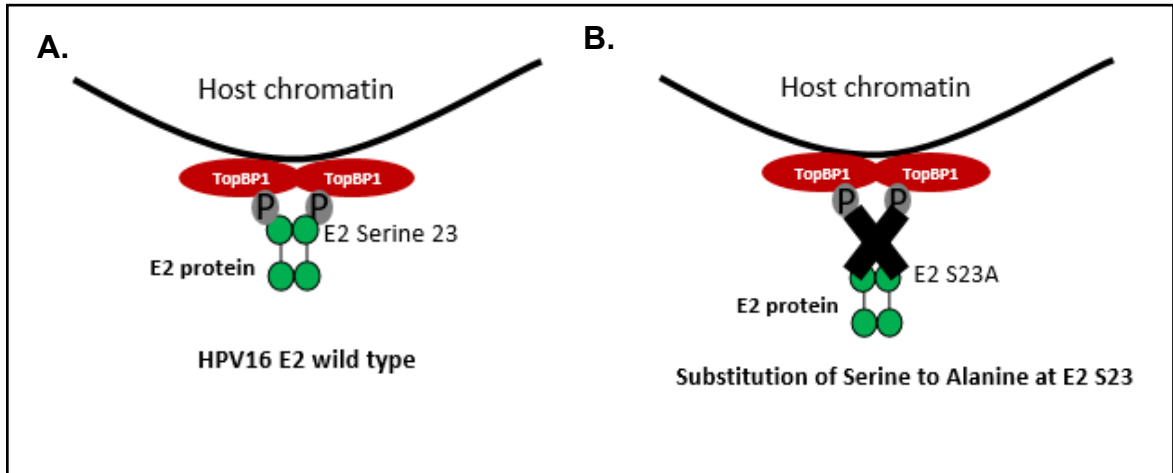


Figure 26. A summary of section 3.1. We developed a system to demonstrate that E2 serine 23 is critical for TopBP1 interaction *in vivo*.

As explained in chapter 1, the E2 viral protein is a central regulator of the HPV lifecycle through its association with other viral and cellular factors. The Morgan lab previously demonstrated an E2-TopBP1 interaction (182) that contributes to E2 replication function and interaction of E2 with interphase chromatin (182-186). In this section, we demonstrate that E2 serine 23 is critical for TopBP1 interaction *in vivo*, that E2-S23A mutation abolished the interaction between E2 and TopBP1 and that S23D maintained this interaction. We further explored the effect of mutating this serine 23 on E2 functions. The mutant E2-S23A activates and represses transcription similarly to E2-WT. Further, E2-S23A and E2-WT cells have identical replication as shown by transient replication assay. On the other hand, E2-S23A has compromised interaction with mitotic chromatin when compared with E2-WT. Both E2 and TopBP1 levels increase during mitosis in E2-WT

cells, which was not observed in E2-S23A cells. Using our novel plasmid retention assay, we demonstrated that E2-S23A is deficient in plasmid retention when compared with E2-WT. siRNA targeted knockdown of TopBP1 abolishes E2-WT plasmid retention function. Our next aim was to demonstrate if phosphorylation of S23 promotes the formation of the E2-TopBP1 complex.

3.2 CK2 phosphorylation of E2 promotes interaction with TopBP1 *in vitro* and *in vivo*.

The data in section 3.1 suggest that phosphorylation of E2 on S23 promotes the interaction with TopBP1 as the E2-S23D mutant (the acidic charge on aspartic acid, D mimicking phosphorylation) binds to TopBP1 while S23A does not. Hence, we investigated if CK2 mediates this phosphorylation. Casein Kinase 2 (CK2) is a ubiquitous kinase. The enzyme exists as a tetramer composed of two catalytic α -subunits (α , α') and two β regulatory subunits. CK2 has been implicated in a lot of cellular processes such as cell cycle control, cell proliferation, cell growth and survival, promoting angiogenesis, and is involved in DNA repair (224). Additionally, CK2 is active during mitosis (225), CK2 can interact with E2 (226), and CK2 phosphorylation promotes interaction of several other proteins with TopBP1 (226-229). Thus, we investigated whether CK2 phosphorylation on E2 S23 promotes complex formation with TopBP1.

3.2.1 Recombinant E2-S23D forms a direct complex with TopBP1, *in vitro*.

Recombinant GST-TopBP1 (full-length), His-E2-WT and His-E2-S23D (amino acids 1-200 for both E2 proteins) were purified from *E. coli* (Figure 27). These proteins were incubated together, and a GST pull-down experiment performed, followed by western blotting (Figure 28A). Lanes 5 and 6 in Figure 28A demonstrate equal levels of E2-S23D and E2-WT input used in the experiment. An interaction between E2-S23D and GST-TopBP1 is seen in lane 1, while it is evident in lane 2 that E2-WT does not interact with TopBP1. Neither protein interacts with the GST-NEDD4 control protein. This experiment was repeated and the results were quantitated (Figure 28B).

3.2.2 CK2 mediates the interaction between recombinant E2-WT and TopBP1, *in vitro*.

Next, to determine whether CK2 phosphorylation of E2-WT can promote interaction with TopBP1, we incubated the recombinant proteins with CK2 enzyme prior to GST pull-down (Figure 29A). In the presence of an enzymatically active CK2, there is an interaction between E2-WT and TopBP1 (lane 1, Figure 29A). By excluding the CK2 co-factors (MgCl₂/ATP) (lane 2) or CK2 enzyme (lane 3, Figure 29A), this interaction is eliminated. CK2 did not promote interaction with the GST-NEDD4 control protein (lanes 5-7, Figure 29A). This experiment was repeated and the results quantitated (Figure 29B).

To confirm whether CK2 phosphorylation promotes the interaction between E2-WT and TopBP1, we repeated the experiment as described in Figure 29, additionally in the presence of lambda phosphatase which eliminated the interaction between E2 and TopBP1 (lane 2, Figure 30A). This experiment was repeated and the results quantitated (Figure 30B). This strongly suggests that phosphorylation of E2-WT by CK2 promotes complex formation with TopBP1 *in vitro*.

3.2.3 CK2 promotes interaction with TopBP1 *in vivo*.

To demonstrate if the knockdown of CK2 components, CK2 α or α' disrupted the E2-TopBP1 interaction *in vivo*, we carried out TopBP1 co-IPs following CK2 α or α' siRNA knockdown. Figure 31A demonstrates a successful knockdown of CK2 α and a reduction in the interaction of E2-WT with TopBP1 in these cells (Lane 2, Figure 31B). The HA control antibody IP does not immunoprecipitate TopBP1 or E2 (Lane 1 and 4, Figure 31B). We also observe higher E2 protein in the absence of CK2 α (lane 2, Figure 31A) and this

was seen repeatedly, making the reduction in E2-TopBP1 complex formation more significant. These experiments were reproduced at least three times and quantitation of the E2 co-IP with TopBP1 demonstrates a significant reduction of complex formation after CK2 α siRNA knockdown (Figure 32). Knockdown of only one CK2 subunit would not negate the CK2 function completely, as there could be an impact from the CK2 α' subunit. For this, we repeated the same experiment as above after CK2 α' knockdown and observe the same phenotype as above (Figure 33 and 34).

The E2-S23D interaction with TopBP1 was not affected by CK2 knockdown. Further, knock down of CK2 α (Figure 31) or CK2 α' (Figure 33) did not affect the protein levels of E2-S23D, as we see with E2-WT. The results from independent experiments were quantitated (Figure 32 and 34).

3.2.4 siRNA knock down of CK2 diminishes E2-WT retention of ptk6E2 plasmid.

Next, we investigated the ability of CK2 knock down to disrupt E2-WT plasmid retention function using our novel assay (Figure 35). We see a sharp reduction in retention of luciferase activity (day 6), but at day 9 there is only a partial loss of activity when compared with the E2-S23A mutant activity. This is probably due to a compensatory mechanism to restore CK2 activity in cells by the other CK2 component when one of them is knockdown. We also confirmed the knock down of CK2 α or α' by western blot with the lysate we used for our retention assay, which remained reduced till day 9 of the assay. (Figure 36). Knock out of both CK2 α and α' component was not successful as the cells were not able to grow out.

3.2.5 CK2 phosphorylates E2 on serine 23 *in vivo*, and CK2 inhibitors disrupt the E2-TopBP1 complex.

A rabbit antibody specific for phosphorylated serine 23 (pS23-Ab) was generated using a phospho-peptide with the region around S23, wherein the serine is phosphorylated (CKILTHYENDS^PTDLR). We used this antibody to investigate if E2 S23 is phosphorylated *in vivo* by CK2. To meet this objective, we knocked down CK2 components using siRNA as shown in Figure 37. CK2 α and α' expression was down-regulated, individually (lanes 2 and 3, respectively Figure 37) and combined (lane 4, Figure 37), following the siRNA knockdown in U2OS pCDNA-Vec and E2-WT. A non-specific scrambled control siRNA (Scr) was used as a control for siRNA treatment (lanes 1 and 5 respectively Figure 37). We observed a partial knockdown of CK2 α and α' , after co-knock down of both CK2 α components which might be a compensatory mechanism the cells use for their continued survival. Immunoprecipitation with pS23-Ab in the U2OS pCDNA-Vec and E2-WT after siRNA knockdown, there was loss of detectable E2 co-immunoprecipitation (co-IP) with the pS23-Ab (lanes 2-4, lower panel Figure 37), whereas in the Scr treated U2OS E2-WT cells, we see a clear co-IP of E2 (lane 5, lower panel Figure 37).

Subsequently, we used a CK2 inhibitor, CX4945 which is currently a drug used in clinical trials for a number of human cancers (230). Following treatment with CX4945 in U2OS E2-WT, the interaction between E2 and TopBP1 was disrupted, and pS23-Ab failed to co-IP E2 (lanes 3-4, Figure 38).

3.2.6 E2 is phosphorylated on serine 23 during mitosis.

Figure 39 reveals that in mitotically enriched U2OS E2-WT and E2-S23A cells, pS23-Ab antibody recognizes E2-WT, but not E2 S23A, both in mitotic and interphase cells. In the E2-WT mitotic and interphase cells following pS23-Ab staining, we observed a strong signal. Whereas with E2-S23A cells, a very marginal signal in mitotic cells and no visible staining in interphase cells is seen after pS23-Ab staining (see arrow pointed, Figure 39). We previously confirmed that the E2-S23A protein is detectable after staining with a non-phospho specific E2 antibody in our immunofluorescence result (Figure 15) and that there is comparable expression of E2-WT and E2-S23A in U2OS cells (Figure 15).

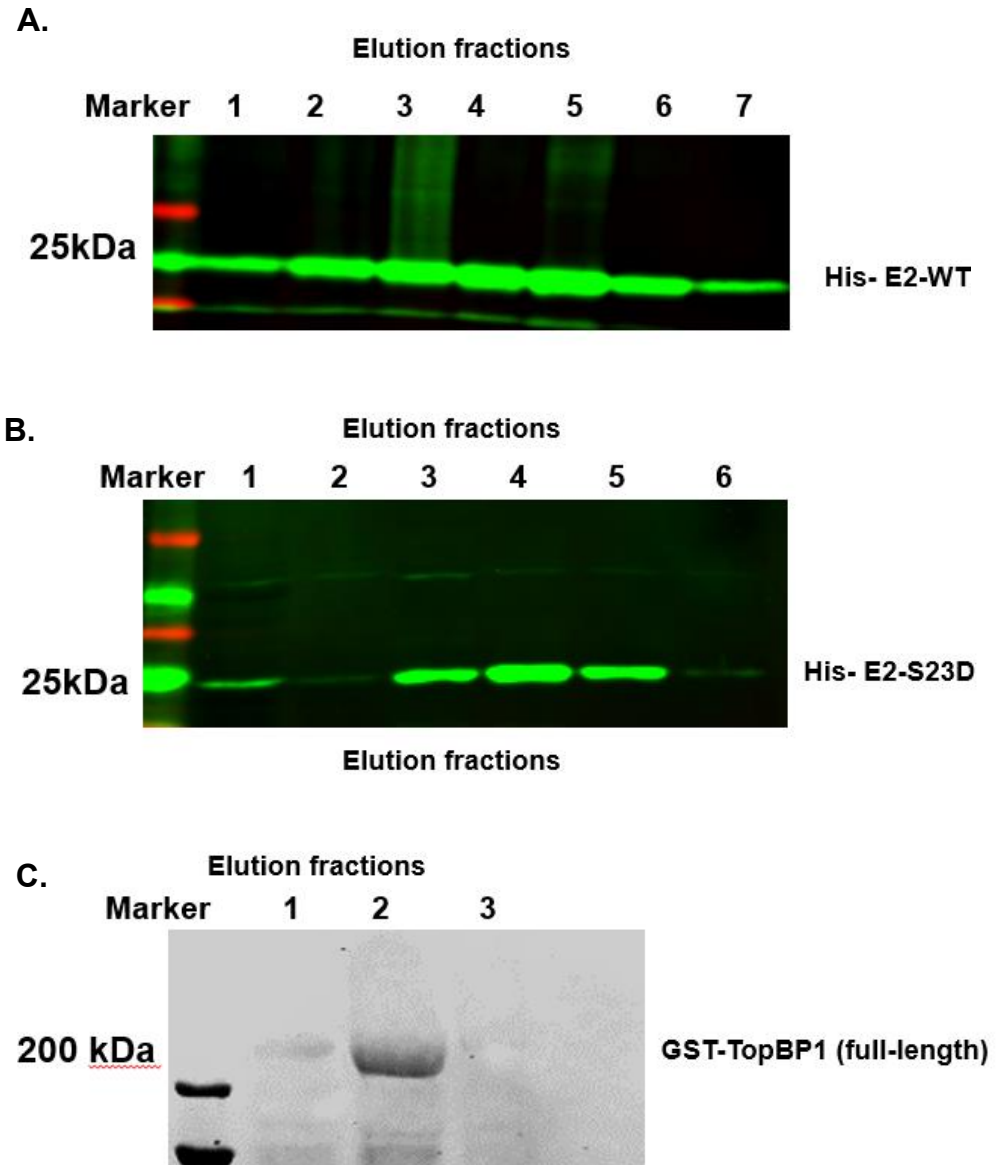


Figure 27. Western blot analysis to confirm and demonstrate purity of recombinant proteins. (A) and (B) Recombinant His-E2-WT and His-E2-S23D (amino acids 1-200 for both E2 proteins) was purified as explained in section 2.9, on a Ni-NTA agarose followed by size-exclusion chromatography. The expression of respective proteins was confirmed by western blot analysis (Green fluorescent bands). (C) Recombinant TopBP1 was produced as a fused protein with a GST-tag (GST TopBP1 (aa 32- 1522) His and purified on Glutathione Sepharose™ 4B as explained in section. The expression of respective proteins was confirmed by western blot analysis.

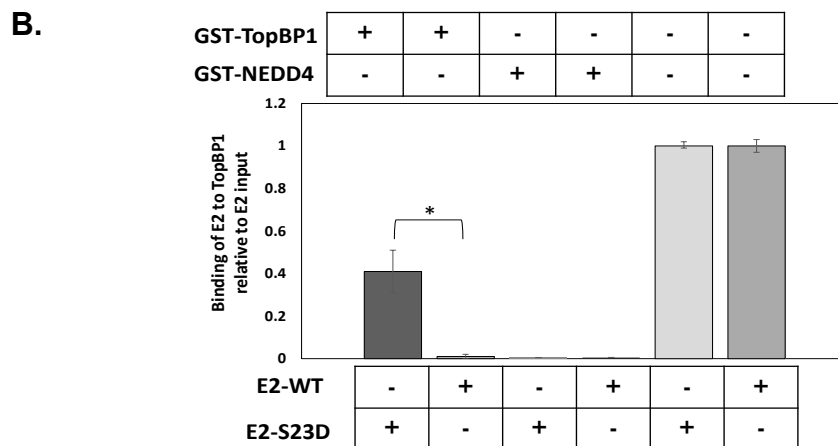
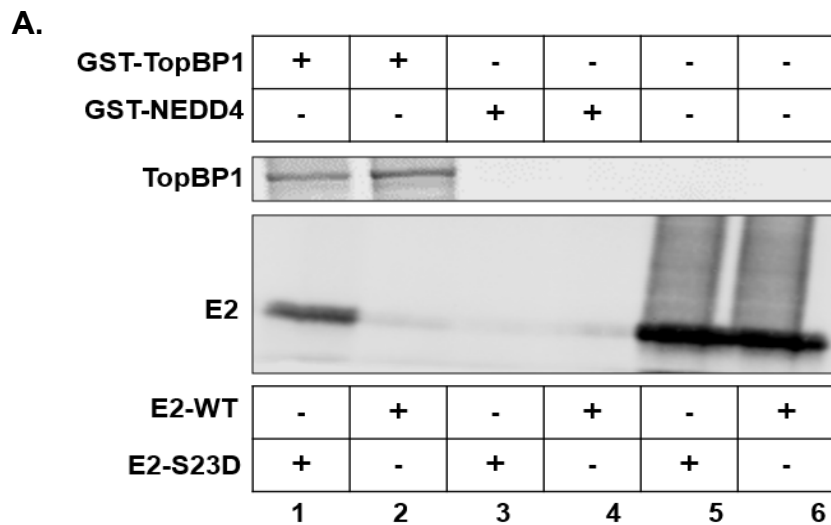


Figure 28. GST pull-down assay followed by western blot analysis using recombinant proteins. (A) 11 pmol of E2 was incubated with 0.65 pmol of GST-TopBP1 or GST-NEDD4 at 4⁰C for one hour with rotation. GST pull-downs followed by western blotting for TopBP1 (top panel) and E2 (bottom panel) were then carried out. Recombinant E2 proteins only were added as input and the TopBP1 pull down demonstrates equivalent levels of TopBP1 in each condition incubated with TopBP1. (B) Quantitation of repeat experiments. The binding of E2 to TopBP1 is repressed relative to the E2 input protein equaling 1. * indicates a significant difference between the two samples under the bracket, p-value < 0.05. Significance was determined using a student's *t* test and standard error was calculated from three independent experiments.

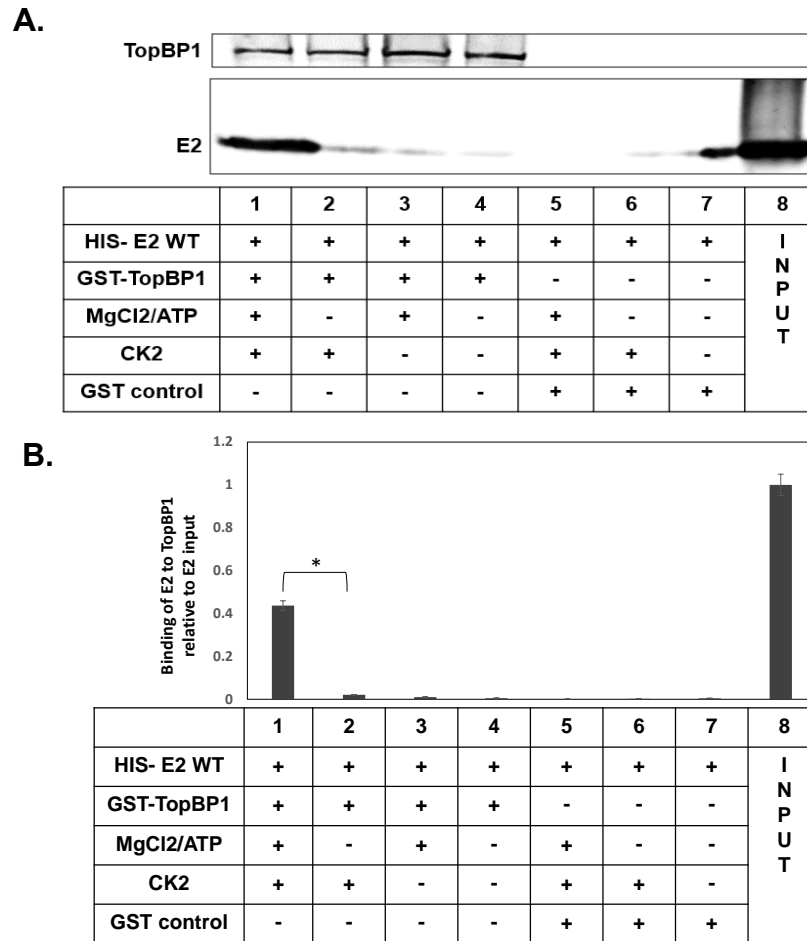


Figure 29. GST pull-down assay followed by western blot analysis using recombinant proteins with CK2 enzyme. (A) The GST pull down was repeated as in Figure 28 following 1 hour at 30°C with CK2 and controls. (B) Quantitation of repeat experiments. The binding of E2 to TopBP1 is expressed relative to the E2 input protein equaling 1. * indicates a significant difference between the two samples under the bracket, p-value < 0.05. Significance was determined using a student's *t* test and standard error was calculated from three independent experiments.

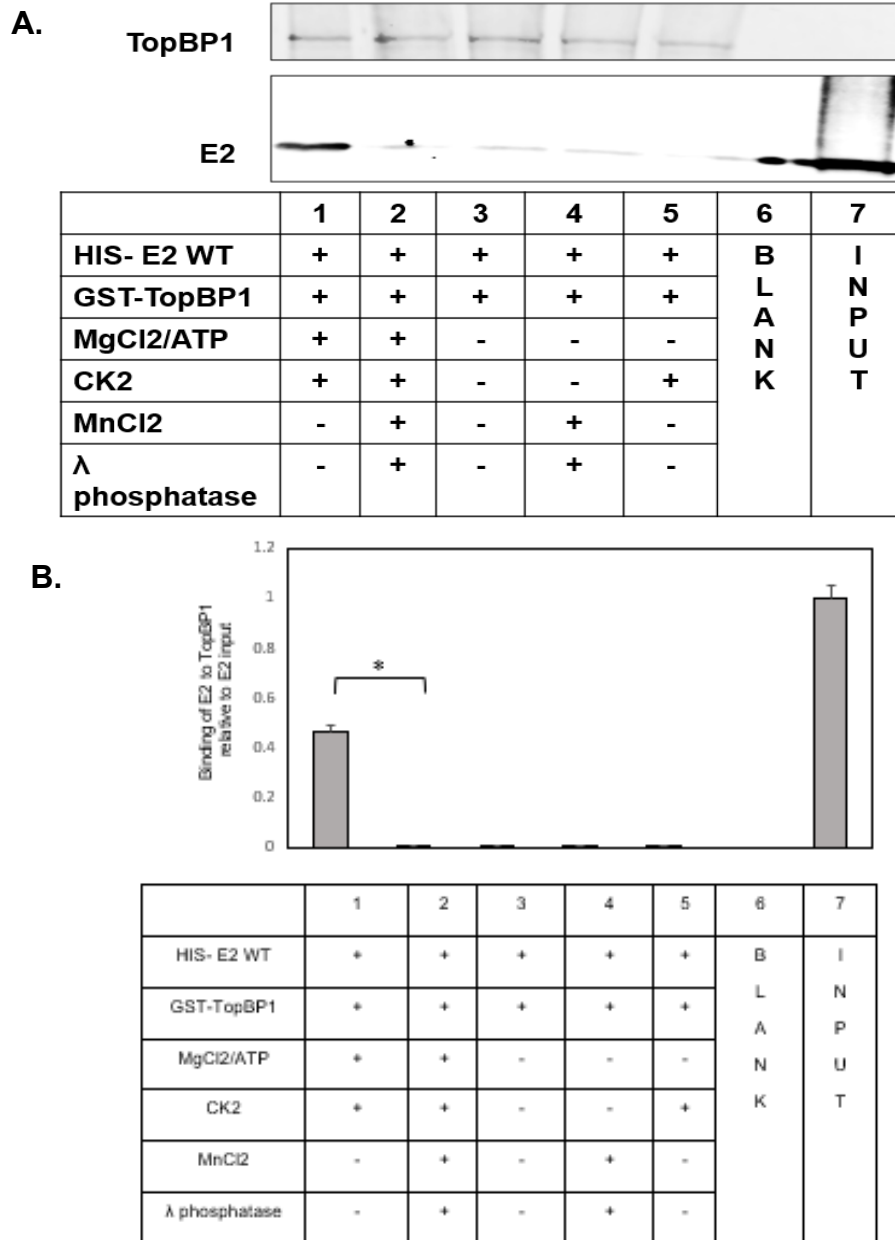


Figure 30. Western blot analysis to demonstrate loss of CK2 mediated E2-WT-TopBP1 interaction in the presence of lambda phosphatase after GST pull-down. (A) Lambda phosphatase was added to the CK2 reaction and GST pull-down assays as mentioned in Figure 28. **(B)** Quantitation of repeat experiments. The binding of E2 to TopBP1 is expressed relative to the E2 input protein equaling 1. * indicates a significant difference between the two samples under the bracket, p-value < 0.05. Significance was determined using a student's *t* test and standard error was calculated from three independent experiments.

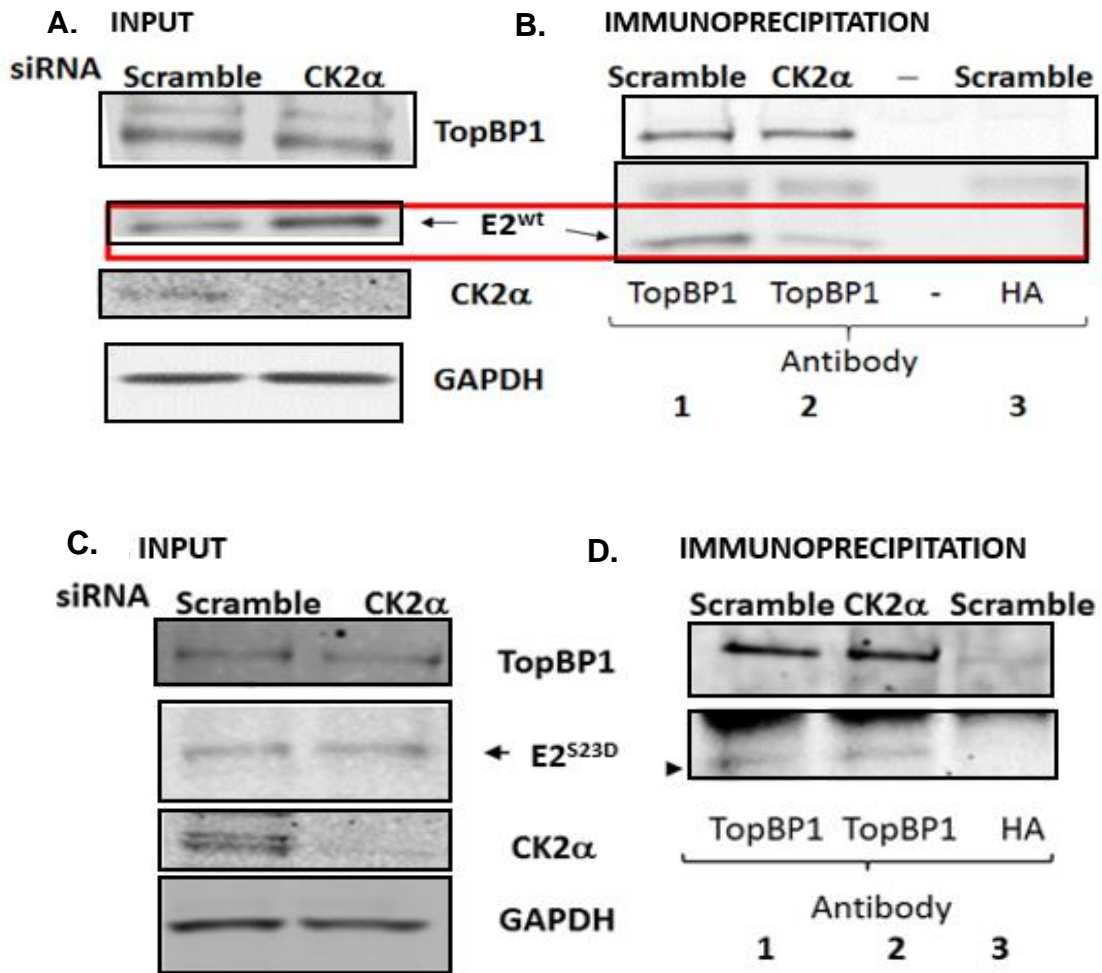


Figure 31. Western blot analysis to demonstrate CK2α knockdown disrupts E2-TopBP1 interaction. Input blots of extracts from indicated siRNA treated U2OS E2-WT cells (A) and E2-S23D cells (B). TopBP1 co-IP of E2-WT (C) and TopBP1 co-IP E2-S23D (D) were carried out following CK2α knockdown.

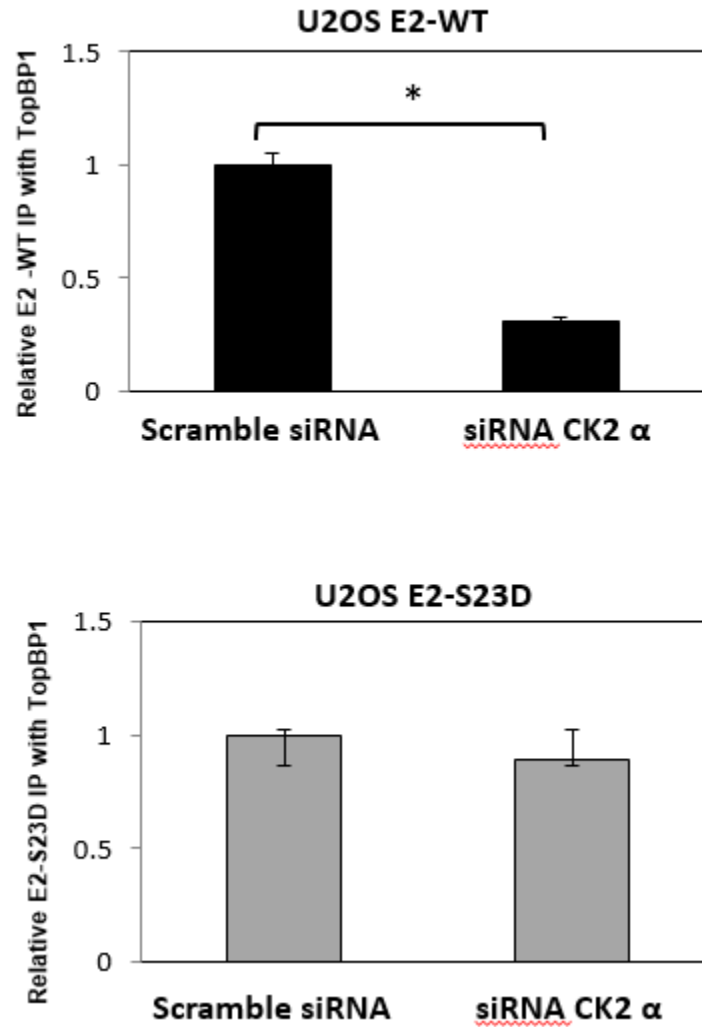


Figure 32. Quantitation of repeat experiments from Figure 31. The co-IPs of E2 with TopBP1 in the presence of Scr and CK2 α siRNA were quantitated relative to the input protein levels. The Scr co-IP levels were set as 1. * indicates a significant difference between the two samples under the bracket, p-value < 0.05. Significance was determined using a student's *t* test and standard error was calculated from three independent experiments.

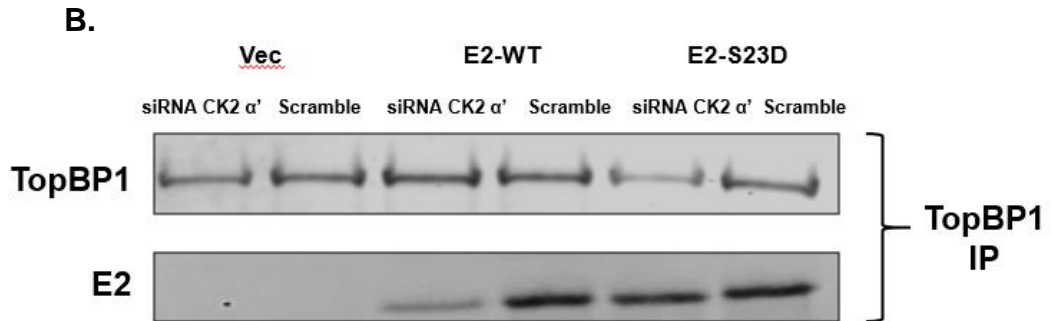
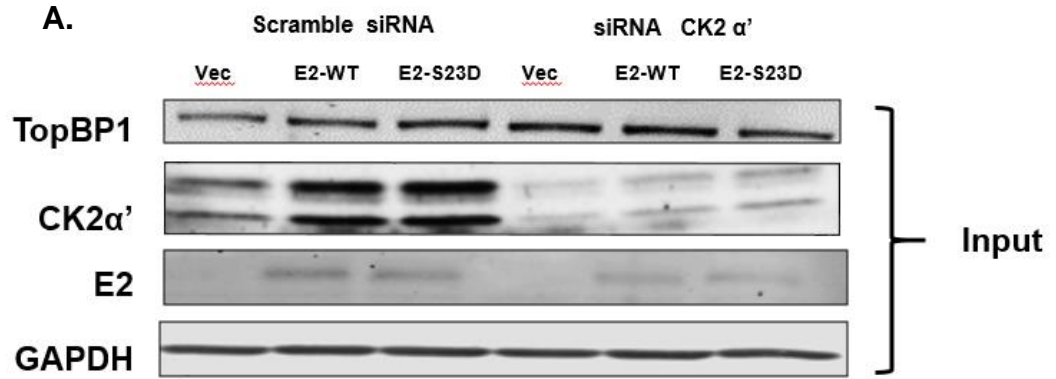


Figure 33. Western blot analysis to demonstrate CK2 α' knockdown disrupts E2-TopBP1 interaction. (A) Input blots of extracts from indicated siRNA-treated U2OS Vec, E2-WT and E2-S23D cells. (B) TopBP1 co-IP of E2-WT or TopBP1 co-IP E2-S23D were carried out following CK2 α' knockdown.

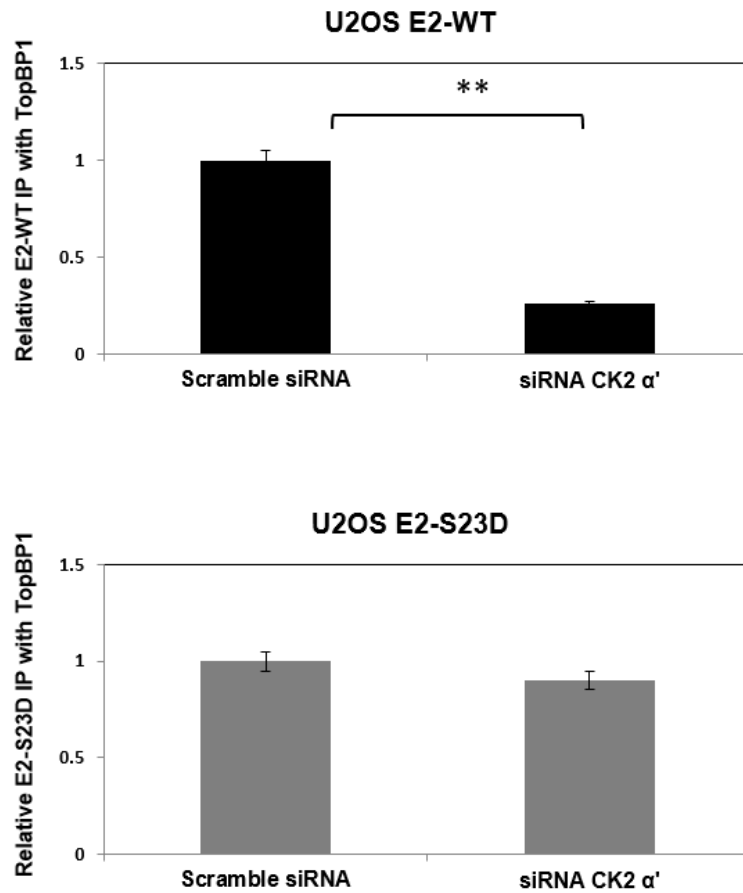


Figure 34. Quantitation of repeat experiments from Figure 33. The co-IPs of E2 with TopBP1 in the presence of Scr and CK2 α' siRNA were quantitated relative to the input protein levels. The Scr co-IP levels were set as 1. * indicates a significant difference between the two samples under the bracket, p-value < 0.05. Significance was determined using a student's *t* test and standard error was calculated from three independent experiments.

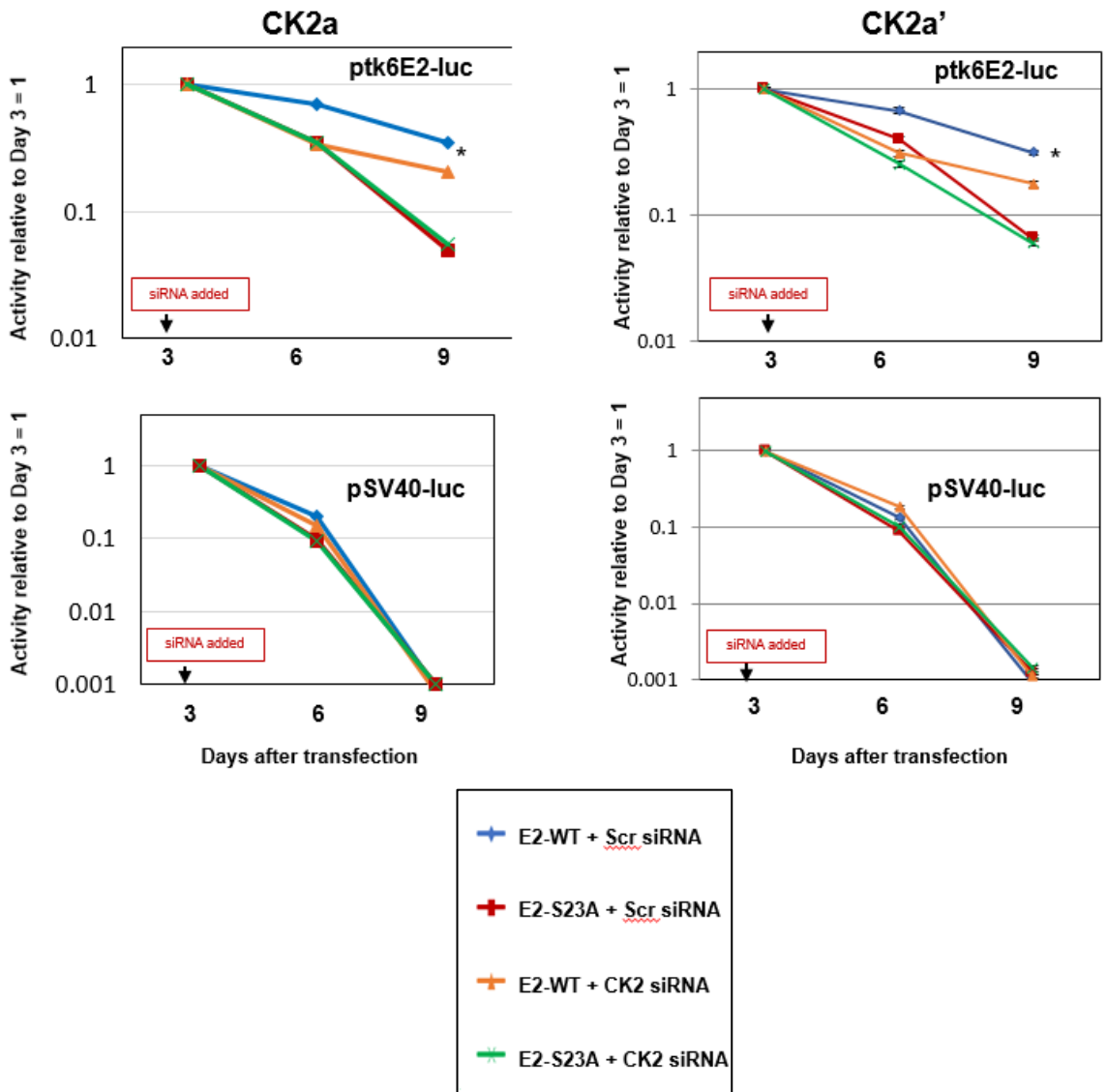


Figure 35. Quantitation of results from plasmid retention assay in U2OS cells followed by siRNA knockdown of CK2 α or CK2 α' . We repeated our previously described plasmid retention assay following the siRNA knockdown of CK2 α or CK2 α' . This is a summary of three independent experiments carried out in duplicate.

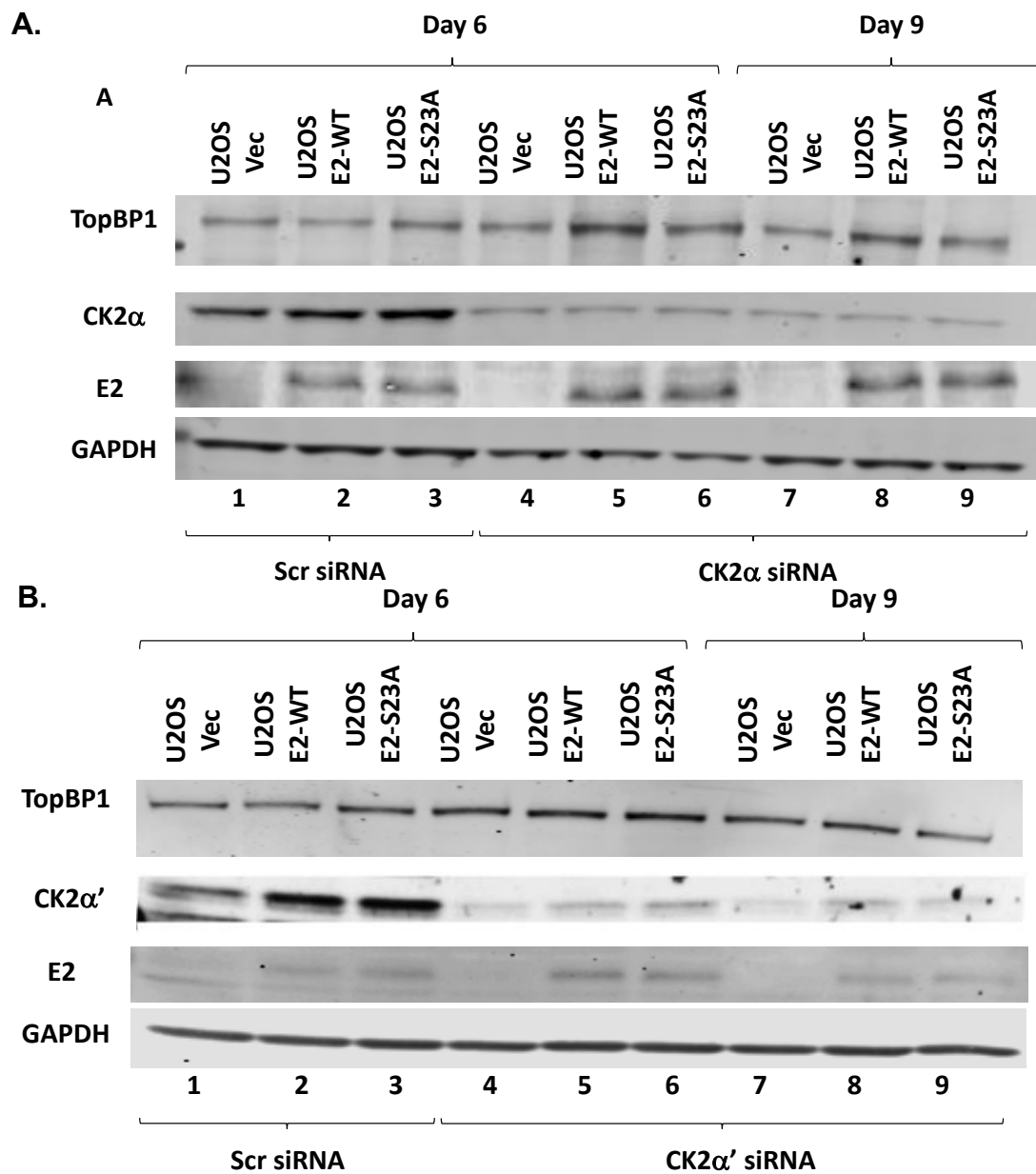


Figure 36. Western blot analysis to confirm siRNA knockdown of CK2α or CK2α' throughout the plasmid retention assay. The indicated U2OS cells were treated with the specified siRNAs and grown over the period indicated.

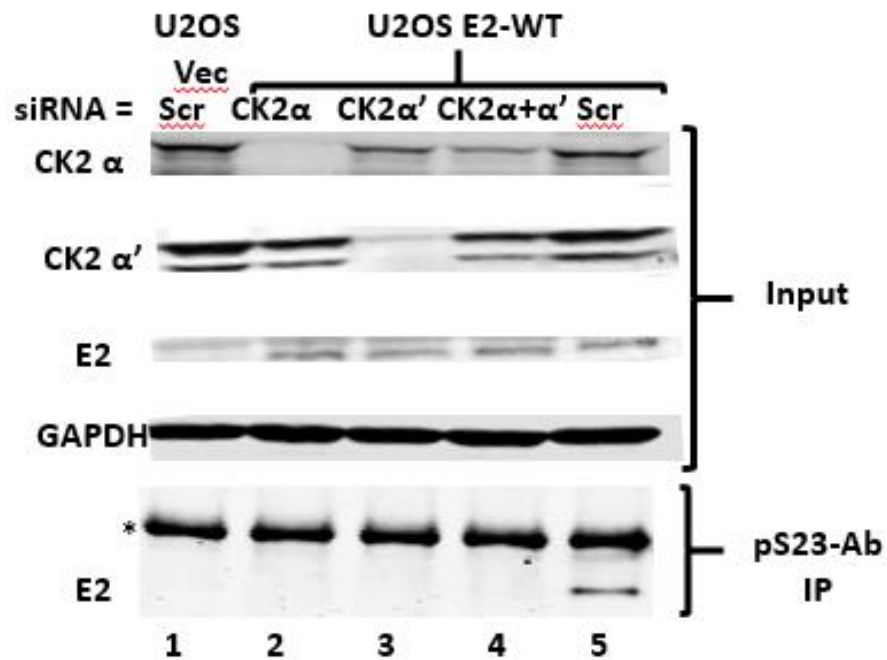


Figure 37. E2 S23 is phosphorylated *in vivo* by CK2. siRNA knockdown of CK2 α and/or CK2 α' , in indicated cell lines was carried out. Scr control siRNA was used in lanes 1 and 5. The top panels demonstrate the input proteins that were used in the immunoprecipitation (IP) with pS23-Ab. Please note the CK2 α blot is independent of the other inputs but the same protein extracts were used. * is an antibody band.

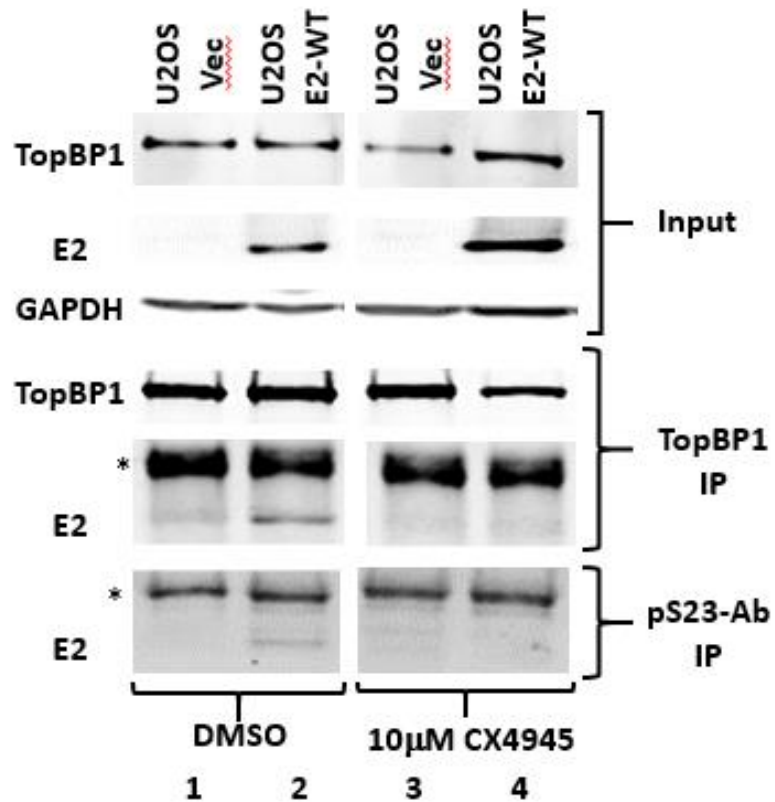


Figure 38. Western blot analysis to demonstrate the effect of CK2 inhibitor on E2-TopBP1 interaction. Cells were treated with DMSO (lanes 1 and 2) or 10uM CX4945 (lanes 3 and 4) for 24 hours and then proteins were harvested. Top panels represent the input levels of E2 and TopBP1, middle panels a TopBP1 co-IP and the bottom panel a pS23-Ab co-IP. Please note a lane removed from these images but they are from the same gel at the same exposure. * is an antibody band.

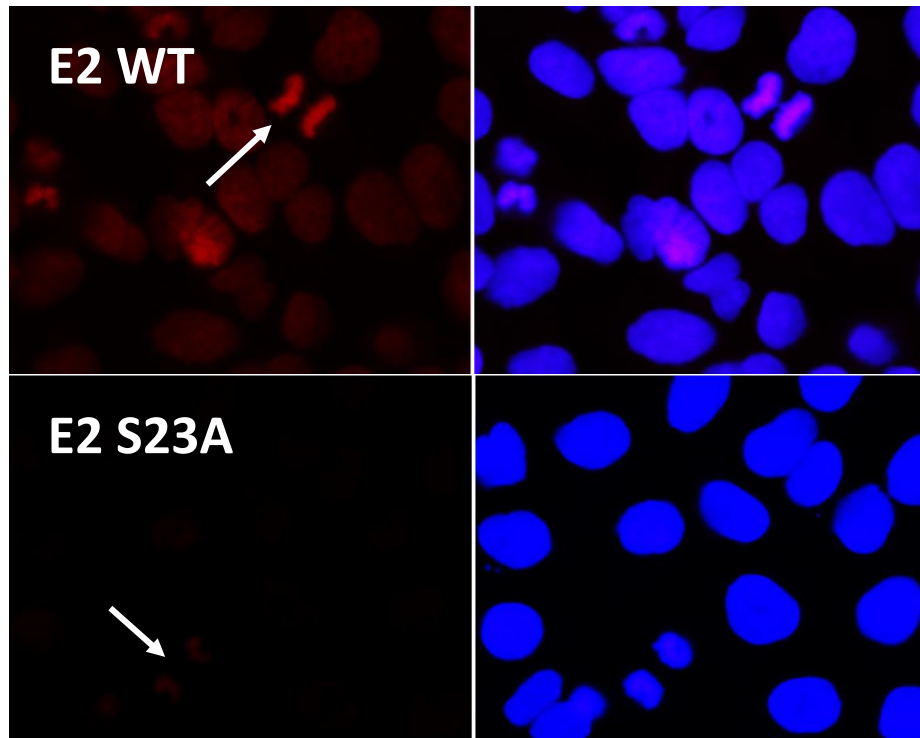


Figure 39. Representative immunofluorescence images of interphase and mitotic cells stained with pS23-Ab. Left hand panels are antibody only, right hand panels are antibody plus DAPI. There was no signal generated with secondary only antibody, and no signal detected in pCDNA-Vec control when the primary antibody was included (not shown).

3.2 Summary

The results in this section demonstrate that CK2 phosphorylation promotes E2 - TopBP1 complex formation *in vivo* and *in vitro* via phosphorylation of serine 23. E2-WT cannot interact with TopBP1 *in vitro*, while E2-S23D can. Incubation of E2-WT with CK2 promoted the interaction between E2 and TopBP1 recombinant proteins, and this was reversed by treatment with lambda phosphatase. Further, by knocking down either α component, or partial knockdown of both, it abolished detectable levels of E2 S23 phosphorylation in U2OS cells and partially disrupted the interaction between E2 and TopBP1. CK2 has two catalytic domains, α and α' . So, knock down of only one CK α subunit would not completely eliminate CK2 function. The role of CK2 phosphorylation of E2 S23 in U2OS cells was further confirmed using a CK2 inhibitor CX4945, which disrupted the E2- TopBP1 interaction and further saw a loss of phosphorylation on the S23 residue, as determined by pS23-Ab co-immunoprecipitation experiment. Additionally, we were able to determine that the pS23-Ab can recognize E2-WT, but not E2-S23A, in mitotic and interphase cells. We also demonstrated that knockdown of CK2 α or α' also compromised the plasmid retention function of E2-WT, further signifying the role CK2 plays in mediating the E2-TopBP1 interaction. Given the many important functions of CK2 at different stages of HPV16 lifecycle, it is an ideal candidate to further investigate the effect of CK2 inhibitors on cancers caused by HPV. We next wanted to expand our aim to further study the role of CK2 phosphorylation of E2 S23 in a more physiological model with the aid of human keratinocytes.

3.3 E2 serine 23 phosphorylation by CK2 is needed for E2-TopBP1 complex formation in human keratinocytes.

In a recently published paper from our lab, it was demonstrated that in N/Tert-1 (TERT immortalized foreskin keratinocytes) cells, E2 can regulate transcription from the host genome that is relevant to the viral lifecycle (231, 232). We used these cells to investigate whether E2 retains plasmid retention function in keratinocytes, and whether CK2 phosphorylates S23.

3.3.1 E2-S23A mutation abolishes TopBP1 interaction and E2 plasmid retention function in N/Tert-1 cells.

Using the N/Tert-1 cells, we generated stable pools of cell lines expressing E2-WT and E2-S23A along with a pcDNA-Vec control. We confirmed the successful establishment of our cell lines by western blot analysis of the cell lysates and Figure 40 A demonstrates the expression of E2-WT and E2-S23A in the N/Tert-1 (lanes 2 and 3, Figure 40A). Co-immunoprecipitation with TopBP1 demonstrates that E2-S23A has a compromised interaction with TopBP1 (compare lane 6 with lane 5, Figure 40B). The experiment was repeated and results quantitated (Figure 40C). We additionally conducted a transient transcription assay using these stable N/Tert-1 cell lines and demonstrated that E2-S23A has similar transcriptional function as E2-WT in these N/Tert-1 cells (not shown).

Next, we carried out our plasmid retention assay in the N/Tert-1 E2-WT and the E2-S23A cells and observed similar results to that in U2OS cells; the E2-S23A mutant has lost the ability to retain the ptk6E2-luc plasmid when compared to E2-WT, and neither retain pSV40-luc (Figure 41).

3.3.2 CK2 phosphorylates E2 on serine 23 *in vivo*, and CK2 inhibitors disrupt the E2-TopBP1 complex in N/Tert-1 cells.

To demonstrate if pS23-Ab recognizes E2-WT in N/Tert-1 cells, we carried out immunoprecipitation with pS23-Ab (Figure 42A). We observed that pS23-Ab pulls down E2-WT (lane 2, Figure 42A) which was lost with the addition of THE CK2 inhibitor, CX4945 (compare lane 5 with lane 2, Figure 42A). In Figure 42B we also observed that CX4945 disrupted the N/Tert-1 E2-WT interaction with TopBP1 (compare lane 6 with lane 3, Figure 42B). TopBP1 pulled-down E2-S23D and CX4945 treatments had no effect on this interaction (compare lane 2 with lane 5, Figure 42B).

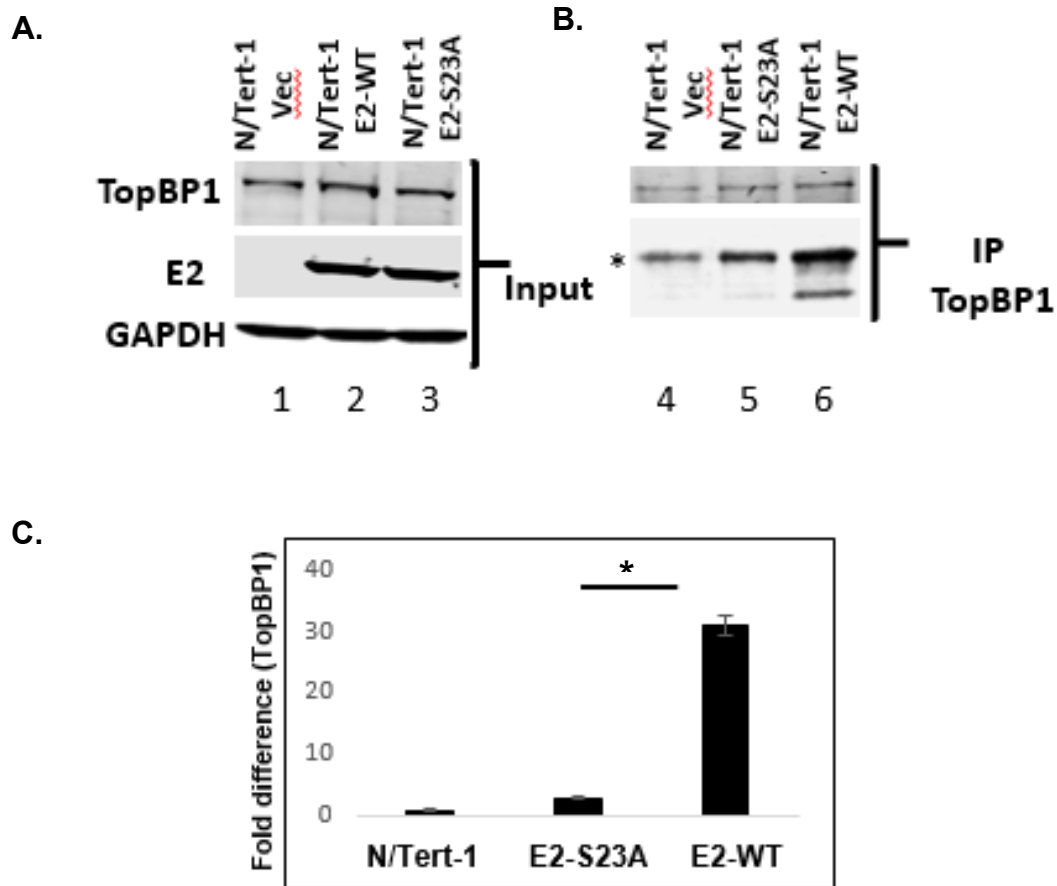


Figure 40. E2–TopBP1 interaction in N/Tert-1. (A) Western blot showing the expression levels of indicated proteins in the stable N/Tert-1 E2 cells. (B) The protein extracts were immunoprecipitated with HA (control) and TopBP1 antibody followed by western blotting for TopBP1 and E2. (C) The experiment described for panel (B) was repeated and the results were quantitated. * indicates a significant decrease in E2-S3A interaction with TopBP1 when compared with E2-WT, p -value < 0.05 . Significance was determined using a student's t test and standard error was calculated from three independent experiments.

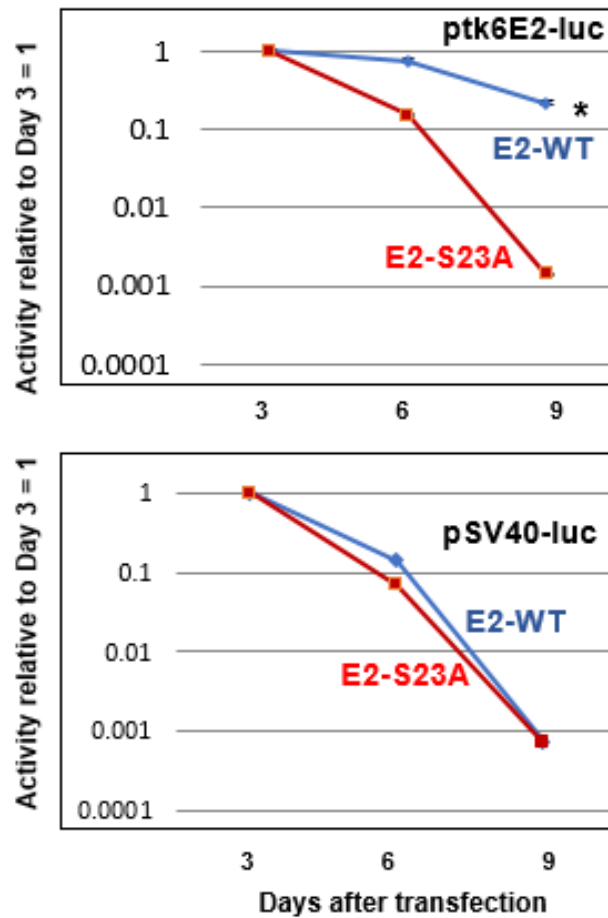


Figure 41. Quantitation of results from plasmid retention assay in N/Tert-1 cells. The plasmid retention assay was carried out as described before in the stable N/Tert-1 E2-WT and S23A cells. The experiment was repeated three times in duplicate. * indicates a significant difference between the E2-WT and E2-S23A luciferase activity at the day 6 and 9 time points, p-value < 0.05.

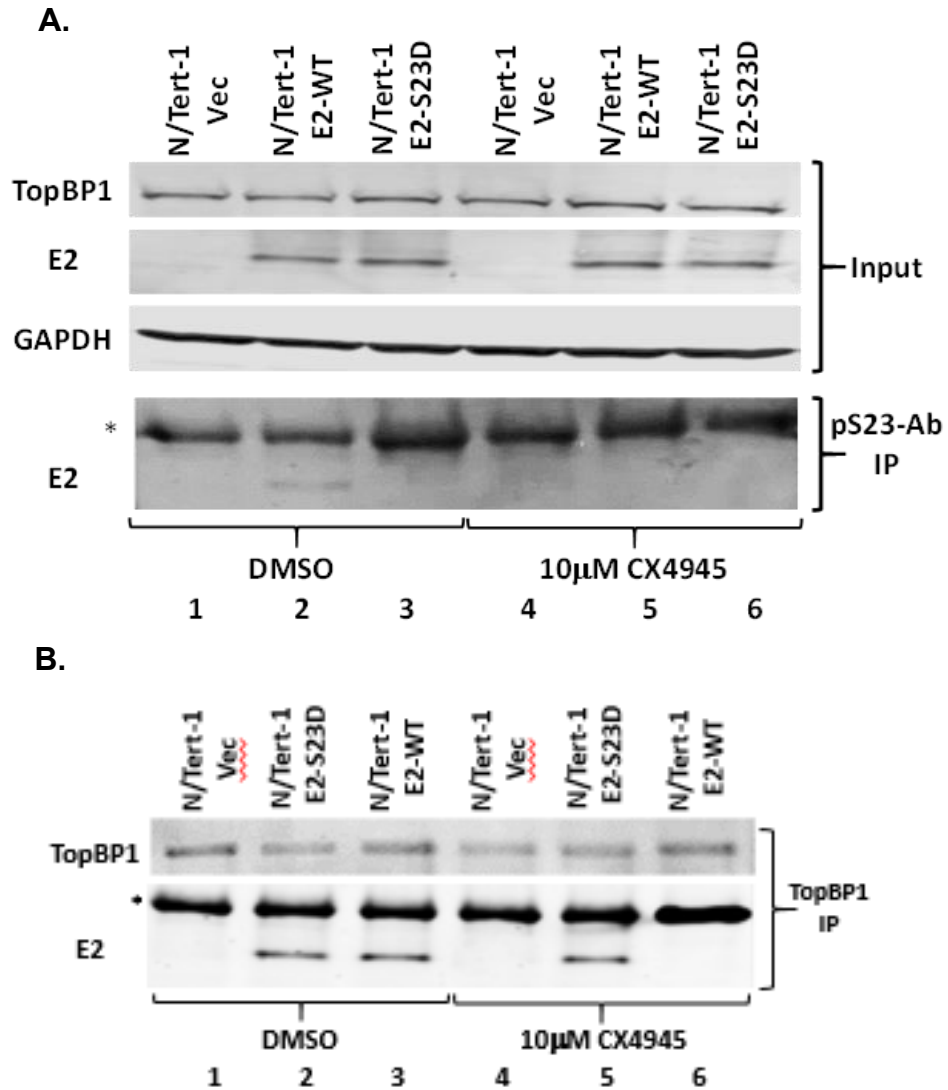


Figure 42. Western blot analysis depicting E2 S23 is phosphorylated *in vivo* by CK2 in N/Tert-1 cell lines. (A) The extracts in the top panels (Input) were immunoprecipitated with pS23-Ab or the extracts were immunoprecipitated with TopBP1 (B) following treatment with the CX4945. DMSO treatment was used as control. * is an antibody band.

3.3 Summary

In this section, we demonstrate that CK2 is responsible for the phosphorylation of E2 serine 23 in N/Tert-1 cells and that this promotes interaction with TopBP1. We successfully established our stable N/Tert-1 cells expressing E2-WT, E2-S23A and E2-S23D and further demonstrated that the E2-S23A mutation also disrupted the E2-TopBP1 interaction in N/Tert-1 cells. We also determine that the E2-TopBP1 interaction in N/Tert-1 cells is mediated by CK2 phosphorylation of serine 23. Our next aim was to explore the role of E2 serine 23 in the HPV lifecycle.

3.4 E2 serine 23 and the HPV16 lifecycle

To date, the results demonstrate that the E2-TopBP1 interaction is promoted by CK2 phosphorylation of E2-S23, and that the E2-TopBP1 complex mediates E2 plasmid retention function. Next, we investigated the role of the E2-TopBP1 interaction during the viral lifecycle.

3.4.1 E2-TopBP1 interaction is required for the HPV16 lifecycle.

We introduced the S23A and S23D mutations into the HPV16 genome and generated stable lines in N/Tert-1 cells, along with WT and pCDNA-Vec control lines. HPV16 transcriptionally reprograms the N/Tert-1 cell lines which support several markers of late stages of the viral lifecycle (232-234). Early passage cells were organotypically rafted to mimic the differentiation process. These were then formalin fixed and paraffin embedded for lifecycle studies.

Figure 43A demonstrates a prominent difference in phenotypes between the N/Tert-1+HPV16 mutants and WT. In Figure 43A (first panel), we observed that the H&E staining demonstrated a more disorganized epithelium and transformed looking with significantly higher koilocytes in N/Tert-1+HPV16-S23A and N/Tert-1+HPV16-S23D when compared with N/Tert-1+HPV16-WT and that of N/Tert-1 pCDNA-Vec control rafts (in which no koilocytes were detected). In HPV16 lesions, detection of koilocytes is potentially diagnostic of HPV infection and disease progression (235). These koilocytes are squamous cells with a large perinuclear vacuole and an acentric nucleus. Subsequently, we stained for E2 and BrdU (to assess cellular proliferation) and detected higher E2 levels in the upper layers of the epithelium in N/Tert-1+HPV16-WT (middle panels, Figure 43A). We

observed a significant reduction in E2 staining in N/Tert-1+HPV16-S23A and N/Tert-1+HPV16-S23D when compared with HPV16-WT cells. Increased BrdU labeling in N/Tert-1+HPV16-WT was observed indicating enhanced basal cell proliferation as described previously (232, 236) and this increase was not seen with the mutant genomes.

During the viral lifecycle, amplification occurs in the upper layers of the epithelium. We made use of FISH, to detect the amplified HPV16 DNA in these cells. There was a significant decrease in cells with amplified HPV16 DNA in the two mutant genomes when compared with the wild type cells (panel three, Figure 43A). We predict that this reduced amplification in mutant cells might be due to failure of stabilization of E2 and TopBP1 proteins during the viral genome amplification, which occurs in cells in G2/M phase during the viral lifecycle (also demonstrated by cell synchronization experiment in Figure 16).

Previously, it was demonstrated that N/Tert-1+HPV16 cells have episomal HPV16 genomes and support late stages of the HPV16 lifecycle (237). We extended our study to investigate whether E2 S23 is phosphorylated during the HPV16 lifecycle. For this purpose, we stained N/Tert-1 and N/Tert-1+HPV16 organotypic raft cultures with the pS23-Ab. We demonstrated that E2 is phosphorylated on serine 23 in the N/Tert-1+HPV16 cells (panel three, Figure 44) when compared to the isogenic control line, N/Tert-1 cells where no positive signal was seen after pS23-Ab staining (panel one, Figure 44). In N/Tert-1+HPV16, p-S23-Ab staining was detected throughout the epithelial layer and is mainly nuclear in most of the cells. The staining outside of nuclei might be due to nuclear breakdown in the upper layers of the differentiated epithelium. We additionally stained W12e rafted cells that can support late stages of the viral lifecycle. W12 are cervical lesion

cells and W12e are a clone that expresses E2 as it retains episomal HPV16. We also see a robust positive signal in W12e rafted cells after staining with p-S23-Ab.

3.4.2 S23A mutation in the HPV16 genome resulted in delayed immortalization of human foreskin keratinocytes and higher episomal viral genome copy number.

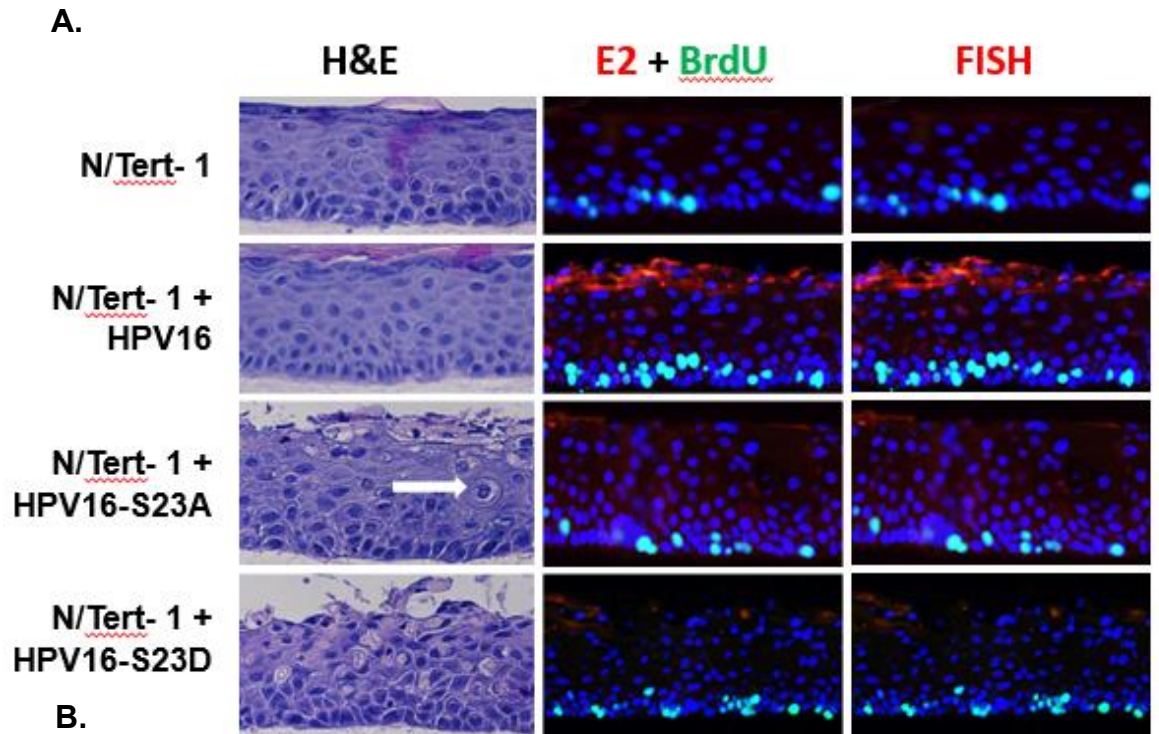
We next set out to investigate the role of E2-TopBP1 interaction during HPV immortalization. We transfected HPV16 genomes containing the E2 S23A and S23D mutations along with the wild type genome (HPV16-WT, HPV16-S23A, HPV16-S23D) into three independent human foreskin keratinocyte (HFK) primary cell cultures to generate immortalized cell lines. Initially, we successfully generated HPV16-WT and HPV16-S23D immortalized cell lines in two out of three donors but failed to immortalize any donor HFK cells by the HPV16-S23A variant (upon selection, HFK + HPV16-S23A cells failed to maintain cell growth). To maximize our chances of obtaining immortalized cell lines, we included feeder cells during transfection and selection. With this protocol, we observed a diminished initial immortalization, with slow growing colonies with HFK+HPV16-S23A as demonstrated by crystal violet staining (middle panel, Figure 45A). Crystal violet staining following immortalization was conducted in duplicates for all three lines, the result of which is summarized in Figure 45B. We observe a reduction in colony formation with HPV16-S23A when compared with HPV16-WT and HPV16-S23D. Following the initial lag, HFK+HPV16-S23A cells eventually grew out and its growth rate was similar to HFK+HPV16-WT and HFK+HPV16-S23D (Figure 46).

Following this, the presence of the viral genome in these immortalized HFK cell lines was investigated using Southern blot analysis (Figure 47) (238). *SphI* cuts the HPV16

genome once and when the DNA from all HFK HPV16 lines was digested with *SphI*, it generated an 8 kbp signal (top panel, Figure 47A). DNA from N/Tert-1 cells was used as control and generated no signal (lane 3). In HFK+HPV16-S23D-3, we observe an additional band of around 10kbp (lane 12 of top panel, Figure 47A). A *HindIII* digestion (bottom panel, Figure 47A) which does not cut the HPV16 genome, generated open circular DNA in all samples, as detected by the presence of slowly migrating species. In all HPV16-S23A samples from all three donors, we observed significantly faster migrating bands when compared with WT and S23D genomes containing cells (compare lanes 7-9 with the other lanes). We detected more DNA present in the HFK lines containing the S23A variant when compared with the WT, following *SphI* digestion (compare lanes 7-9 with 4-6). Figure 47B depicts the quantitation of the signals generated in the HPV16 lines relative to the 50 copy number (lane 2) in the *SphI* digest. In S23A samples, we see a statistically significant increase in HPV16 genome copy number when compared to WT.

To determine whether E2 S23 mutation alters the episomal/integrated status of the HPV16 genomes, we made use of a recent technique which utilizes exonuclease resistant DNA as a measure of episomal status (221, 239, 240). This assay determines the resistance of HPV16 genomes to exonuclease V (ExoV), which degrades linear but not circular DNA. GAPDH was used as our linear standard and designated the dCt between samples plus and minus ExoV as 100% degradation. We then took the dCt for a mitochondrial marker (a circular genome) and E2 and E6 and determined the percent of degradation by comparing the dCt difference with that of GAPDH. The assay was conducted using DNA from three independent cell lines generated and results are summarized in Figure 48. The circular

mitochondrial DNA is around 90% resistant in all samples. E2 and E6 are between approximately 50 and 80% resistant. Table in Figure 48B summarizes the results from these assays. Interestingly, HFK+HPV16-S23D-C is predominantly integrated, and the additional band on the Southern blot (Figure 47A, lane 12) may be related to this. From this experiment, with regards the episomal status of the viral genomes, we observe no significant difference between HFK+HPV16-WT and HFK+HPV16-S23A/S23D. Hence, the introduction of these mutations does not promote integration of the viral genome into that of the host.



	N/Tert-1	+HPV16 WT	+HPV16 S23A	+HPV16 S23D
Koilocytes (a)	0	0.49+/-0.04	1.8+/-0.3*	1.7+/-0.2*
BrdU (b)	25.2+/-0.7	43.8+/-1.5^	20.5+/-0.5	24.6+/-0.6
E2 (c)	0	3.7+/-0.24	1.6+/-0.1*	1.5+/-0.2*
FISH (d)	0	10.2+/-0.5	3.1+/-0.2*	1.1+/-0.1*

(a) Percent of cells that are koilocytes, relative to the number of DAPI cells
 (b) Percent of basal cells that are BrdU positive, relative to DAPI
 (c) Percent of cells positive for E2 staining, relative to DAPI
 (d) Percent of FISH positive cells, relative to DAPI
 (e) *significantly lower than wild HPV16WT; ^significantly higher than other lines

Figure 43. E2-TopBP1 mutation disrupts the HPV16 lifecycle. (A) N/Tert-1 cells containing the E2-WT and E2-ToPBP1 mutations were rafted, formalin fixed, paraffin embedded and sectioned for lifecycle studies. Left panels are H&E staining (koilocytes are indicated by white arrow). E2 staining (in red) and BrdU incorporation (in green) were carried out (middle panels). HPV16 DNA amplification was determined by FISH (in red, right panels). (B) Quantitation of images in (A). The quantitation was carried out using artificial intelligence via a Vectra Polaris as previously described (232-234). **These results are the work of Dr. Claire James.**

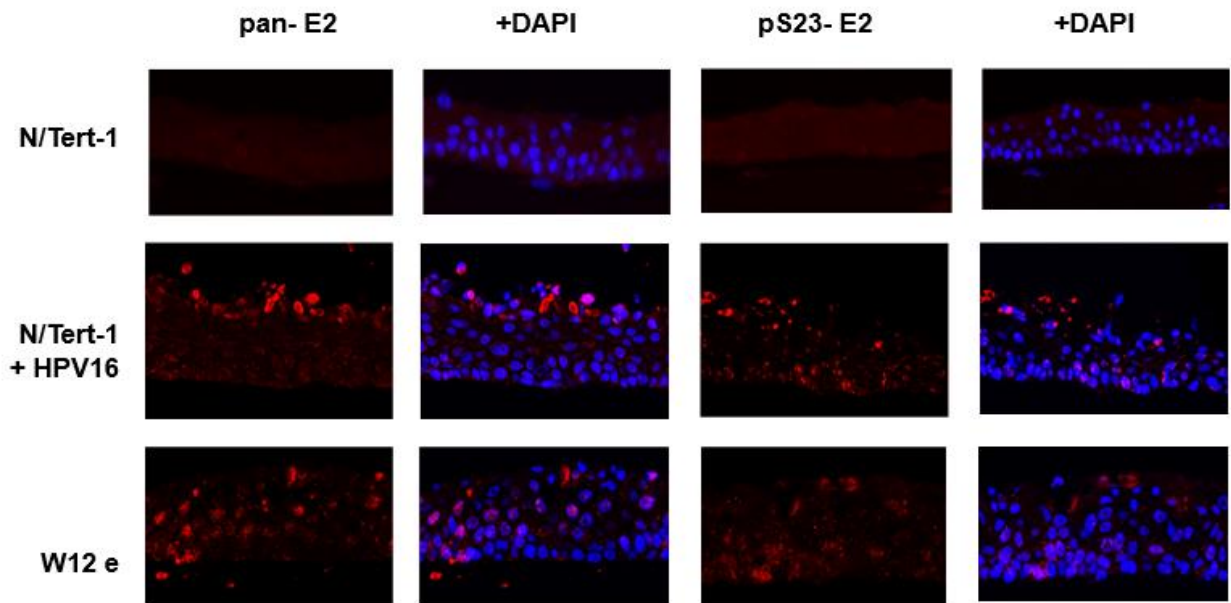


Figure 44. Detection of E2 S23 phosphorylation in HPV16 lifecycle models. The indicated cell lines were organotypically rafted, formalin fixed and paraffin embedded then sectioned. pS23-Ab (third panel) was carried out in N/Tert-1, N/Tert-1+HPV16 and W12e. Pan-E2 staining served as the control. Lane 2 and 4 depicts merge of pan-E2 and pS23-E2 staining, respectively with DAPI staining. **These results are the work of Dr. Claire James.**

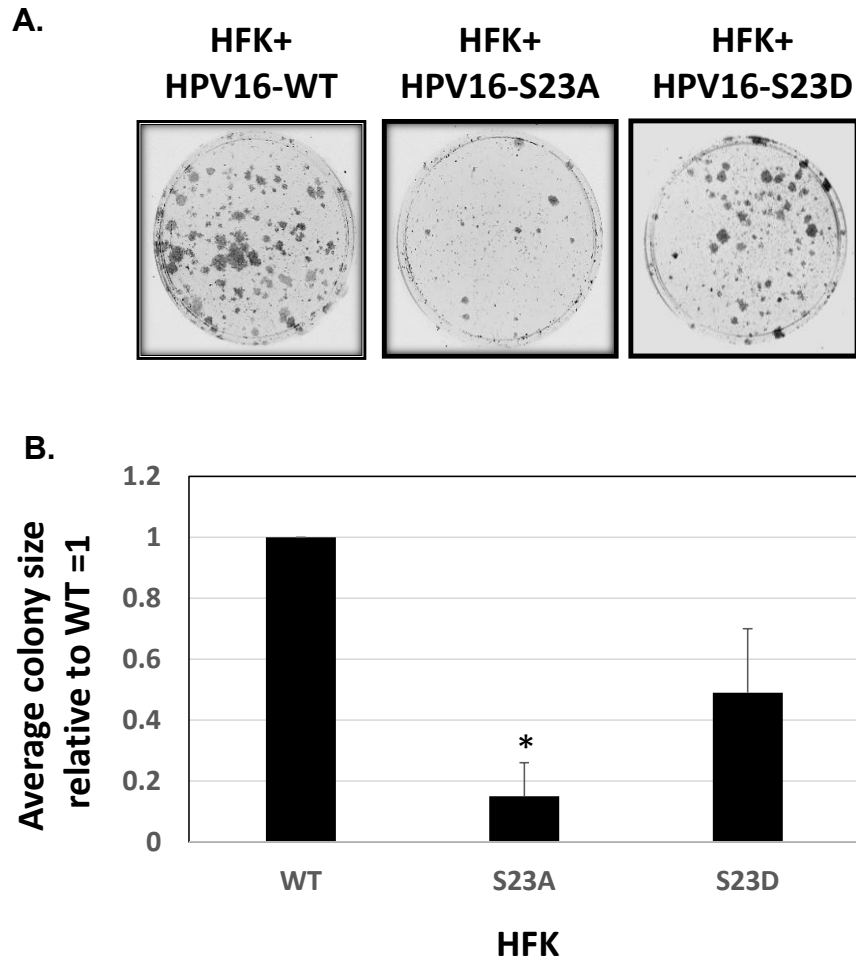


Figure 45. HPV16 S23A has diminished immortalization properties. (A) Primary human foreskin keratinocytes (HFK) were transfected with the indicated HPV16 genomes and cell colonies formed 2 weeks after transfection and selection with G418. Three independent HFK donors were used. (B) Quantitation of the result shown in (A). * indicates a significant reduction in colony size for E2-S23A, p-value < 0.05. **These results are the work of Dr. Claire James.**

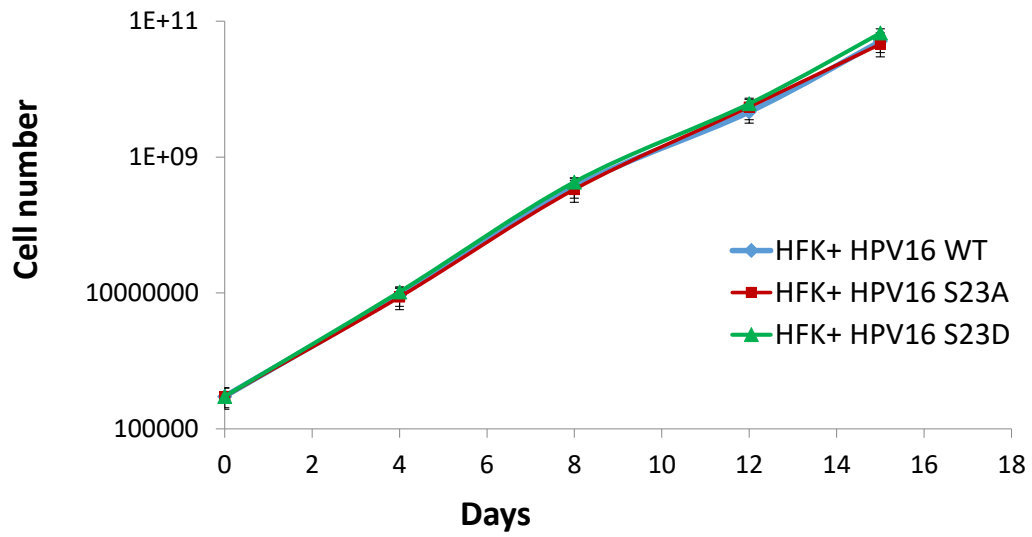


Figure 46. The growth rates of the indicated cell lines following immortalization. A growth curve was carried out over 15 days and the accumulated number of cells is plotted on a log graph. Cell numbers were not statistically significant at any point.

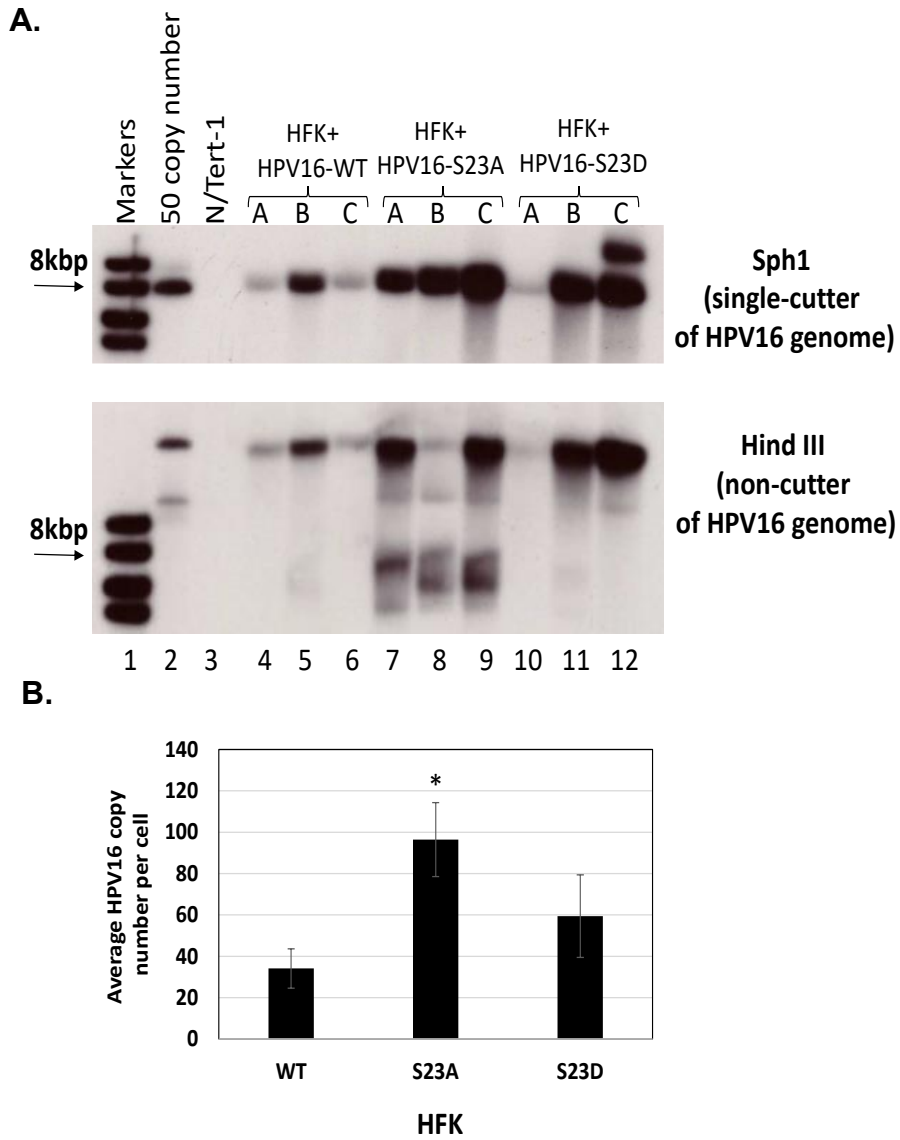
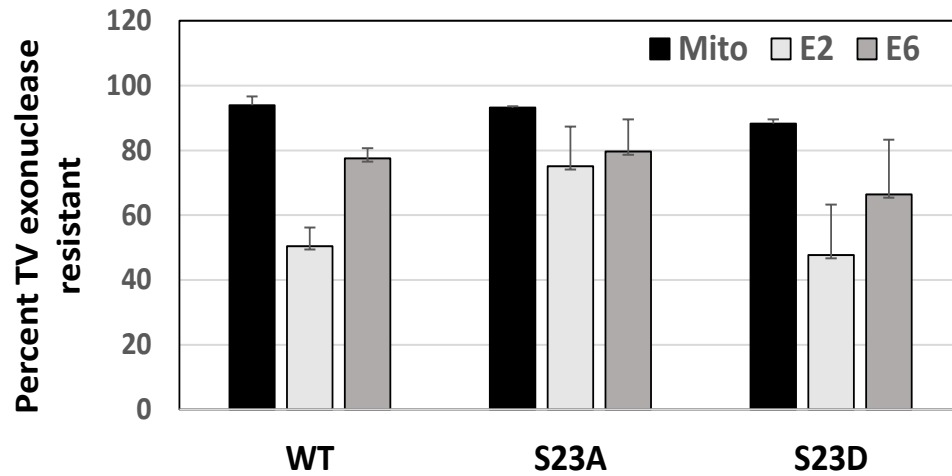


Figure 47. Southern blot analysis to determine the status of the HPV16 genomes in the immortalized cells. (A) DNA extracted from the indicated cell lines were probed with the HPV16 genome in Southern blots. Samples were digested with the HPV16 genome single cutter Sph1 (top panel). Hind III does not cut the HPV16 genome (bottom panel). **(B)** The bands in the top panel of A (Sph1 cut) were quantitated and are summarized here. * indicates a significant increase in HPV16-S23A genome copy number, p-value < 0.05. **These results are the work of Dr. Claire James.**

A.



B.

HFK	GAPDH	MITO	E2	E6	MITO	E2	E6
06087 E2WT-A	-8.85	-0.45	-5.29	-2.14	94.90%	40.3	75.8
06087 S23A-A	-9.93	-0.74	-4.87	-3.96	92.5	51	60.1
06087 S23D-A	-9.35	-1.24	-2.8	-1.47	86.7	70	84.3
06447 E2WT-B	-8.56	-0.17	-4.23	-2.3	98	50.6	73.1
06447 S23A-B	-9.08	-0.64	-0.84	-0.77	93	90.7	91.5
06447 S23D-B	-4.04	-0.37	-1.8	-0.72	90.8	55.4	82.2
08415 E2WT-C	-8.17	-0.92	-3.24	-1.34	88.7	60.3	83.6
08415 S23A-C	-7.33	-0.43	-1.2	-0.92	94.1	83.6	87.4
08415 S23D-C	-7.93	-0.99	-6.53	-5.34	87.5	17.7	32.7

Figure 48. Quantitation of result from the TV exonuclease assay. (A) To investigate the episomal status of the HPV16 genomes in all cell lines we used the TV exonuclease assay. Table in **(B)** details the result seen above. See section 3.4.2 for explanation. **These results are the work of Raymonde Otoa.**

3.4 Summary

In this section, we investigated the role of the E2-TopBP1 interaction during the viral lifecycle. We introduced the S23A and S23D mutations into the HPV16 genome. Wild type (WT) and mutant genomes were then transfected into N/Tert-1 cells to form stable cell lines, which were rafted. Introduction of mutations resulted in more dysplasia with increased koilocytes, decreased E2 stabilization and decreased viral genome amplification during the viral lifecycle. We further demonstrated that E2 is phosphorylated on S23 during the HPV16 lifecycle.

Additionally, when HPV16-S23A was introduced into HFK, it demonstrated delayed ability to immortalize these cells. Moreover, the resultant immortalized cell lines that eventually grow out from the HPV16-S23A transfected cells revealed increased episomal viral genomes when compared with HPV16-WT. By using the recently developed TV exonuclease assay, we have shown that the introduction of these mutations does not promote integration of the viral genome into that of the host. This is further discussed in chapter 4.

CHAPTER 4

Discussion

HPV16 E2 protein is a multi-functional protein which has many vital roles during the viral lifecycle. There is a gap in our understanding of host partner proteins and their roles in E2 functions. In this study, we demonstrate that CK2 phosphorylation of E2 serine 23 leads to a complex formation with TopBP1, both *in vitro* and *in vivo*.

Serine 23 is conserved in all alpha-type HPV, which also includes high-risk HPVs, without any known function (Figure 11). Further, the negative aspartic and glutamic acid residues at -1 and -3 respectively, could indicate a potential CK2 target residue (241). *In vivo*, mutation of S23 to alanine disrupts the co-immunoprecipitation of E2 with TopBP1, while an aspartic acid mutation (which mimics the negative charge of phosphorylation) retains interaction similar to E2-WT (Figure 13B). To demonstrate phosphorylation of S23 *in vivo*, we generated a phospho-specific antibody (pS23-Ab) which recognizes E2-WT, including during mitosis, but not E2-S23A (Figure 39). CK2 exists as a tetramer composed of two catalytic α -subunits (α , α') and two β regulatory subunits (241). When either α component is knocked down, or by partial knockdown of both components, we completely eliminate detectable levels of E2 S23 phosphorylation in U2OS cells (Figure 37) and further observe that knockdown partially disrupted the interaction between E2 and TopBP1 (Figure 38). The reason for this complete loss of phosphorylation, and only a partial loss of interaction, could be due to the failure to detect residual E2 phosphorylation following knockdown of the CK2 components. Unfortunately, pS23-Ab did not work in the western

blots, it is possible the antibody only recognizes native E2 and not the denatured versions needed for western blotting.

The loss of detectable phosphorylation on S23 residue with addition of the CK2 inhibitor CX4945 as shown by pS23-Ab immunoprecipitation in U2OS cells (Figure 37), further confirms the role of CK2 in the phosphorylation of S23. We also see a disruption of E2-TopBP1 interaction following the CK2 inhibitor CX4945 treatment (Figure 38). We next expanded our studies in a more physiologically relevant model with the use of N/Tert-1 cells, to demonstrate that S23 is critical for the E2-TopBP1 interaction (Figure 40) and to further validate that that CX4945 abolishes detectable phosphorylation of E2 on S23 residue and blocks the E2-TopBP1 interaction in N/Tert-1 cells (Figure 42). We also observed detectable E2 S23 phosphorylation during the HPV16 lifecycle in N/Tert-1 cells (Figure 44). Our results additionally illustrate that CK2 phosphorylation of S23 mediates the E2-TopBP1 interaction *in vivo*, we also demonstrated that CK2 controls this interaction *in vitro*. E2-WT cannot interact with TopBP1 *in vitro*, but E2-S23D can (Figure 28). Incubation of E2-WT with CK2 enzyme promotes the interaction between E2 and TopBP1 recombinant proteins (Figure 29), and this can be reversed by treatment with lambda phosphatase (Figure 30). As E2 has been shown to interact with CK2 components (226), this loss of interaction after the lambda phosphatase treatment demonstrates that the enzymatic function of CK2 is required to promote the E2-TopBP1 interaction via phosphorylation and that CK2 does not act as a “bridge” to bring the two proteins together. We were not successful to express and purify recombinant E2-S23A to use as a control in our *in vitro* studies. Nevertheless, the combination of *in vivo* and *in vitro* results

demonstrates that CK2 phosphorylation of E2 S23 is crucial for E2-TopBP1 complex formation.

The significance of investigating the role of CK2 in mediating HPV16 E2 function is that CK2 has been implicated in several aspects of papillomavirus functions. CK2 phosphorylates BPV1 E2 on the 301 residue and this further regulates E2 protein stability (242). This is not the case with HPV16 E2 as this residue is not conserved on HPV16 E2, which is also shown in this study by the relatively equivalent expression levels of E2-WT and E2-S23A in both U2OS and N/Tert-1 cells. CK2 can also regulate the DNA binding of BPV and HPV E1 proteins and can control their DNA replication functions (243). CK2 phosphorylates and regulates HPV18 E1 function and is important in the lifecycle of HPV18 and 11 (222, 244). CK2 α was the critical component involved in regulating E1, CK2 α' was not involved. CK2 phosphorylation of BRD4 is important for mediating HPV16 E2 transcription and replication function, and studies from the Morgan lab along with other groups have also demonstrated that a direct interaction between E2 and BRD4 is required for E2 transcription function (245-247). As well as regulating E1-E2 functions, CK2 can also regulate the function of E7 proteins. Phosphorylation of a CK2 consensus sequence on E7 is important for E7 degradation of p130 and the promotion of S-phase in differentiated keratinocytes (248), and a HPV18 E7 CK2 target residue is required for maintaining the transformed phenotype of cervical cancer cells (249). Overall, this critical role of CK2 during multiple stages of viral lifecycle reiterates the need to investigate the anti-viral and therapeutic effects of CK2 inhibition on HPV infection. The outcome from this study is a step towards enhancing our understanding of the E2-TopBP1 interaction

mediated by CK2 phosphorylation and to expand its importance and relevance into other HR-HPV types.

E2 has three major functions in the viral lifecycle. From our transient assay results we demonstrate the E2-S23A replication and transcription function is similar to E2-WT (Figure 14). E2 also has an important third role, to mediate viral genome segregation into daughter cells by actively associating with viral and human DNA simultaneously during mitosis (250). E2 can bind to mitotic chromatin, and previously it was demonstrated that E2 and TopBP1 co-localize on mitotic chromatin (187). We thus were intrigued to investigate the interaction of E2-WT and E2-S23A with mitotic chromatin (Figure 15). E2-WT showed robust staining on mitotic chromatin, and in addition it recruited TopBP1 onto the mitotic chromatin. In control cells with no E2, TopBP1 does not “coat” the mitotic chromatin as it does with E2-WT. Therefore, like BPV1 E2 and BRD4, E2 alters TopBP1 interaction with mitotic chromatin (251). Although we see that E2-S23A could retain some mitotic E2 staining and could also recruit TopBP1, we observed a reduced E2 staining on mitotic chromatin in our E2-S23A mutant when compared to E2-WT and this result was reproducible. Cell cycle analysis demonstrates that E2-WT levels are increased during mitosis, while E2-S23A levels are not, supporting our immunofluorescence results. Furthermore, in this study we observed that E2-WT increases the levels of TopBP1 during mitosis while E2-S23A cannot. Therefore, E2-WT and E2-S23A have distinct phenotypes during mitosis. We are currently investigating whether E2 is stabilized during mitosis. Subsequently, we investigated whether this difference could contribute to the ability of E2 to retain plasmids in the U2OS cells. Our results in Figure 21 demonstrates that E2-WT

retains the plasmid with E2 binding site, over an extended period, while E2-S23A could not. A non-E2 binding site plasmid could not be retained by either E2 protein. siRNA knockdown of TopBP1 abrogated the ability of E2-WT to retain the E2 binding site plasmid in this assay. Knockdown of CK2 α or α' also compromised the plasmid retention function of E2-WT, further demonstrating the critical role CK2 plays in mediating the E2-TopBP1 interaction. These results demonstrate that an interaction between E2 and TopBP1 is critical for the plasmid retention function of E2-WT. The observation that E2-S23A retains interaction with mitotic chromatin was interesting as previous work has demonstrated that interaction with mitotic chromatin alone is not enough to mediate plasmid retention function by E2, two properties seem to be required: chromatin attachment and transactivation functions must be in sync for proper plasmid segregation (179). We propose that there is an additional factor that could mediate the interaction of HPV16 E2-S23A with mitotic chromatin and this is under active investigation, with our focus on BRD4.

To further study the effect of E2-S23A mutation on the viral lifecycle, we introduced S23A and S23D mutations into the HPV16 genome and used this to prepare N/Tert-1+ HPV16 cells lines. In a previous study from the Morgan lab, it was demonstrated that in N/Tert-1 cells with the entire HPV16 genome (N/Tert-1+HPV16), the viral genome is episomal and is amplified in the upper layers of organotypic raft cultures (232). From our rafting study results we observe that morphology of the N/Tert-1+HPV16-S23A and HPV16-S23D cells was disorganized and more transformed looking, when compared with the wild type genome (Figure 43), and there were also occasional sections of thickened

epithelium. There was an increase in FISH signal with both mutant genomes, and more detectable replication towards the basal layers (Figure 43). N/Tert-1+HPV16 only demonstrated a FISH signal in the upper layers of the epithelium, as expected. We then stained the rafted N/Tert-1+HPV16 and vec control, along with W12e cells which were isolated from cervical lesion and are a clone that retains episomal HPV16, and therefore E2 expression. From Figure 44 it is evident that E2 is phosphorylated on S23 during the HPV16 lifecycle.

We further saw E2-S23A genomes lagged in their ability to immortalize human foreskin keratinocytes (HFK) (Figure 45). Also, the resultant immortalized cell lines that ultimately grow out from the HPV16-S23A transfected cells have increased episomal viral genomes when compared with HPV16-WT (Figure 47). The results from the recently developed TV exonuclease assay also support this (Figure 48). One explanation to this is that possibly, at the early stages of establishing immortalization, the viral genome segregation function of E2 is critical to spread the viral genome to daughter cells, and with the S23A mutant genomes this is not occurring. This might explain the delay in initial immortalization in S23A mutant. This process may also explain the increase in viral genome copy number with the S23A mutant as the viral genomes may be mis-segregated into a smaller number of cells, resulting in the ultimate growth of immortalized HFK that have increased viral genomes. Additionally, in the HFK+HPV16-S23A immortalized cell lines, there is a significant increase in faster mobility genomes when compared with HFK+HPV16-WT on Southern blots where the viral genomes have not been cut (Figure 47A). During mitosis, TopBP1 is required for decatenation of the host genome to promote

the correct segregation of the host chromosomes into daughter nuclei (252, 253). Probably, the E2-TopBP1 interaction plays a similar role for the circular viral genome during mitosis, ensuring that individual viral genomes reside in the daughter nuclei and are therefore substrates for replication. Therefore, the faster migrating genomes observed in Southern blot analysis of HFK+HPV16-S23A cells could be those that remain catenated. This defect in decatenation could also delay the growth of immortalized HFK.

Moreover, in monolayer cell culture, the HFK lines grew equally well (Figure 46) which would suggest that the viral genomes are not being lost in HFK+HPV16-S23A during this period, as loss of viral genomes would result in a reduction in proliferation. As the monolayer cell culture model does not support and depict the actual different viral lifecycle stages, perhaps during the culture of the HFK in monolayer, the E2-TopBP1 episome retention mechanism is not required to maintain viral genome copy numbers. This needs to be further explored to determine the contribution of the E2-TopBP1 interaction to multiple stages of the viral lifecycle.

Previously, it was demonstrated that E2 regulates host gene transcription and that this property is essential for the viral lifecycle (231, 254). TopBP1 regulates transcription of E2F and p53 and therefore interaction with E2 could disrupt this process (255, 256). Studies have also demonstrated that TopBP1 regulates host gene transcription during keratinocyte differentiation (257). Although we cannot detect any difference in the replication functions of E2-WT and E2-S23A in our transient replication assays, it is possible that the S23A mutation could compromise the replication function of E2 during immortalization. We are presently investigating to identify what aspects of the lifecycle is

affected by the introduction of the S23A mutation into the HPV16 genome which resulted in an aberrant HPV16 lifecycle in human keratinocytes seen in our results.

Overall, in this study, we have demonstrated that CK2 phosphorylation of E2 on serine 23 promotes interaction with TopBP1, and that this is crucial during the viral lifecycle. The difference in phenotypes observed in our results is suggestive that disrupting this interaction further abrogates the plasmid retention function of E2. As CK2 is essential in different stages of HPV16 lifecycle, we propose that CK2 could be a potential therapeutic target for treating HPV16 related HNSCC.

CHAPTER 5

Conclusion and future work

The prevalence of HPV positive HNSCC are on the rise, especially among men, despite the availability of vaccine against HPV16, 18 and also HPV 6 and 11. There is an urgent need to develop novel antiviral therapeutics targeting the HR-HPVs as the vaccine is only prophylactic and cannot treat pre-existing HPV infections and related conditions. Only with a deeper understanding of the HPV lifecycle, it is possible to develop a successful strategy to treat HPV related cancers.

In this study, for the first time, we have identified the chromatin receptor for HPV16 E2, demonstrating that the E2-TopBP1 interaction is promoted by CK2 phosphorylation and can mediate plasmid segregation function and regulate the viral lifecycle (Figure 49). The outcomes of this study will enhance our understanding of HPV lifecycles which are major human pathogens responsible for 5% of all cancers.

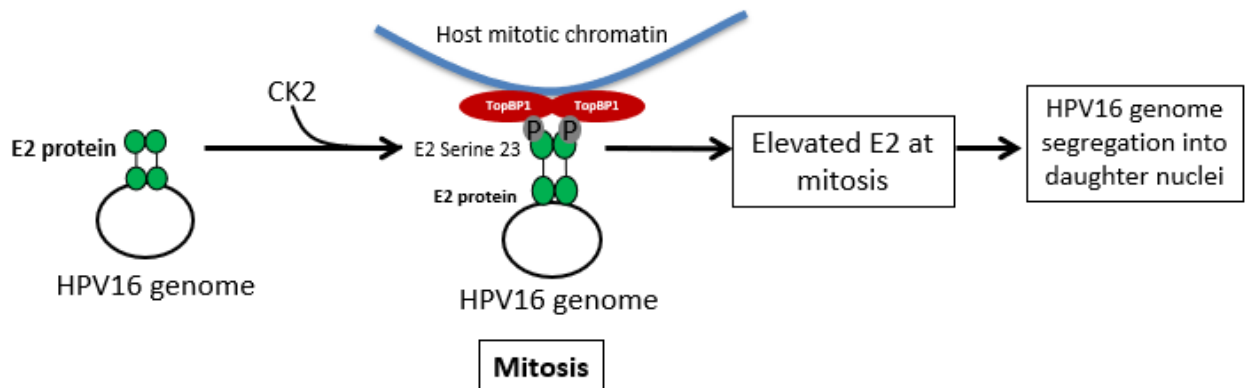


Figure 49. A schematic model depicting a summary of the results deduced from this study.

Targeting the E2-TopBP1 interaction can be promising for the reasons listed below:

1. The interaction between TopBP1 is confirmed in BPV1 E2, which is suggestive that the interaction might be conserved across all PV types. TopBP1 is the mitotic chromatin receptor for HPV16 E2, it further aids E2 to regulate the host genome and is essential for optimal viral DNA replication mediated by E2, making this an ideal target for viral therapy development.

2. CK2 has been implicated with regards to several PV functions. Furthermore, in this study, we demonstrate that CK2 phosphorylates E2 on serine 23 *in vivo*, and that CK2 inhibitors disrupt the E2-TopBP1 complex. Our results suggest that CK2 inhibitors such as CX4945, a drug in clinical trials for several human cancers (230), may be useful to disrupt the E2-TopBP1 dependent HPV16 lifecycle and potentially kill HPV16 positive cancers (Figure 50).

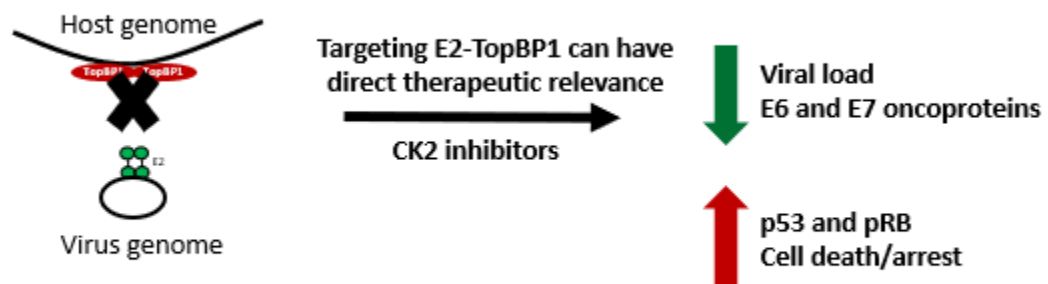


Figure 50. A schematic depicting a potential impact E2-TopBP1 interaction could have with regards to a direct therapeutic relevance.

Future directions

The bromo-domain protein, Brd4 is the host mitotic receptor for BPV1 E2 (258-261). Further, HPV16 E2 transcription and replication function is mediated by CK2 phosphorylation of Brd4 (123, 262). Previously, it has been established that Brd4 to be an essential transcriptional co-activator for all E2 proteins (245-247) and Brd4 is a ubiquitous protein found in all proliferating cells (155). In our immunofluorescence results (Figure 15), we observed that E2-S23A could retain interaction with mitotic chromatin despite not being able to complex with TopBP1. This prompted us to explore if this interaction of E2-S23A with mitotic chromatin is mediated by an additional factor. Given its various important roles, in our future studies, we aim at exploring if Brd4 could be a part of the complex that could potentially mediate the E2-S23 interaction with host mitotic chromatin. Our preliminary data seems to support this.

To understand the role of Brd4 in the complex, we made a stable E2 cell line in U2OS carrying the mutant E2-R37A (arginine to alanine at position 37) which was previously characterized (158, 176, 263). We then harvested the lysate and repeated the immunoprecipitation with TopBP1 antibody as before. From Figure 52, we observe that E2-R37A mutant interacts with TopBP1 similarly to E2-WT and E2-S23D phospho mutant, and unlike E2-S23A, where this interaction is lost. Furthermore, IP with Brd4 pulls down both E2-S23A and E2-WT (Figure 53). Next, when we synchronized the U2OS cells using double thymidine block, we observed that there was a significant increase in E2 and TopBP1 levels 8 hours following release in the E2-WT cells, but an increase of neither E2 nor TopBP1 in E2-R37A or Vec control cells (Figure 54). This solidified our theory that

E2-S23 is the site of interaction between E2 and TopBP1 and not mediated by E2-R37. We are currently expanding the study with the use of a E2-S23A+R37A double mutant, to further dissect the role of Brd4 in the complex. In our future studies, we aim to make use of the E2-R37A and the E2-S23A+R37A double mutant to study the effect of these Brd4 mutation on the mitotic interaction of E2. We further want to study the effect this double mutation has on the transcription function of E2 and its role in the viral lifecycle.

We propose a model that during mitosis, TopBP1 might function as a chaperon that interacts with E2 one side and this interaction leads to stabilization of both proteins on the mitotic chromatin. Next, with its other side, TopBP1 may bind to one of Brd4's bromodomains. Brd4 would then interact with both the host chromatin and transcription factors, potentially recruiting the E2-TopBP1 complex to open sites of chromatin and the promoters of host genes for their regulation. This could further play a role in mediating genome segregation as well as DNA replication and transcription functions of the E2 protein, needed for the virus to carry its lifecycle (Figure 51).

Additionally, future studies will also focus on more in-depth lifecycle studies to determine the contribution of the E2-TopBP1 interaction to multiple stages of the viral lifecycle.

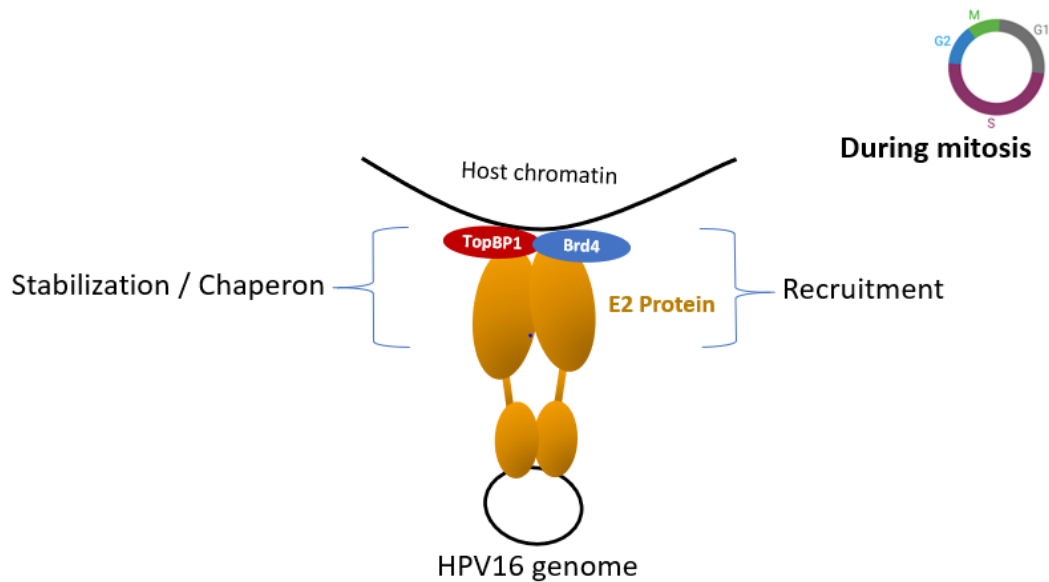
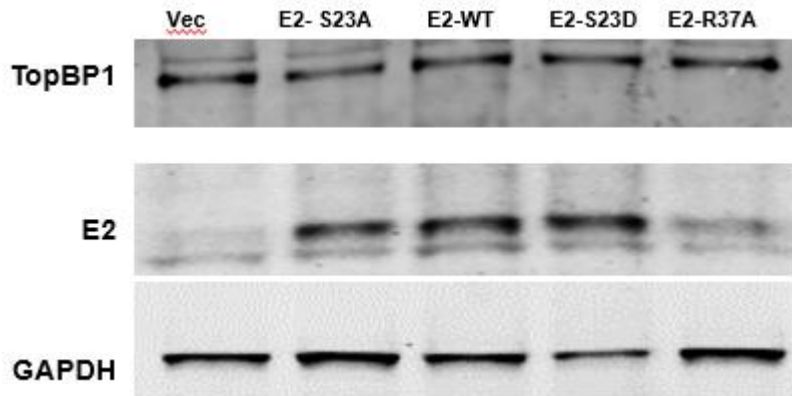


Figure 51. A proposed model and roles of a potential TopBP1-Brd4- E2 complex.

Furthermore, we aim to identify the TopBP1 domain that E2 interacts with to form the complex. Previous studies have identified several TopBP1 domains that interact with phosphorylated peptides (228). The region around E2 S23 does not correspond to a consensus sequence for interacting with any of these TopBP1 domains and in fact, an E2 pS23 peptide does not interact with any of these domains (Figure 55). This indicates that E2 interacts with a yet to be identified domain of TopBP1. Our aim is to identify this domain, as this will help us to determine whether E2 has evolved a unique way to interact with TopBP1 that does not disrupt the ability of TopBP1 to interact with host proteins involved in the DNA damage response, a process essential for HPV lifecycles (205). Identifying this TopBP1 functional domains involved in the HPV16 genome segregation, could serve as potential therapeutic target.

A.



B.

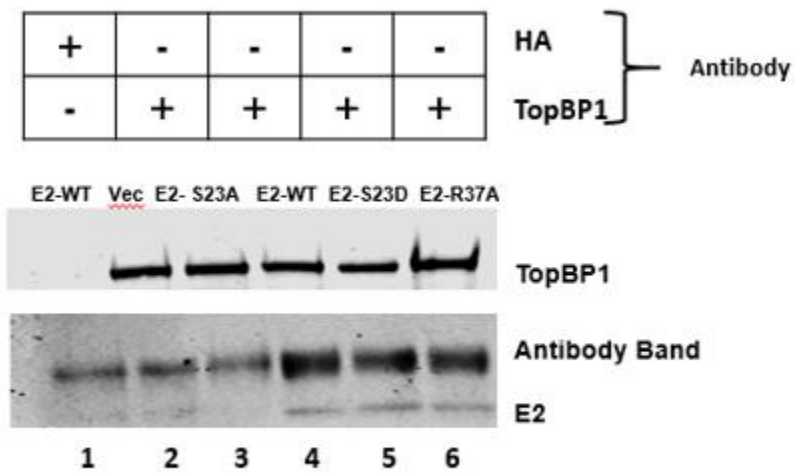


Figure 52. Western blot analysis to demonstrate E2-TopBP1 interaction in E2-R37A mutant. (A) Western blot showing the expression levels of indicated proteins in stable U2OS E2 cells. (B) The protein extracts were immunoprecipitated with HA (control) or TopBP1 antibodies followed by western blotting for TopBP1 and E2.

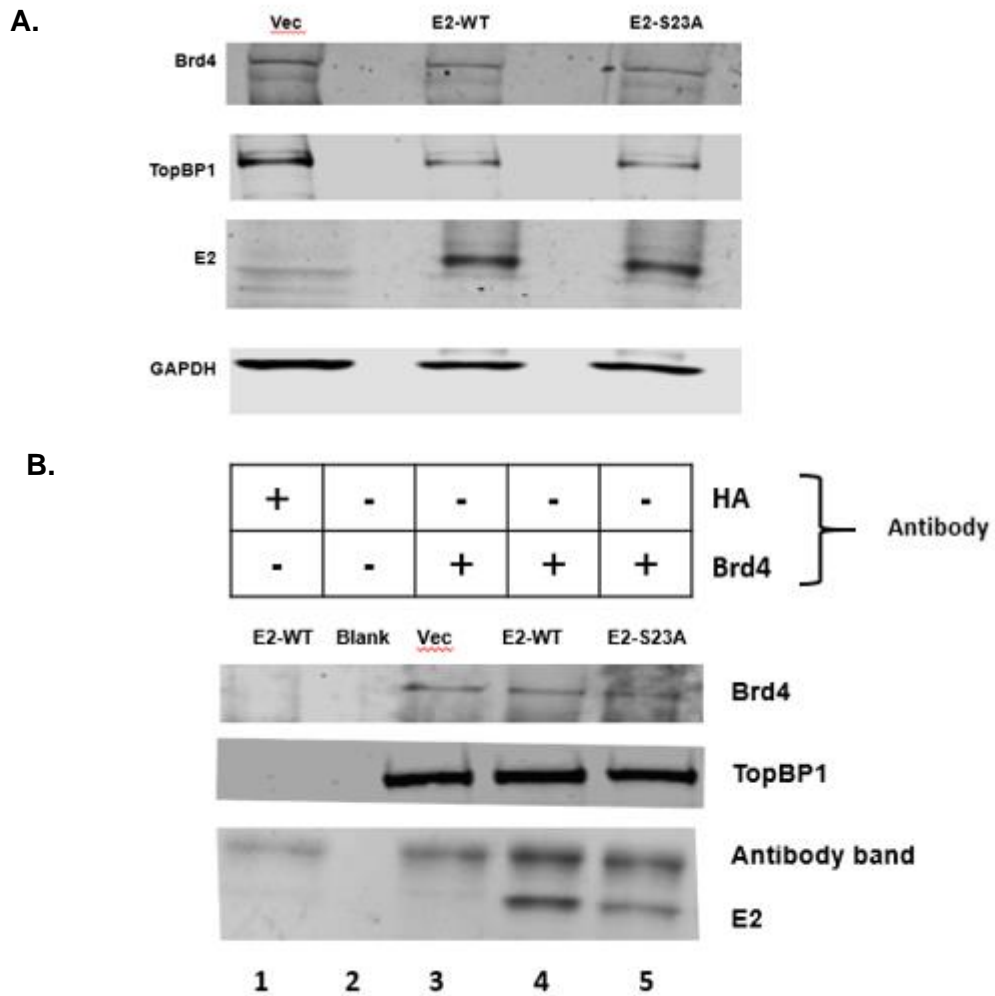


Figure 53. Western blot analysis to demonstrate E2-Brd4 interaction (A) Western blot showing the expression levels of indicated proteins in stable U2OS E2 cells. **(B)** The protein extracts were immunoprecipitated with HA (control) or Brd4 antibodies followed by western blotting for TopBP1, Brd4 and E2.

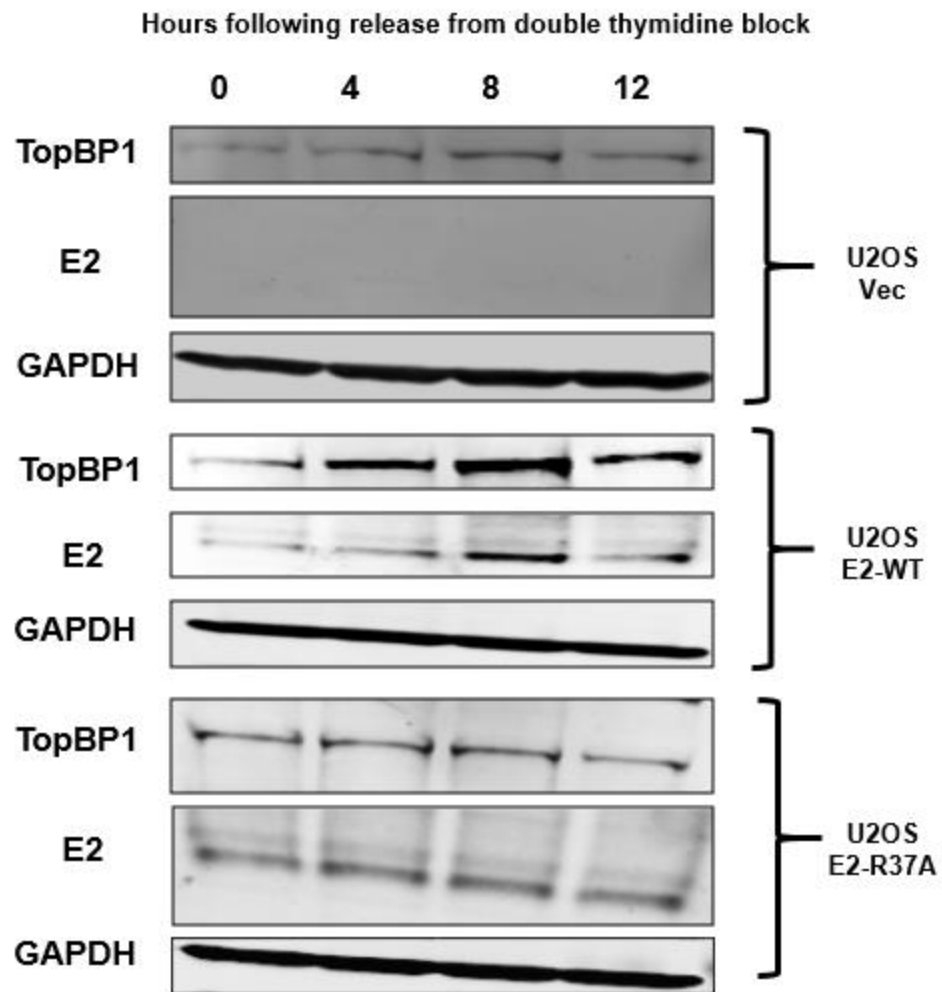


Figure 54. Cell synchronization and western blot analysis on U2OS E2 cell lines. U2OS lines as indicated, were double thymidine blocked to coordinate them in G1. The cells were then released for the time points shown, and protein extracts harvested and western blots carried out.

TOPBP1 BRCT domain modules vs E2 pS23 peptide and controls

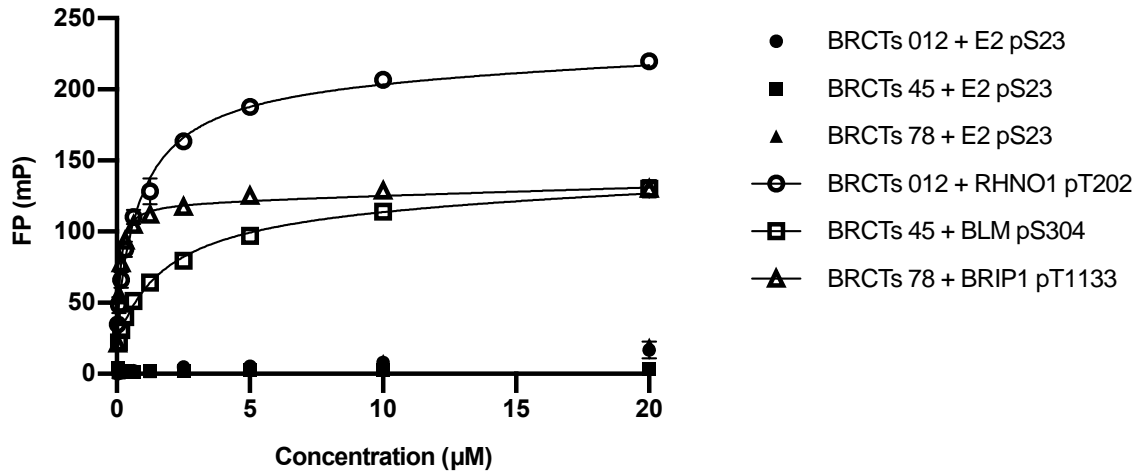


Figure 55. The E2 pS23 peptide does not interact with well characterized phosphopeptide binding domains of TopBP1. Fluorescent polarization assays were carried out with the indicated peptides and TopBP1 BRCT containing domains. The control peptides are known interactors of the indicated TopBP1 domains, see (228) for details.

REFERENCES

1. **Johnson DE, Burtness B, Leemans CR, Lui VWY, Bauman JE, Grandis JR.** 2020. Head and neck squamous cell carcinoma. *Nature Reviews Disease Primers* **6**:92.
2. **Aupérin A.** 2020. Epidemiology of head and neck cancers: an update. *Curr Opin Oncol* **32**:178-186.
3. **SocietyAmericancancer.** 2020. Cancer Facts & Figures 2020. <https://www.cancer.org/content/dam/cancer-org/research/cancer-facts-and-statistics/annual-cancer-facts-and-figures/2020/cancer-facts-and-figures-2020.pdf>. Accessed
4. **Hoang T, Zhang C, Geye HM, Speer T, Yu M, Wiederholt PA, Kakuske JC, Traynor AM, Cleary JF, Dailey SH, Ford CN, McCulloch TM, Hartig GK, Harari PM.** 2012. Gender associations in head and neck squamous cell carcinoma (HNSCC). *Journal of Clinical Oncology* **30**:e16010-e16010.
5. **Chaturvedi AK, Engels EA, Anderson WF, Gillison ML.** 2008. Incidence trends for human papillomavirus-related and -unrelated oral squamous cell carcinomas in the United States. *J Clin Oncol* **26**:612-619.
6. **Ragin CC, Modugno F, Gollin SM.** 2007. The epidemiology and risk factors of head and neck cancer: a focus on human papillomavirus. *J Dent Res* **86**:104-114.
7. **Ramqvist T, Dalianis T.** 2010. Oropharyngeal cancer epidemic and human papillomavirus. *Emerg Infect Dis* **16**:1671-1677.

8. **D'Souza G, Dempsey A.** 2011. The role of HPV in head and neck cancer and review of the HPV vaccine. *Prev Med* **53 Suppl 1**:S5-s11.
9. **Moore KA, Mehta V.** 2015. The Growing Epidemic of HPV-Positive Oropharyngeal Carcinoma: A Clinical Review for Primary Care Providers. *The Journal of the American Board of Family Medicine* **28**:498-503.
10. **CDC.** October 7, 2020. Head and Neck Cancers. <https://www.cdc.gov/cancer/headneck/index.htm>. Accessed
11. **McMurray HR, Nguyen D, Westbrook TF, McAnce DJ.** 2001. Biology of human papillomaviruses. *Int J Exp Pathol* **82**:15-33.
12. **Liao JB.** 2006. Viruses and human cancer. *Yale J Biol Med* **79**:115-122.
13. **de Martel C, Plummer M, Vignat J, Franceschi S.** 2017. Worldwide burden of cancer attributable to HPV by site, country and HPV type. *Int J Cancer* **141**:664-670.
14. **CDC.** September 2020. Cancers Associated with Human Papillomavirus, United States—2013–2017. *US Cancer Statistics Data Briefs*, No 18.
15. **Chaturvedi AK.** 2010. Beyond cervical cancer: burden of other HPV-related cancers among men and women. *J Adolesc Health* **46**:S20-26.
16. **Giannoudis A, Herrington CS.** 2001. Human papillomavirus variants and squamous neoplasia of the cervix. *J Pathol* **193**:295-302.
17. **Doorbar J, Egawa N, Griffin H, Kranjec C, Murakami I.** 2015. Human papillomavirus molecular biology and disease association. *Reviews in medical virology* **25 Suppl 1**:2-23.

18. **Burd EM.** 2003. Human papillomavirus and cervical cancer. *Clin Microbiol Rev* **16**:1-17.
19. **Klussmann JP, Weissenborn SJ, Wieland U, Dries V, Kolligs J, Jungehueling M, Eckel HE, Dienes HP, Pfister HJ, Fuchs PG.** 2001. Prevalence, distribution, and viral load of human papillomavirus 16 DNA in tonsillar carcinomas. *Cancer* **92**:2875-2884.
20. **Gillison ML, Koch WM, Capone RB, Spafford M, Westra WH, Wu L, Zahurak ML, Daniel RW, Viglione M, Symer DE, Shah KV, Sidransky D.** 2000. Evidence for a Causal Association Between Human Papillomavirus and a Subset of Head and Neck Cancers. *JNCI: Journal of the National Cancer Institute* **92**:709-720.
21. **Vokes EE, Agrawal N, Seiwert TY.** 2015. HPV-Associated Head and Neck Cancer. *JNCI: Journal of the National Cancer Institute* **107**.
22. **Smeets SJ, Braakhuis BJ, Abbas S, Snijders PJ, Ylstra B, van de Wiel MA, Meijer GA, Leemans CR, Brakenhoff RH.** 2006. Genome-wide DNA copy number alterations in head and neck squamous cell carcinomas with or without oncogene-expressing human papillomavirus. *Oncogene* **25**:2558-2564.
23. **El-Mofty SK, Lu DW.** 2003. Prevalence of human papillomavirus type 16 DNA in squamous cell carcinoma of the palatine tonsil, and not the oral cavity, in young patients: a distinct clinicopathologic and molecular disease entity. *Am J Surg Pathol* **27**:1463-1470.

24. **You EL, Henry M, Zeitouni AG.** 2019. Human papillomavirus-associated oropharyngeal cancer: review of current evidence and management. *Curr Oncol* **26**:119-123.
25. **Fakhry C, Westra WH, Li S, Cmelak A, Ridge JA, Pinto H, Forastiere A, Gillison ML.** 2008. Improved survival of patients with human papillomavirus-positive head and neck squamous cell carcinoma in a prospective clinical trial. *J Natl Cancer Inst* **100**:261-269.
26. **Ang KK, Harris J, Wheeler R, Weber R, Rosenthal DI, Nguyen-Tân PF, Westra WH, Chung CH, Jordan RC, Lu C, Kim H, Axelrod R, Silverman CC, Redmond KP, Gillison ML.** 2010. Human papillomavirus and survival of patients with oropharyngeal cancer. *N Engl J Med* **363**:24-35.
27. **Mirghani H, Blanchard P.** 2018. Treatment de-escalation for HPV-driven oropharyngeal cancer: Where do we stand? *Clin Transl Radiat Oncol* **8**:4-11.
28. **Zheng ZM, Baker CC.** 2006. Papillomavirus genome structure, expression, and post-transcriptional regulation. *Front Biosci* **11**:2286-2302.
29. **Doorbar J, Egawa N, Griffin H, Kranjec C, Murakami I.** 2015. Human papillomavirus molecular biology and disease association. *Rev Med Virol* **25 Suppl 1**:2-23.
30. **Chiang CM, Ustav M, Stenlund A, Ho TF, Broker TR, Chow LT.** 1992. Viral E1 and E2 proteins support replication of homologous and heterologous papillomaviral origins. *Proceedings of the National Academy of Sciences* **89**:5799-5803.

31. **Ustav M, Ustav E, Szymanski P, Stenlund A.** 1991. Identification of the origin of replication of bovine papillomavirus and characterization of the viral origin recognition factor E1. *Embo j* **10**:4321-4329.
32. **Thierry F.** 2009. Transcriptional regulation of the papillomavirus oncogenes by cellular and viral transcription factors in cervical carcinoma. *Virology* **384**:375-379.
33. **McBride AA.** 2013. The papillomavirus E2 proteins. *Virology* **445**:57-79.
34. **Hummel M, Hudson JB, Laimins LA.** 1992. Differentiation-induced and constitutive transcription of human papillomavirus type 31b in cell lines containing viral episomes. *Journal of Virology* **66**:6070-6080.
35. **Nasseri M, Hirochika R, Broker TR, Chow LT.** 1987. A human papilloma virus type 11 transcript encoding an E1^{E4} protein. *Virology* **159**:433-439.
36. **Doorbar J.** 2013. The E4 protein; structure, function and patterns of expression. *Virology* **445**:80-98.
37. **DiMaio D, Mattoon D.** 2001. Mechanisms of cell transformation by papillomavirus E5 proteins. *Oncogene* **20**:7866-7873.
38. **Venuti A, Paolini F, Nasir L, Corteggio A, Roperto S, Campo MS, Borzacchiello G.** 2011. Papillomavirus E5: the smallest oncoprotein with many functions. *Molecular Cancer* **10**:140.
39. **Wasson CW, Morgan EL, Müller M, Ross RL, Hartley M, Roberts S, Macdonald A.** 2017. Human papillomavirus type 18 E5 oncogene supports cell

- cycle progression and impairs epithelial differentiation by modulating growth factor receptor signalling during the virus lifecycle. *Oncotarget* **8**:103581-103600.
40. **DiMaio D, Petti LM.** 2013. The E5 proteins. *Virology* **445**:99-114.
 41. **Goldstein DJ, Andresson T, Sparkowski JJ, Schlegel R.** 1992. The BPV-1 E5 protein, the 16 kDa membrane pore-forming protein and the PDGF receptor exist in a complex that is dependent on hydrophobic transmembrane interactions. *The EMBO journal* **11**:4851-4859.
 42. **Tomakidi P, Cheng H, Kohl A, Komposch G, Alonso A.** 2000. Modulation of the epidermal growth factor receptor by the human papillomavirus type 16 E5 protein in raft cultures of human keratinocytes. *Eur J Cell Biol* **79**:407-412.
 43. **Pim D, Collins M, Banks L.** 1992. Human papillomavirus type 16 E5 gene stimulates the transforming activity of the epidermal growth factor receptor. *Oncogene* **7**:27-32.
 44. **de Freitas AC, de Oliveira THA, Barros MR, Jr., Venuti A.** 2017. hrHPV E5 oncoprotein: immune evasion and related immunotherapies. *J Exp Clin Cancer Res* **36**:71.
 45. **de Freitas AC, de Oliveira THA, Barros MR, Jr., Venuti A.** 2017. hrHPV E5 oncoprotein: immune evasion and related immunotherapies. *Journal of experimental & clinical cancer research : CR* **36**:71-71.
 46. **Genther SM, Sterling S, Duensing S, Münger K, Sattler C, Lambert PF.** 2003. Quantitative role of the human papillomavirus type 16 E5 gene during the productive stage of the viral lifecycle. *J Virol* **77**:2832-2842.

47. **Münger K, Baldwin A, Edwards KM, Hayakawa H, Nguyen CL, Owens M, Grace M, Huh K.** 2004. Mechanisms of Human Papillomavirus-Induced Oncogenesis. *Journal of Virology* **78**:11451-11460.
48. **Yim EK, Park JS.** 2005. The role of HPV E6 and E7 oncoproteins in HPV-associated cervical carcinogenesis. *Cancer Res Treat* **37**:319-324.
49. **Li X, Coffino P.** 1996. High-risk human papillomavirus E6 protein has two distinct binding sites within p53, of which only one determines degradation. *Journal of virology* **70**:4509-4516.
50. **Mansur CP, Marcus B, Dalal S, Androphy EJ.** 1995. The domain of p53 required for binding HPV 16 E6 is separable from the degradation domain. *Oncogene* **10**:457-465.
51. **Münger K, Scheffner M, Huibregtse JM, Howley PM.** 1992. Interactions of HPV E6 and E7 oncoproteins with tumour suppressor gene products. *Cancer Surv* **12**:197-217.
52. **Kao WH, Beaudenon SL, Talis AL, Huibregtse JM, Howley PM.** 2000. Human papillomavirus type 16 E6 induces self-ubiquitination of the E6AP ubiquitin-protein ligase. *J Virol* **74**:6408-6417.
53. **Watson RA, Thomas M, Banks L, Roberts S.** 2003. Activity of the human papillomavirus E6 PDZ-binding motif correlates with an enhanced morphological transformation of immortalized human keratinocytes. *Journal of Cell Science* **116**:4925-4934.

54. **Songock WK, Kim SM, Bodily JM.** 2017. The human papillomavirus E7 oncoprotein as a regulator of transcription. *Virus Res* **231**:56-75.
55. **Shin MK, Balsitis S, Brake T, Lambert PF.** 2009. Human papillomavirus E7 oncoprotein overrides the tumor suppressor activity of p21Cip1 in cervical carcinogenesis. *Cancer Res* **69**:5656-5663.
56. **Gonzalez SL, Stremlau M, He X, Basile JR, Münger K.** 2001. Degradation of the Retinoblastoma Tumor Suppressor by the Human Papillomavirus Type 16 E7 Oncoprotein Is Important for Functional Inactivation and Is Separable from Proteasomal Degradation of E7. *Journal of Virology* **75**:7583-7591.
57. **Chellappan S, Kraus VB, Kroger B, Munger K, Howley PM, Phelps WC, Nevins JR.** 1992. Adenovirus E1A, simian virus 40 tumor antigen, and human papillomavirus E7 protein share the capacity to disrupt the interaction between transcription factor E2F and the retinoblastoma gene product. *Proceedings of the National Academy of Sciences* **89**:4549-4553.
58. **James CD, Saini S, Sesay F, Ko K, Felthousen-Rusbasan J, Iness AN, Nulton T, Windle B, Dozmorov MG, Morgan IM, Litovchick L.** 2021. Restoring the DREAM Complex Inhibits the Proliferation of High-Risk HPV Positive Human Cells. *Cancers* **13**:489.
59. **Shin MK, Sage J, Lambert PF.** 2012. Inactivating all three rb family pocket proteins is insufficient to initiate cervical cancer. *Cancer Res* **72**:5418-5427.
60. **James CD, Saini S, Sesay F, Ko K, Felthousen-Rusbasan J, Iness AN, Nulton T, Windle B, Dozmorov MG, Morgan IM, Litovchick L.** 2021. Restoring the

DREAM Complex Inhibits the Proliferation of High-Risk HPV Positive Human Cells. *Cancers (Basel)* **13**.

61. **Finnen RL, Erickson KD, Chen XS, Garcea RL.** 2003. Interactions between papillomavirus L1 and L2 capsid proteins. *J Virol* **77**:4818-4826.
62. **D'Abramo C, Archambault J.** 2011. Small Molecule Inhibitors of Human Papillomavirus Protein - Protein Interactions. *The open virology journal* **5**:80-95.
63. **Graham SV.** 2010. Human papillomavirus: gene expression, regulation and prospects for novel diagnostic methods and antiviral therapies. *Future Microbiol* **5**:1493-1506.
64. **Nulton TJ, Olex AL, Dozmorov M, Morgan IM, Windle B.** 2017. Analysis of The Cancer Genome Atlas sequencing data reveals novel properties of the human papillomavirus 16 genome in head and neck squamous cell carcinoma. *Oncotarget* **8**.
65. **Vinokurova S, Wentzensen N, Kraus I, Klaes R, Driesch C, Melsheimer P, Kisseljov F, Dürst M, Schneider A, von Knebel Doeberitz M.** 2008. Type-dependent integration frequency of human papillomavirus genomes in cervical lesions. *Cancer Res* **68**:307-313.
66. **Cooper K, Herrington CS, Lo ES, Evans MF, McGee JO.** 1992. Integration of human papillomavirus types 16 and 18 in cervical adenocarcinoma. *J Clin Pathol* **45**:382-384.

67. **Fukushima M, Yamakawa Y, Shimano S, Hashimoto M, Sawada Y, Fujinaga K.** 1990. The physical state of human papillomavirus 16 DNA in cervical carcinoma and cervical intraepithelial neoplasia. *Cancer* **66**:2155-2161.
68. **Dürst M, Kleinheinz A, Hotz M, Gissmann L.** 1985. The physical state of human papillomavirus type 16 DNA in benign and malignant genital tumours. *J Gen Virol* **66 (Pt 7)**:1515-1522.
69. **Arias-Pulido H, Peyton CL, Joste NE, Vargas H, Wheeler CM.** 2006. Human papillomavirus type 16 integration in cervical carcinoma in situ and in invasive cervical cancer. *J Clin Microbiol* **44**:1755-1762.
70. **McBride AA, Warburton A.** 2017. The role of integration in oncogenic progression of HPV-associated cancers. *PLoS pathogens* **13**:e1006211-e1006211.
71. **Parfenov M, Pedomallu CS, Gehlenborg N, Freeman SS, Danilova L, Bristow CA, Lee S, Hadjipanayis AG, Ivanova EV, Wilkerson MD, Protopopov A, Yang L, Seth S, Song X, Tang J, Ren X, Zhang J, Pantazi A, Santoso N, Xu AW, Mahadeshwar H, Wheeler DA, Haddad RI, Jung J, Ojesina AI, Issaeva N, Yarbrough WG, Hayes DN, Grandis JR, El-Naggar AK, Meyerson M, Park PJ, Chin L, Seidman JG, Hammerman PS, Kucherlapati R.** 2014. Characterization of HPV and host genome interactions in primary head and neck cancers. *Proceedings of the National Academy of Sciences* **111**:15544-15549.
72. **Peter M, Stransky N, Couturier J, Hupé P, Barillot E, de Cremoux P, Cottu P, Radvanyi F, Sastre-Garau X.** 2010. Frequent genomic structural alterations at HPV insertion sites in cervical carcinoma. *J Pathol* **221**:320-330.

73. **Network CGA.** 2015. Comprehensive genomic characterization of head and neck squamous cell carcinomas. *Nature* **517**:576-582.
74. **Kalantari M, Blennow E, Hagmar B, Johansson B.** 2001. Physical State of HPV16 and Chromosomal Mapping of the Integrated Form in Cervical Carcinomas. *Diagnostic Molecular Pathology* **10**.
75. **Morgan IM, DiNardo LJ, Windle B.** 2017. Integration of Human Papillomavirus Genomes in Head and Neck Cancer: Is It Time to Consider a Paradigm Shift? *Viruses* **9**.
76. **Nulton TJ, Kim N-K, DiNardo LJ, Morgan IM, Windle B.** 2018. Patients with integrated HPV16 in head and neck cancer show poor survival. *Oral Oncology* **80**:52-55.
77. **Kelly JR, Husain ZA, Burtness B.** 2016. Treatment de-intensification strategies for head and neck cancer. *Eur J Cancer* **68**:125-133.
78. **Lim MY, Dahlstrom KR, Sturgis EM, Li G.** 2016. Human papillomavirus integration pattern and demographic, clinical, and survival characteristics of patients with oropharyngeal squamous cell carcinoma. *Head Neck* **38**:1139-1144.
79. **Kajitani N, Satsuka A, Kawate A, Sakai H.** 2012. Productive Lifecycle of Human Papillomaviruses that Depends Upon Squamous Epithelial Differentiation. *Front Microbiol* **3**:152.
80. **Jones KB, Klein OD.** 2013. Oral epithelial stem cells in tissue maintenance and disease: the first steps in a long journey. *International Journal of Oral Science* **5**:121-129.

81. **Kajitani N, Satsuka A, Kawate A, Sakai H.** 2012. Productive Lifecycle of Human Papillomaviruses that Depends Upon Squamous Epithelial Differentiation. *Frontiers in Microbiology* **3**.
82. **Moody CA, Laimins LA.** 2010. Human papillomavirus oncoproteins: pathways to transformation. *Nat Rev Cancer* **10**:550-560.
83. **Archambault J, Melendy T.** 2013. Targeting human papillomavirus genome replication for antiviral drug discovery. *Antiviral therapy* **18**:271-283.
84. **Rocque WJ, Porter DJ, Barnes JA, Dixon EP, Lobe DC, Su JL, Willard DH, Gaillard R, Condreay JP, Clay WC, Hoffman CR, Overton LK, Pahel G, Kost TA, Phelps WC.** 2000. Replication-associated activities of purified human papillomavirus type 11 E1 helicase. *Protein Expr Purif* **18**:148-159.
85. **Woodman C, Collins S, Young L.** 2007. The natural history of cervical HPV infection: unresolved issues. *Nature Reviews Cancer* **7**:11-22.
86. **Hernandez-Ramon EE, Burns JE, Zhang W, Walker HF, Allen S, Antson AA, Maitland NJ.** 2008. Dimerization of the Human Papillomavirus Type 16 E2 N Terminus Results in DNA Looping within the Upstream Regulatory Region. *Journal of Virology* **82**:4853-4861.
87. **Blakaj DM, Fernandez-Fuentes N, Chen Z, Hegde R, Fiser A, Burk RD, Brenowitz M.** 2009. Evolutionary and biophysical relationships among the papillomavirus E2 proteins. *Frontiers in bioscience (Landmark edition)*. **14**(900-917). doi:10.2741/3285.

88. **Giri I, Yaniv M.** 1988. Structural and mutational analysis of E2 trans-activating proteins of papillomaviruses reveals three distinct functional domains. *Embo j* **7**:2823-2829.
89. **McBride AA, Byrne JC, Howley PM.** 1989. E2 polypeptides encoded by bovine papillomavirus type 1 form dimers through the common carboxyl-terminal domain: transactivation is mediated by the conserved amino-terminal domain. *Proc Natl Acad Sci U S A* **86**:510-514.
90. **McBride AA, Schlegel R, Howley PM.** 1988. The carboxy-terminal domain shared by the bovine papillomavirus E2 transactivator and repressor proteins contains a specific DNA binding activity. *Embo j* **7**:533-539.
91. **Antson AA, Burns JE, Moroz OV, Scott DJ, Sanders CM, Bronstein IB, Dodson GG, Wilson KS, Maitland NJ.** 2000. Structure of the intact transactivation domain of the human papillomavirus E2 protein. *Nature* **403**:805-809.
92. **Phelps WC, Howley PM.** 1987. Transcriptional trans-activation by the human papillomavirus type 16 E2 gene product. *J Virol* **61**:1630-1638.
93. **Skiadopoulos MH, McBride AA.** 1998. Bovine papillomavirus type 1 genomes and the E2 transactivator protein are closely associated with mitotic chromatin. *J Virol* **72**:2079-2088.
94. **Bernard BA, Bailly C, Lenoir MC, Darmon M, Thierry F, Yaniv M.** 1989. The human papillomavirus type 18 (HPV18) E2 gene product is a repressor of the HPV18 regulatory region in human keratinocytes. *J Virol* **63**:4317-4324.

95. **Wu SY, Lee AY, Hou SY, Kemper JK, Erdjument-Bromage H, Tempst P, Chiang CM.** 2006. Brd4 links chromatin targeting to HPV transcriptional silencing. *Genes Dev* **20**:2383-2396.
96. **Bedrosian CL, Bastia D.** 1990. The DNA-binding domain of HPV-16 E2 protein interaction with the viral enhancer: protein-induced DNA bending and role of the nonconserved core sequence in binding site affinity. *Virology* **174**:557-575.
97. **Hegde RS, Androphy EJ.** 1998. Crystal structure of the E2 DNA-binding domain from human papillomavirus type 16: implications for its DNA binding-site selection mechanism. *J Mol Biol* **284**:1479-1489.
98. **Garnett TO, Duerksen-Hughes PJ.** 2006. Modulation of apoptosis by human papillomavirus (HPV) oncoproteins. *Archives of virology* **151**:2321-2335.
99. **Wells SI, Francis DA, Karpova AY, Dowhanick JJ, Benson JD, Howley PM.** 2000. Papillomavirus E2 induces senescence in HPV-positive cells via pRB- and p21(CIP)-dependent pathways. *Embo j* **19**:5762-5771.
100. **Jang MK, Shen K, McBride AA.** 2014. Papillomavirus genomes associate with BRD4 to replicate at fragile sites in the host genome. *PLoS Pathog* **10**:e1004117.
101. **Sakakibara N, Mitra R, McBride AA.** 2011. The papillomavirus E1 helicase activates a cellular DNA damage response in viral replication foci. *J Virol* **85**:8981-8995.
102. **Reinson T, Toots M, Kadaja M, Pipitch R, Allik M, Ustav E, Ustav M.** 2013. Engagement of the ATR-dependent DNA damage response at the human

- papillomavirus 18 replication centers during the initial amplification. *J Virol* **87**:951-964.
103. **Ustav E, Ustav M, Szymanski P, Stenlund A.** 1993. The bovine papillomavirus origin of replication requires a binding site for the E2 transcriptional activator. *Proc Natl Acad Sci U S A* **90**:898-902.
 104. **Võsa L, Sudakov A, Remm M, Ustav M, Kurg R.** 2012. Identification and analysis of papillomavirus E2 protein binding sites in the human genome. *Journal of virology* **86**:348-357.
 105. **Mohr IJ, Clark R, Sun S, Androphy EJ, MacPherson P, Botchan MR.** 1990. Targeting the E1 Replication Protein to the Papillomavirus Origin of Replication by Complex Formation with the E2 Transactivator. *Science* **250**:1694-1699.
 106. **Sanders CM, Stenlund A.** 1998. Recruitment and loading of the E1 initiator protein: an ATP-dependent process catalysed by a transcription factor. *The EMBO journal* **17**:7044-7055.
 107. **Sedman J, Stenlund A.** 1995. Co-operative interaction between the initiator E1 and the transcriptional activator E2 is required for replicator specific DNA replication of bovine papillomavirus in vivo and in vitro. *The EMBO Journal* **14**:6218-6228.
 108. **Conger KL, Liu JS, Kuo SR, Chow LT, Wang TS.** 1999. Human papillomavirus DNA replication. Interactions between the viral E1 protein and two subunits of human dna polymerase alpha/primase. *J Biol Chem* **274**:2696-2705.

109. **Loo YM, Melendy T.** 2004. Recruitment of replication protein A by the papillomavirus E1 protein and modulation by single-stranded DNA. *J Virol* **78**:1605-1615.
110. **Clower RV, Fisk JC, Melendy T.** 2006. Papillomavirus E1 protein binds to and stimulates human topoisomerase I. *Journal of virology* **80**:1584-1587.
111. **Melendy T, Sedman J, Stenlund A.** 1995. Cellular factors required for papillomavirus DNA replication. *Journal of Virology* **69**:7857-7867.
112. **Bergvall M, Melendy T, Archambault J.** 2013. The E1 proteins. *Virology* **445**:35-56.
113. **Chojnacki M, Melendy T.** 2018. The human papillomavirus DNA helicase E1 binds, stimulates, and confers processivity to cellular DNA polymerase epsilon. *Nucleic acids research* **46**:229-241.
114. **Schuck S, Ruse C, Stenlund A.** 2013. CK2 phosphorylation inactivates DNA binding by the papillomavirus E1 and E2 proteins. *Journal of virology* **87**:7668-7679.
115. **Li R, Botchan MR.** 1994. Acidic transcription factors alleviate nucleosome-mediated repression of DNA replication of bovine papillomavirus type 1. *Proceedings of the National Academy of Sciences of the United States of America* **91**:7051-7055.
116. **Chen G, Stenlund A.** 1998. Characterization of the DNA-binding domain of the bovine papillomavirus replication initiator E1. *J Virol* **72**:2567-2576.

117. **Bouvard V, Storey A, Pim D, Banks L.** 1994. Characterization of the human papillomavirus E2 protein: evidence of trans-activation and trans-repression in cervical keratinocytes. *Embo j* **13**:5451-5459.
118. **Cripe TP, Haugen TH, Turk JP, Tabatabai F, Schmid PG, 3rd, Dürst M, Gissmann L, Roman A, Turek LP.** 1987. Transcriptional regulation of the human papillomavirus-16 E6-E7 promoter by a keratinocyte-dependent enhancer, and by viral E2 trans-activator and repressor gene products: implications for cervical carcinogenesis. *Embo j* **6**:3745-3753.
119. **Vance KW, Campo MS, Morgan IM.** 2001. A Novel Silencer Element in the Bovine Papillomavirus Type 4 Promoter Represses the Transcriptional Response to Papillomavirus E2 Protein. *Journal of Virology* **75**:2829-2838.
120. **Vance KW, Campo MS, Morgan IM.** 1999. An enhanced epithelial response of a papillomavirus promoter to transcriptional activators. *J Biol Chem* **274**:27839-27844.
121. **Demeret C, Desaintes C, Yaniv M, Thierry F.** 1997. Different mechanisms contribute to the E2-mediated transcriptional repression of human papillomavirus type 18 viral oncogenes. *J Virol* **71**:9343-9349.
122. **Cha S, Seo T.** 2011. hSNF5 is required for human papillomavirus E2-driven transcriptional activation and DNA replication. *Intervirology* **54**:66-77.
123. **Schweiger M-R, You J, Howley PM.** 2006. Bromodomain Protein 4 Mediates the Papillomavirus E2 Transcriptional Activation Function. *Journal of Virology* **80**:4276-4285.

124. **Smith JA, White EA, Sowa ME, Powell MLC, Ottinger M, Harper JW, Howley PM.** 2010. Genome-wide siRNA screen identifies SMCX, EP400, and Brd4 as E2-dependent regulators of human papillomavirus oncogene expression. *Proceedings of the National Academy of Sciences* **107**:3752-3757.
125. **Gauson EJ, Windle B, Donaldson MM, Caffarel MM, Dornan ES, Coleman N, Herzyk P, Henderson SC, Wang X, Morgan IM.** 2014. Regulation of human genome expression and RNA splicing by human papillomavirus 16 E2 protein. *Virology* **468-470**:10-18.
126. **Evans MR, James CD, Bristol ML, Nulton TJ, Wang X, Kaur N, White EA, Windle B, Morgan IM.** 2019. Human Papillomavirus 16 E2 Regulates Keratinocyte Gene Expression Relevant to Cancer and the Viral Lifecycle. *Journal of Virology* **93**:e01941-01918.
127. **Fontan CT, Das D, Bristol ML, James CD, Wang X, Lohner H, Atfi A, Morgan IM.** 2020. Human papillomavirus 16 E2 repression of TWIST1 transcription is a potential mediator of HPV16 cancer outcomes. *bioRxiv* doi:10.1101/2020.09.25.314484;2020.2009.2025.314484.
128. **Taylor ER, Boner W, Dornan ES, Corr EM, Morgan IM.** 2003. UVB irradiation reduces the half-life and transactivation potential of the human papillomavirus 16 E2 protein. *Oncogene* **22**:4469-4477.
129. **Lee D, Hwang SG, Kim J, Choe J.** 2002. Functional interaction between p/CAF and human papillomavirus E2 protein. *J Biol Chem* **277**:6483-6489.

130. **Müller A, Ritzkowsky A, Steger G.** 2002. Cooperative activation of human papillomavirus type 8 gene expression by the E2 protein and the cellular coactivator p300. *J Virol* **76**:11042-11053.
131. **Rehtanz M, Schmidt HM, Warthorst U, Steger G.** 2004. Direct interaction between nucleosome assembly protein 1 and the papillomavirus E2 proteins involved in activation of transcription. *Mol Cell Biol* **24**:2153-2168.
132. **Bellanger S, Tan CL, Xue YZ, Teissier S, Thierry F.** 2011. Tumor suppressor or oncogene? A critical role of the human papillomavirus (HPV) E2 protein in cervical cancer progression. *American journal of cancer research* **1**:373-389.
133. **Gammoh N, Gardiol D, Massimi P, Banks L.** 2009. The Mdm2 Ubiquitin Ligase Enhances Transcriptional Activity of Human Papillomavirus E2. *Journal of Virology* **83**:1538-1543.
134. **Sunthamala N, Thierry F, Teissier S, Pientong C, Kongyingyoes B, Tangsiriwatthana T, Sangkomkamhang U, Ekalaksananan T.** 2014. E2 proteins of high risk human papillomaviruses down-modulate STING and IFN- κ transcription in keratinocytes. *PloS one* **9**:e91473-e91473.
135. **McBride AA.** 2008. Replication and partitioning of papillomavirus genomes. *Adv Virus Res* **72**:155-205.
136. **Ilves I, Kivi S, Ustav M.** 1999. Long-term episomal maintenance of bovine papillomavirus type 1 plasmids is determined by attachment to host chromosomes, which is mediated by the viral E2 protein and its binding sites. *J Virol* **73**:4404-4412.

137. **Poddar A, Reed SC, McPhillips MG, Spindler JE, McBride AA.** 2009. The human papillomavirus type 8 E2 tethering protein targets the ribosomal DNA loci of host mitotic chromosomes. *J Virol* **83**:640-650.
138. **McBride AA, Sakakibara N, Stepp WH, Jang MK.** 2012. Hitchhiking on host chromatin: how papillomaviruses persist. *Biochim Biophys Acta* **1819**:820-825.
139. **Kurg R, Sild K, Ilves A, Sepp M, Ustav M.** 2005. Association of Bovine Papillomavirus E2 Protein with Nuclear Structures In Vivo. *Journal of Virology* **79**:10528-10539.
140. **McBride A, De Oliveira J, McPhillips M.** 2006. Partitioning Viral Genomes in Mitosis: Same Idea, Different Targets. *Cell cycle (Georgetown, Tex)* **5**:1499-1502.
141. **Knipe DM, Lieberman PM, Jung JU, McBride AA, Morris KV, Ott M, Margolis D, Nieto A, Nevels M, Parks RJ, Kristie TM.** 2013. Snapshots: chromatin control of viral infection. *Virology* **435**:141-156.
142. **Bentley P, Tan MJA, McBride AA, White EA, Howley PM.** 2018. The SMC5/6 Complex Interacts with the Papillomavirus E2 Protein and Influences Maintenance of Viral Episomal DNA. *J Virol* **92**.
143. **Sekhar V, McBride AA.** 2012. Phosphorylation Regulates Binding of the Human Papillomavirus Type 8 E2 Protein to Host Chromosomes. *Journal of Virology* **86**:10047-10058.
144. **Sekhar V, Reed SC, McBride AA.** 2010. Interaction of the betapapillomavirus E2 tethering protein with mitotic chromosomes. *Journal of virology* **84**:543-557.

145. **Nasmyth K.** 2002. Segregating sister genomes: the molecular biology of chromosome separation. *Science* **297**:559-565.
146. **Lehman CW, Botchan MR.** 1998. Segregation of viral plasmids depends on tethering to chromosomes and is regulated by phosphorylation. *Proc Natl Acad Sci U S A* **95**:4338-4343.
147. **Ilves I, Kivi S, Ustav M.** 1999. Long-term episomal maintenance of bovine papillomavirus type 1 plasmids is determined by attachment to host chromosomes, which is mediated by the viral E2 protein and its binding sites. *Journal of virology* **73**:4404-4412.
148. **You J, Croyle JL, Nishimura A, Ozato K, Howley PM.** 2004. Interaction of the bovine papillomavirus E2 protein with Brd4 tethers the viral DNA to host mitotic chromosomes. *Cell* **117**:349-360.
149. **Skidopoulos MH, McBride AA.** 1998. Bovine Papillomavirus Type 1 Genomes and the E2 Transactivator Protein Are Closely Associated with Mitotic Chromatin. *Journal of Virology* **72**:2079-2088.
150. **Muller M, Demeret C.** 2012. The HPV E2-Host Protein-Protein Interactions: A Complex Hijacking of the Cellular Network. *Open Virol J* **6**:173-189.
151. **Yang Z, Yik JH, Chen R, He N, Jang MK, Ozato K, Zhou Q.** 2005. Recruitment of P-TEFb for stimulation of transcriptional elongation by the bromodomain protein Brd4. *Mol Cell* **19**:535-545.
152. **Malik S, Roeder RG.** 2000. Transcriptional regulation through Mediator-like coactivators in yeast and metazoan cells. *Trends Biochem Sci* **25**:277-283.

153. **Wu SY, Chiang CM.** 2007. The double bromodomain-containing chromatin adaptor Brd4 and transcriptional regulation. *J Biol Chem* **282**:13141-13145.
154. **Mochizuki K, Nishiyama A, Jang MK, Dey A, Ghosh A, Tamura T, Natsume H, Yao H, Ozato K.** 2008. The bromodomain protein Brd4 stimulates G1 gene transcription and promotes progression to S phase. *J Biol Chem* **283**:9040-9048.
155. **Houzelstein D, Bullock SL, Lynch DE, Grigorieva EF, Wilson VA, Beddington RSP.** 2002. Growth and Early Postimplantation Defects in Mice Deficient for the Bromodomain-Containing Protein Brd4. *Molecular and Cellular Biology* **22**:3794-3802.
156. **Donati B, Lorenzini E, Ciarrocchi A.** 2018. BRD4 and Cancer: going beyond transcriptional regulation. *Molecular cancer* **17**:164-164.
157. **Ives I, Mäemets K, Silla T, Janikson K, Ustav M.** 2006. Brd4 Is Involved in Multiple Processes of the Bovine Papillomavirus Type 1 Lifecycle. *Journal of Virology* **80**:3660-3665.
158. **McPhillips MG, Oliveira JG, Spindler JE, Mitra R, McBride AA.** 2006. Brd4 is required for e2-mediated transcriptional activation but not genome partitioning of all papillomaviruses. *Journal of virology* **80**:9530-9543.
159. **Sénéchal H, Poirier GG, Coulombe B, Laimins LA, Archambault J.** 2007. Amino acid substitutions that specifically impair the transcriptional activity of papillomavirus E2 affect binding to the long isoform of Brd4. *Virology* **358**:10-17.
160. **Baxter MK, McPhillips MG, Ozato K, McBride AA.** 2005. The Mitotic Chromosome Binding Activity of the Papillomavirus E2 Protein Correlates with

- Interaction with the Cellular Chromosomal Protein, Brd4. *Journal of Virology* **79**:4806-4818.
161. **Jang MK, Kwon D, McBride AA.** 2009. Papillomavirus E2 Proteins and the Host Brd4 Protein Associate with Transcriptionally Active Cellular Chromatin. *Journal of Virology* **83**:2592-2600.
162. **Abbate EA, Voitenleitner C, Botchan MR.** 2006. Structure of the papillomavirus DNA-tethering complex E2:Brd4 and a peptide that ablates HPV chromosomal association. *Mol Cell* **24**:877-889.
163. **Abroi A, Kurg R, Ustav M.** 1996. Transcriptional and replicational activation functions in the bovine papillomavirus type 1 E2 protein are encoded by different structural determinants. *J Virol* **70**:6169-6179.
164. **Cooper CS, Upmeyer SN, Winokur PL.** 1998. Identification of single amino acids in the human papillomavirus 11 E2 protein critical for the transactivation or replication functions. *Virology* **241**:312-322.
165. **Ferguson MK, Botchan MR.** 1996. Genetic analysis of the activation domain of bovine papillomavirus protein E2: its role in transcription and replication. *J Virol* **70**:4193-4199.
166. **Winokur PL, McBride AA.** 1992. Separation of the transcriptional activation and replication functions of the bovine papillomavirus-1 E2 protein. *Embo j* **11**:4111-4118.
167. **Breiding DE, Grossel MJ, Androphy EJ.** 1996. Genetic analysis of the bovine papillomavirus E2 transcriptional activation domain. *Virology* **221**:34-43.

168. **Sakai H, Yasugi T, Benson JD, Dowhanick JJ, Howley PM.** 1996. Targeted mutagenesis of the human papillomavirus type 16 E2 transactivation domain reveals separable transcriptional activation and DNA replication functions. *J Virol* **70**:1602-1611.
169. **Yan J, Li Q, Lievens S, Tavernier J, You J.** 2010. Abrogation of the Brd4-positive transcription elongation factor B complex by papillomavirus E2 protein contributes to viral oncogene repression. *J Virol* **84**:76-87.
170. **Smith JA, White EA, Sowa ME, Powell ML, Ottinger M, Harper JW, Howley PM.** 2010. Genome-wide siRNA screen identifies SMCX, EP400, and Brd4 as E2-dependent regulators of human papillomavirus oncogene expression. *Proc Natl Acad Sci U S A* **107**:3752-3757.
171. **Schweiger MR, Ottinger M, You J, Howley PM.** 2007. Brd4-independent transcriptional repression function of the papillomavirus e2 proteins. *J Virol* **81**:9612-9622.
172. **Gauson EJ, Wang X, Dornan ES, Herzyk P, Bristol M, Morgan IM.** 2016. Failure to interact with Brd4 alters the ability of HPV16 E2 to regulate host genome expression and cellular movement. *Virus Res* **211**:1-8.
173. **Wang X, Helfer CM, Pancholi N, Bradner JE, You J.** 2013. Recruitment of Brd4 to the Human Papillomavirus Type 16 DNA Replication Complex Is Essential for Replication of Viral DNA. *Journal of Virology* **87**:3871-3884.

174. **Baxter MK, McPhillips MG, Ozato K, McBride AA.** 2005. The mitotic chromosome binding activity of the papillomavirus E2 protein correlates with interaction with the cellular chromosomal protein, Brd4. *J Virol* **79**:4806-4818.
175. **Baxter MK, McBride AA.** 2005. An acidic amphipathic helix in the Bovine Papillomavirus E2 protein is critical for DNA replication and interaction with the E1 protein. *Virology* **332**:78-88.
176. **Gauson EJ, Donaldson MM, Dornan ES, Wang X, Bristol M, Bodily JM, Morgan IM.** 2015. Evidence Supporting a Role for TopBP1 and Brd4 in the Initiation but Not Continuation of Human Papillomavirus 16 E1/E2-Mediated DNA Replication. *Journal of Virology* **89**:4980-4991.
177. **Abroi A, Ilves I, Kivi S, Ustav M.** 2004. Analysis of chromatin attachment and partitioning functions of bovine papillomavirus type 1 E2 protein. *J Virol* **78**:2100-2113.
178. **Bastien N, McBride AA.** 2000. Interaction of the papillomavirus E2 protein with mitotic chromosomes. *Virology* **270**:124-134.
179. **Silla T, Männik A, Ustav M.** 2010. Effective formation of the segregation-competent complex determines successful partitioning of the bovine papillomavirus genome during cell division. *Journal of virology* **84**:11175-11188.
180. **McPhillips MG, Ozato K, McBride AA.** 2005. Interaction of bovine papillomavirus E2 protein with Brd4 stabilizes its association with chromatin. *J Virol* **79**:8920-8932.

181. **Oliveira JG, Colf LA, McBride AA.** 2006. Variations in the association of papillomavirus E2 proteins with mitotic chromosomes. *Proc Natl Acad Sci U S A* **103**:1047-1052.
182. **Boner W, Taylor ER, Tsirimonaki E, Yamane K, Campo MS, Morgan IM.** 2002. A Functional interaction between the human papillomavirus 16 transcription/replication factor E2 and the DNA damage response protein TopBP1. *J Biol Chem* **277**:22297-22303.
183. **Boner W, Morgan IM.** 2002. Novel cellular interacting partners of the human papillomavirus 16 transcription/replication factor E2. *Virus Res* **90**:113-118.
184. **Gauson EJ, Donaldson MM, Dornan ES, Wang X, Bristol M, Bodily JM, Morgan IM.** 2015. Evidence supporting a role for TopBP1 and Brd4 in the initiation but not continuation of human papillomavirus 16 E1/E2-mediated DNA replication. *J Virol* **89**:4980-4991.
185. **Donaldson MM, Mackintosh LJ, Bodily JM, Dornan ES, Laimins LA, Morgan IM.** 2012. An Interaction between Human Papillomavirus 16 E2 and TopBP1 Is Required for Optimum Viral DNA Replication and Episomal Genome Establishment. *Journal of Virology* **86**:12806-12815.
186. **Kanginakudru S, DeSmet M, Thomas Y, Morgan IM, Androphy EJ.** 2015. Levels of the E2 interacting protein TopBP1 modulate papillomavirus maintenance stage replication. *Virology* **478**:129-135.

187. **Donaldson MM, Boner W, Morgan IM.** 2007. TopBP1 Regulates Human Papillomavirus Type 16 E2 Interaction with Chromatin. *Journal of Virology* **81**:4338-4342.
188. **Wardlaw CP, Carr AM, Oliver AW.** 2014. TopBP1: A BRCT-scaffold protein functioning in multiple cellular pathways. *DNA Repair (Amst)* **22**:165-174.
189. **Wright RH, Dornan ES, Donaldson MM, Morgan IM.** 2006. TopBP1 contains a transcriptional activation domain suppressed by two adjacent BRCT domains. *Biochem J* **400**:573-582.
190. **Yu X, Chini CC, He M, Mer G, Chen J.** 2003. The BRCT domain is a phospho-protein binding domain. *Science* **302**:639-642.
191. **Day M, Rappas M, Ptasinska K, Boos D, Oliver AW, Pearl LH.** 2018. BRCT domains of the DNA damage checkpoint proteins TOPBP1/Rad4 display distinct specificities for phosphopeptide ligands. *eLife* **7**:e39979.
192. **Rappas M, Oliver AW, Pearl LH.** 2010. Structure and function of the Rad9-binding region of the DNA-damage checkpoint adaptor TopBP1. *Nucleic Acids Research* **39**:313-324.
193. **Qu M, Rappas M, Wardlaw Christopher P, Garcia V, Ren J-Y, Day M, Carr Antony M, Oliver Antony W, Du L-L, Pearl Laurence H.** 2013. Phosphorylation-Dependent Assembly and Coordination of the DNA Damage Checkpoint Apparatus by Rad4TopBP1. *Molecular Cell* **51**:723-736.
194. **Liu K, Paik JC, Wang B, Lin FT, Lin WC.** 2006. Regulation of TopBP1 oligomerization by Akt/PKB for cell survival. *Embo j* **25**:4795-4807.

195. **Herold S, Wanzel M, Beuger V, Frohme C, Beul D, Hillukkala T, Syvaioja J, Saluz HP, Haenel F, Eilers M.** 2002. Negative regulation of the mammalian UV response by Myc through association with Miz-1. *Mol Cell* **10**:509-521.
196. **Kumagai A, Shevchenko A, Shevchenko A, Dunphy WG.** 2010. Treslin collaborates with TopBP1 in triggering the initiation of DNA replication. *Cell* **140**:349-359.
197. **Boos D, Sanchez-Pulido L, Rappas M, Pearl LH, Oliver AW, Ponting CP, Diffley JF.** 2011. Regulation of DNA replication through Sld3-Dpb11 interaction is conserved from yeast to humans. *Curr Biol* **21**:1152-1157.
198. **Boos D, Yekezare M, Diffley JF.** 2013. Identification of a heteromeric complex that promotes DNA replication origin firing in human cells. *Science* **340**:981-984.
199. **Sansam CG, Goins D, Siefert JC, Clowdus EA, Sansam CL.** 2015. Cyclin-dependent kinase regulates the length of S phase through TICRR/TRESLIN phosphorylation. *Genes Dev* **29**:555-566.
200. **Mordes DA, Glick GG, Zhao R, Cortez D.** 2008. TopBP1 activates ATR through ATRIP and a PIKK regulatory domain. *Genes & development* **22**:1478-1489.
201. **Yoo HY, Kumagai A, Shevchenko A, Shevchenko A, Dunphy WG.** 2007. Ataxia-telangiectasia mutated (ATM)-dependent activation of ATR occurs through phosphorylation of TopBP1 by ATM. *J Biol Chem* **282**:17501-17506.
202. **Anacker DC, Moody CA.** 2017. Modulation of the DNA damage response during the lifecycle of human papillomaviruses. *Virus research* **231**:41-49.

203. **Anacker DC, Aloor HL, Shepard CN, Lenzi GM, Johnson BA, Kim B, Moody CA.** 2016. HPV31 utilizes the ATR-Chk1 pathway to maintain elevated RRM2 levels and a replication-competent environment in differentiating Keratinocytes. *Virology* **499**:383-396.
204. **Gautam D, Moody CA.** 2016. Impact of the DNA Damage Response on Human Papillomavirus Chromatin. *PLoS pathogens* **12**:e1005613.
205. **Moody CA, Laimins LA.** 2009. Human papillomaviruses activate the ATM DNA damage pathway for viral genome amplification upon differentiation. *PLoS pathogens* **5**:e1000605.
206. **Hong S, Cheng S, Iovane A, Laimins LA.** 2015. STAT-5 Regulates Transcription of the Topoisomerase IIbeta-Binding Protein 1 (TopBP1) Gene To Activate the ATR Pathway and Promote Human Papillomavirus Replication. *mBio* **6**:e02006-02015.
207. **Rappas M, Oliver AW, Pearl LH.** 2013. Structure and function of the Rad9-binding region of the DNA-damage checkpoint adaptor TopBP1. *Nucleic Acids Research* **41**:4741-4741.
208. **Bang SW, Kim GS, Hwang DS.** 2013. Oligomerization of TopBP1 is necessary for the localization of TopBP1 to mitotic centrosomes. *Biochem Biophys Res Commun* **436**:31-34.
209. **Pedersen RT, Kruse T, Nilsson J, Oestergaard VH, Lisby M.** 2015. TopBP1 is required at mitosis to reduce transmission of DNA damage to G1 daughter cells. *J Cell Biol* **210**:565-582.

210. **Broderick R, Nieminuszczy J, Blackford AN, Winczura A, Niedzwiedz W.** 2015. TOPBP1 recruits TOP2A to ultra-fine anaphase bridges to aid in their resolution. *Nature Communications* **6**:6572.
211. **Leimbacher PA, Jones SE, Shorrocks AK, de Marco Zompit M, Day M, Blaauwendraad J, Bundschuh D, Bonham S, Fischer R, Fink D, Kessler BM, Oliver AW, Pearl LH, Blackford AN, Stucki M.** 2019. MDC1 Interacts with TOPBP1 to Maintain Chromosomal Stability during Mitosis. *Mol Cell* **74**:571-583.e578.
212. **Takeishi Y, Ohashi E, Ogawa K, Masai H, Obuse C, Tsurimoto T.** 2010. Casein kinase 2-dependent phosphorylation of human Rad9 mediates the interaction between human Rad9-Hus1-Rad1 complex and TopBP1. *Genes Cells* **15**:761-771.
213. **Liu K, Lin FT, Ruppert JM, Lin WC.** 2003. Regulation of E2F1 by BRCT domain-containing protein TopBP1. *Mol Cell Biol* **23**:3287-3304.
214. **Liu K, Bellam N, Lin HY, Wang B, Stockard CR, Grizzle WE, Lin WC.** 2009. Regulation of p53 by TopBP1: a potential mechanism for p53 inactivation in cancer. *Mol Cell Biol* **29**:2673-2693.
215. **Bouvard V, Storey A, Pim D, Banks L.** 1994. Characterization of the human papillomavirus E2 protein: evidence of trans-activation and trans-repression in cervical keratinocytes. *The EMBO Journal* **13**:5451-5459.
216. **Wieland A, Patel MR, Cardenas MA, Eberhardt CS, Hudson WH, Obeng RC, Griffith CC, Wang X, Chen ZG, Kissick HT, Saba NF, Ahmed R.** 2020.

Defining HPV-specific B cell responses in patients with head and neck cancer.
Nature doi:10.1038/s41586-020-2931-3.

217. **Bristol ML, James CD, Wang X, Fontan CT, Morgan IM.** 2020. Estrogen Attenuates the Growth of Human Papillomavirus-Positive Epithelial Cells. *mSphere* **5**.
218. **Berge U, Bochenek D, Schnabel R, Wehling A, Schroeder T, Stadler T, Kroschewski R.** 2019. Asymmetric division events promote variability in cell cycle duration in animal cells and *Escherichia coli*. *Nat Commun* **10**:1901.
219. **Meyers C, Frattini M, Hudson J, Laimins L.** 1992. Biosynthesis of human papillomavirus from a continuous cell line upon epithelial differentiation. *Science* **257**:971-973.
220. **Dollard SC, Wilson JL, Demeter LM, Bonnez W, Reichman RC, Broker TR, Chow LT.** 1992. Production of human papillomavirus and modulation of the infectious program in epithelial raft cultures. *Genes Dev* **6**:1131-1142.
221. **Bienkowska-Haba M, Luszczek W, Myers JE, Keiffer TR, DiGiuseppe S, Polk P, Bodily JM, Scott RS, Sapp M.** 2018. A new cell culture model to genetically dissect the complete human papillomavirus lifecycle. *PLoS Pathog* **14**:e1006846.
222. **Piirsoo A, Piirsoo M, Kala M, Sankovski E, Lototskaja E, Levin V, Salvi M, Ustav M.** 2019. Activity of CK2 α protein kinase is required for efficient replication of some HPV types. *PLoS Pathog* **15**:e1007788.

223. **Taylor ER, Morgan IM.** 2003. A novel technique with enhanced detection and quantitation of HPV-16 E1- and E2-mediated DNA replication. *Virology* **315**:103-109.
224. **Litchfield DW.** 2003. Protein kinase CK2: structure, regulation and role in cellular decisions of life and death. *Biochem J* **369**:1-15.
225. **Rusin SF, Adamo ME, Kettenbach AN.** 2017. Identification of Candidate Casein Kinase 2 Substrates in Mitosis by Quantitative Phosphoproteomics. *Front Cell Dev Biol* **5**:97.
226. **Jang MK, Anderson DE, van Doorslaer K, McBride AA.** 2015. A proteomic approach to discover and compare interacting partners of papillomavirus E2 proteins from diverse phylogenetic groups. *Proteomics* **15**:2038-2050.
227. **Bigot N, Day M, Baldock RA, Watts FZ, Oliver AW, Pearl LH.** 2019. Phosphorylation-mediated interactions with TOPBP1 couple 53BP1 and 9-1-1 to control the G1 DNA damage checkpoint. *Elife* **8**.
228. **Day M, Rappas M, Ptasinska K, Boos D, Oliver AW, Pearl LH.** 2018. BRCT domains of the DNA damage checkpoint proteins TOPBP1/Rad4 display distinct specificities for phosphopeptide ligands. *Elife* **7**.
229. **Takeishi Y, Ohashi E, Ogawa K, Masai H, Obuse C, Tsurimoto T.** 2010. Casein kinase 2-dependent phosphorylation of human Rad9 mediates the interaction between human Rad9-Hus1-Rad1 complex and TopBP1. *Genes to Cells* **15**:761-771.

230. **Cozza G, Pinna LA, Moro S.** 2013. Kinase CK2 inhibition: an update. *Curr Med Chem* **20**:671-693.
231. **Evans MR, James CD, Bristol ML, Nulton TJ, Wang X, Kaur N, White EA, Windle B, Morgan IM.** 2019. Human Papillomavirus 16 E2 Regulates Keratinocyte Gene Expression Relevant to Cancer and the Viral Lifecycle. *J Virol* **93**.
232. **Evans MR, James CD, Loughran O, Nulton TJ, Wang X, Bristol ML, Windle B, Morgan IM.** 2017. An oral keratinocyte lifecycle model identifies novel host genome regulation by human papillomavirus 16 relevant to HPV positive head and neck cancer. *Oncotarget* doi:10.18632/oncotarget.18328 [doi].
233. **James CD, Das D, Morgan EL, Otoa R, Macdonald A, Morgan IM.** 2020. Werner Syndrome Protein (WRN) Regulates Cell Proliferation and the Human Papillomavirus 16 Lifecycle during Epithelial Differentiation. *mSphere* **5**.
234. **James CD, Prabhakar AT, Otoa R, Evans MR, Wang X, Bristol ML, Zhang K, Li R, Morgan IM.** 2019. SAMHD1 Regulates Human Papillomavirus 16-Induced Cell Proliferation and Viral Replication during Differentiation of Keratinocytes. *mSphere* **4**.
235. **Krawczyk E, Supryniewicz FA, Liu X, Dai Y, Hartmann DP, Hanover J, Schlegel R.** 2008. Koilocytosis: a cooperative interaction between the human papillomavirus E5 and E6 oncoproteins. *Am J Pathol* **173**:682-688.

236. **Xue Y, Bellanger S, Zhang W, Lim D, Low J, Lunny D, Thierry F.** 2010. HPV16 E2 is an immediate early marker of viral infection, preceding E7 expression in precursor structures of cervical carcinoma. *Cancer research* **70**:5316-5325.
237. **Wang HK, Duffy AA, Broker TR, Chow LT.** 2009. Robust production and passaging of infectious HPV in squamous epithelium of primary human keratinocytes. *Genes Dev* **23**:181-194.
238. **Morgan IM, Taylor ER.** 2005. Detection and quantitation of HPV DNA replication by Southern blotting and real-time PCR. *Methods Mol Med* **119**:349-362.
239. **Myers JE, Zwolinska K, Sapp MJ, Scott RS.** 2020. An Exonuclease V-qPCR Assay to Analyze the State of the Human Papillomavirus 16 Genome in Cell Lines and Tissues. *Curr Protoc Microbiol* **59**:e119.
240. **Myers JE, Guidry JT, Scott ML, Zwolinska K, Raikhy G, Prasai K, Bienkowska-Haba M, Bodily JM, Sapp MJ, Scott RS.** 2019. Detecting episomal or integrated human papillomavirus 16 DNA using an exonuclease V-qPCR-based assay. *Virology* **537**:149-156.
241. **Nuñez de Villavicencio-Diaz T, Rabalski AJ, Litchfield DW.** 2017. Protein Kinase CK2: Intricate Relationships within Regulatory Cellular Networks. *Pharmaceuticals (Basel)* **10**.
242. **Penrose KJ, Garcia-Alai M, de Prat-Gay G, McBride AA.** 2004. Casein Kinase II phosphorylation-induced conformational switch triggers degradation of the papillomavirus E2 protein. *The Journal of biological chemistry* **279**:22430-22439.

243. **Schuck S, Ruse C, Stenlund A.** 2013. CK2 phosphorylation inactivates DNA binding by the papillomavirus E1 and E2 proteins. *J Virol* **87**:7668-7679.
244. **Piirsoo A, Kala M, Sankovski E, Ustav M, Piirsoo M.** 2020. Uncovering the Role of the E1 Protein in Different Stages of Human Papillomavirus 18 Genome Replication. *J Virol* **94**.
245. **Wu SY, Nin DS, Lee AY, Simanski S, Kodadek T, Chiang CM.** 2016. BRD4 Phosphorylation Regulates HPV E2-Mediated Viral Transcription, Origin Replication, and Cellular MMP-9 Expression. *Cell reports* **16**:1733-1748.
246. **Gauson EJ, Donaldson MM, Dornan ES, Wang X, Bristol M, Bodily JM, Morgan IM.** 2015. Evidence supporting a role for TopBP1 and Brd4 in the initiation but not continuation of human papillomavirus 16 E1/E2 mediated DNA replication. *Journal of virology* **89**:17684-17699.
247. **Schweiger MR, You J, Howley PM.** 2006. Bromodomain protein 4 mediates the papillomavirus E2 transcriptional activation function. *Journal of virology* **80**:4276-4285.
248. **Genovese NJ, Banerjee NS, Broker TR, Chow LT.** 2008. Casein kinase II motif-dependent phosphorylation of human papillomavirus E7 protein promotes p130 degradation and S-phase induction in differentiated human keratinocytes. *J Virol* **82**:4862-4873.
249. **Basukala O, Mittal S, Massimi P, Bestagno M, Banks L.** 2019. The HPV-18 E7 CKII phospho acceptor site is required for maintaining the transformed phenotype of cervical tumour-derived cells. *PLoS Pathog* **15**:e1007769.

250. **McBride AA, Sakakibara N, Stepp WH, Jang MK.** 2012. Hitchhiking on host chromatin: how papillomaviruses persist. *Biochimica et biophysica acta* **1819**:820-825.
251. **McPhillips MG, Ozato K, McBride AA.** 2005. Interaction of Bovine Papillomavirus E2 Protein with Brd4 Stabilizes Its Association with Chromatin Interaction of Bovine Papillomavirus E2 Protein with Brd4 Stabilizes Its Association with Chromatin. **79**.
252. **Broderick R, Niedzwiedz W.** 2015. Sister chromatid decatenation: bridging the gaps in our knowledge. *Cell Cycle* **14**:3040-3044.
253. **Broderick R, Nieminuszczy J, Blackford AN, Winczura A, Niedzwiedz W.** 2015. TOPBP1 recruits TOP2A to ultra-fine anaphase bridges to aid in their resolution. *Nature communications* **6**:6572-6572.
254. **Fontan CT, Das D, Bristol ML, James CD, Wang X, Lohner H, Atfi A, Morgan IM.** 2020. Human Papillomavirus 16 (HPV16) E2 Repression of TWIST1 Transcription Is a Potential Mediator of HPV16 Cancer Outcomes. *mSphere* **5**.
255. **Liu K, Lin FT, Ruppert JM, Lin WC.** 2003. Regulation of E2F1 by BRCT domain-containing protein TopBP1. *Molecular and cellular biology* **23**:3287-3304.
256. **Liu K, Ling S, Lin WC.** 2011. TopBP1 mediates mutant p53 gain of function through NF-Y and p63/p73. *Molecular and cellular biology* **31**:4464-4481.
257. **Hong S, Xu J, Li Y, Andrade J, Hoover P, Kaminski PJ, Laimins LA.** 2019. Topoisomerase II β -binding protein 1 activates expression of E2F1 and p73 in HPV-

- positive cells for genome amplification upon epithelial differentiation. *Oncogene* **38**:3274-3287.
258. **You J, Croyle JL, Nishimura A, Ozato K, Howley PM.** 2004. Interaction of the bovine papillomavirus E2 protein with Brd4 tethers the viral DNA to host mitotic chromosomes. *Cell* **117**:349-360.
259. **Oliveira JG, Colf LA, McBride AA.** 2006. Variations in the association of papillomavirus E2 proteins with mitotic chromosomes. *Proceedings of the National Academy of Sciences of the United States of America* **103**:1047-1052.
260. **Brannon AR, Maresca JA, Boeke JD, Basrai MA, McBride AA.** 2005. Reconstitution of papillomavirus E2-mediated plasmid maintenance in *Saccharomyces cerevisiae* by the Brd4 bromodomain protein. *Proceedings of the National Academy of Sciences of the United States of America* **102**:2998-3003.
261. **McPhillips MG, Ozato K, McBride AA.** 2005. Interaction of bovine papillomavirus E2 protein with Brd4 stabilizes its association with chromatin. *Journal of virology* **79**:8920-8932.
262. **Wu SY, Nin DS, Lee AY, Simanski S, Kodadek T, Chiang CM.** 2016. BRD4 Phosphorylation Regulates HPV E2-Mediated Viral Transcription, Origin Replication, and Cellular MMP-9 Expression. *Cell Rep* **16**:1733-1748.
263. **Gauson EJ, Wang X, Dornan ES, Herzyk P, Bristol M, Morgan IM.** 2016. Failure to interact with Brd4 alters the ability of HPV16 E2 to regulate host genome expression and cellular movement. *Virus research* **211**:1-8.

VITA

Apurva Tadimari Prabhakar was born on August 17th, 1989 in Bangalore, Karnataka and is an Indian citizen. Apurva is a dentist who received her dental degree from M.S.Ramaiah dental college and hospital, Bangalore in 2012. She then moved to Louisville, Kentucky to pursue her Master of Science degree in oral biology from University of Louisville school of dentistry in 2016. The same year, her search to be a clinician-researcher led her to Virginia Commonwealth University, to pursue her doctoral training in the oral health research program at the Philips Institute, VCU school of dentistry, in the lab of Dr. Iain Morgan.

EDUCATION

- **VIRGINIA COMMONWEALTH UNIVERSITY**

Richmond, Virginia 08/2016 – Present

Doctoral Candidate, Oral Health Research

GPA- 3.375

Mentor- Dr. Iain Morgan

My dissertation focuses on studying the interaction between HPV16 E2 protein and host protein TopBP1. The study will enhance our understanding of HPV lifecycle, considering HPVs are major human pathogens responsible for 5% of all cancers.

- **UNIVERSITY OF LOUISVILLE DENTAL SCHOOL**

Louisville, Kentucky 08/2014 – 08/2016

Master of Science in Oral Biology

GPA- 3.742

Mentor- Dr. Jan Potempa

My thesis focused on characterization of PorZ, an essential bacterial surface component of the type-IX secretion system of human oral-microbiomic *Porphyromonas gingivalis*.

- **M.S. RAMAIAH DENTAL COLLEGE AND HOSPITAL**

Bangalore, India 08/2007 – 09/2012

Bachelor of Dental Surgery

GPA- 3.94

CERTIFICATE

- **Summer Leadership Series at Virginia Commonwealth University**

Richmond, Virginia 06/2018 – 07/2018

EXTERNSHIP

- **St. Luke's Dental Hospital, General Practice Residency**

Bethlehem, PA 06/2013 – 10/2013

25 hours/week of observership, shadowing attendings and residents, taking course lectures. I was exposed to advanced restorative, prosthodontics, periodontal, surgical and implant cases.

PUBLICATIONS

- **Prabhakar AT**, James CD, Das D, Otoa R, Day M, Burgner J, Fontan CT, Wang X, Wieland A, Donaldson MM, Bristol ML, Li R, Oliver AW, Pearl LH, Smith BO, Morgan IM. 2021. CK2 phosphorylation of human papillomavirus 16 E2 on serine 23 promotes interaction with TopBP1 and is critical for E2 plasmid retention function. bioRxiv doi:10.1101/2021.02.17.431757:2021.2002.2017.431757.
(Preprint)
<https://www.biorxiv.org/content/10.1101/2021.02.17.431757v1>
- James CD, Fontan CT, Otoa R, Das D, **Prabhakar AT**, Wang X, Bristol ML, Morgan IM. 2020. Human Papillomavirus 16 E6 and E7 Synergistically Repress Innate Immune Gene Transcription, msphere, vol. 5.
<https://msphere.asm.org/content/5/1/e00828-19>
- James CD, **Prabhakar AT**, Otoa R, Evans MR, Wang X, Bristol ML, Zhang K, Li R, Morgan IM. 2019. SAMHD1 Regulates Human Papillomavirus 16-Induced Cell Proliferation and Viral Replication during Differentiation of Keratinocytes, mSphere, vol. 4.
<https://msphere.asm.org/content/4/4/e00448-19>
- **Apurva Tadimari P**, Ranadheer Ramachandra, Krishnappa Pushpanjali, Shivakumar K. V. (2017). Oral Health Related Knowledge, Attitude and Practices among High School Students in Bangalore – A Cross Sectional Study. Journal of Dental & Oro-facial Research, 2, 13.
<http://www.jdorjournal.com/pdf/archives/August2017/3.pdf>

- Lasica, A. M., Goulas, T., Mizgalska, D., Zhou, X., de Diego, I., Ksiazek, M., Madej, M., Guo, Y., Guevara, T., Nowak, M., Potempa, B, Goel, A., Sztukowska, M., **Prabhakar, A.**, Bzowska, M., Widziolek, M., Thøgersen, I., Enghild. J., Simonian, M., Kulczyk. A., Nguyen, K., Potempa, J., Gomis-Rüth, F. X. (2016). Structural and functional probing of PorZ, an essential bacterial surface component of the type-IX secretion system of human oral-microbiomic *Porphyromonas gingivalis*. *Scientific Reports*, 6, 37708.

<https://www.nature.com/articles/srep37708>

SCIENTIFIC PRESENTATIONS

- Poster presentation at the VCU School of Dentistry’ Research day 2020, **Richmond VA** titled “Role of E2-TopBP1 interaction in human papilloma virus type 16 genome segregation” **Tadimari Prabhakar, Apurva**, James C, Das D, Morgan IM, Philips Institute for Oral Health Research, Virginia Commonwealth University, School of Dentistry.
- International oral presentation at DNA Tumour Viruses Meeting, ICGEB, **Trieste Italy** titled “Interaction with a TopBP1 cellular complex is required for the plasmid segregation function of human papillomavirus16 E2” **Tadimari Prabhakar, Apurva**, Das D, Morgan IM, Philips Institute for Oral Health Research, Virginia Commonwealth University, School of Dentistry.
- Poster presentation at the Massey Cancer Center Research Retreat 2019, **Richmond VA** titled “Role of E2-TopBP1 interaction in human papilloma virus

type 16 genome segregation” **Tadimari Prabhakar, Apurva**, Das D, Morgan IM, Philips Institute for Oral Health Research, Virginia Commonwealth University, School of Dentistry.

- Poster presentation at the VCU School of Dentistry’ Research day 2019, **Richmond VA** titled “Role of E2-TopBP1 interaction in human papilloma virus type 16 genome segregation” **Tadimari Prabhakar, Apurva**, Das D, Morgan IM, Philips Institute for Oral Health Research, Virginia Commonwealth University, School of Dentistry.
- Poster presentation at the VCU School of Dentistry’ Research day 2018, **Richmond VA** titled “SAMHD1 vs HPV16 - A tale of restriction” **Tadimari Prabhakar, Apurva**, James, Claire D, Bristol, Molly L, Evans, Michael R, Wang, Xu, Loughran, Oonagh and Morgan, Iain M, Philips Institute for Oral Health Research, Virginia Commonwealth University, School of Dentistry.
- Poster presentation at the Mid-Atlantic Microbial Pathogenesis Meeting 2017 **Wintergreen, VA** on the topic “Large Scale Expression and Preliminary Structural Characterization of Cdh (Pgn_1373)” **Apurva Tadimari Prabhakar**, Barbara Potempa, Anna Lasica, Mirosław Ksiazek, Richard Lamont, Jan Potempa, Oral Immunology and Infectious Diseases, University of Louisville.
- Poster presentation at the Research **Louisville 2016** on the topic “Large Scale Expression and Preliminary Structural Characterization of Cdh (Pgn_1373)” **Apurva Tadimari Prabhakar**, Barbara Potempa, Anna Lasica, Mirosław Ksiazek,

Richard Lamont, Jan Potempa, Oral Immunology and Infectious Diseases, University of Louisville.

- Poster Presentation on the topic “Cargo Proteins of Type 9 Secretion System in Porphyromonas gingivalis” **Apurva Tadimari Prabhakar**, Barbara Potempa, Anna Lasica, Jan Potempa, Oral Immunology and Infectious Diseases at the Graduate Student Council Research Symposium, University of Louisville, April 2016.
- **A. Tadimari Prabhakar**; A. Goel; B. Potempa; D. Mizgalska; K.Nguyen; J. Potempa; A. Lasica, *J Dent Res* Vol 95 Spec Iss A: 2410758, 2016. Poster Presentation at the International Association of Dental Research Conference- Poster Presentation to be held at **Los Angeles, California**, March 2016.
- Poster Presentation at the Research Louisville 2015 on the topic “Cargo Proteins of Type 9 Secretion System” **Apurva Tadimari Prabhakar**, Barbara Potempa, Anna Lasica, Jan Potempa, Oral Immunology and Infectious Diseases, University of Louisville.
- **Best paper presentation Award** in the National B.D.S seminar in Oral Medicine and Radiology, held in Chennai, India, on the topic “Diagnostic tests for cancer detection.”

CONFERENCES ATTENDED

- ICGEB DNA Tumour Viruses Meeting
Trieste, Italy 07/2019
- Massey Cancer Research Retreat
Richmond, VA 06/2019
- Massey Cancer Research Retreat
Richmond, VA 06/2018
- Massey Cancer Research Retreat
Richmond, VA 06/2017
- Mid - Atlantic Microbial Pathogenesis Meeting
Wintergreen, VA 03/2017
- Graduate Research Symposium, University of Louisville
Louisville, KY 04/2016
- IADR/AADR 45th Annual Meeting
Los Angeles, CA 03/2016
- UPENN- Penn Periodontal Conference
Philadelphia, PA 06/2015
- IDA Colgate Future Dental Professional Program
Bangalore, India 05/2012
- IDA Colgate Future Dental Professional Program
Bangalore, India 05/2011
- National B.D.S Seminar in Oral Medicine and Radiology
Chennai, India 12/2010

TEACHING

- Speaker, HONR 399 Mouth Microbes and Medical Research, Virginia Commonwealth University, February 2021
- Speaker, OCMB 604 An introduction to oral research, Virginia Commonwealth University, March 2021
- Speaker, undergraduate summer research Near Peer seminar series, Virginia Commonwealth University, June 2019

POSITIONS HELD

- **Director**, Graduate and Professional Student Programming Board (GSPB) at Virginia Commonwealth University 2018- 2020
- **Member**, Diversity, Equity, and Inclusion committee at School of dentistry, Virginia Commonwealth University 2020- Present
- **Member**, student mental health and well-being council at Virginia Commonwealth University 2019- Present
- **Student member**, Faculty Promotion and Tenure committee, Promotion and Tenure Committee Member Department of Oral and Craniofacial Molecular Biology, School of dentistry, Virginia Commonwealth University 2018- 2020
- **Executive committee member, Events coordinator**, Graduate and Professional Student Programming Board (GSPB) at Virginia Commonwealth University 2018- 2020

- **Student Representative** for Graduate Recruitment Council, Strategic Enrollment Management (SEM) at Virginia Commonwealth University

2018- Present
- **Member**, Student Leadership Council at Virginia Commonwealth University

2018- Present
- **Graduate student representative** for School of Dentistry, Graduate student association at Virginia Commonwealth University

2017- Present
- **Member**, Women in Science at Virginia Commonwealth University

2017- Present
- **Co-Chair** of Health Science Cluster at Graduate Student Council at University of Louisville

2015-2016
- **Vice-President** for Student Research Group at University of Louisville School of Dentistry

2015-2016
- **Student Body General Secretary**, M.S.Ramaiah Dental College

2010-2011
- **Science Club Secretary**, M.S.Ramaiah Dental College

2009 -2010

ACADEMIC AWARDS AND NOMINATIONS

- **Graduate Research Award, Research day, VCU School of Dentistry, 2020**
- **George W Burke, Jr Award for the best PhD student working in the School of Dentistry, 2019**
- **International Student Scholarship** from VCU Business Services, 2019
- **Travel grant** to attend the ICGEB DNATV 2019 Meeting in Trieste, Italy, 2019
- **VCU Graduate School, Travel Award, 2019**
- **Summer Research Scholarship**, from University of Louisville School of Dentistry, 2016 and 2015
- **Oral Biology program tuition scholarship award**, School of Interdisciplinary and Graduate Studies, 2016 and 2015
- **Graduate Student Council travel award**, University of Louisville, 2016
- **Graduate Merit Scholarship**, University of Louisville 2016
- **Best Outgoing Student 2007- 2012 award** from M.S. Ramaiah Dental College and hospital
- Public health dentistry, General Surgery and Oral Pathology and Microbiology University **Subject Topper Awards**
- Awarded **Certificates of Merit** for being the topper in all the 4 years of Bachelor of Dental Surgery, 2007- 2012, M.S.Ramaiah Dental College
- **IDA Scholarship for the year 2009-2010** for being the topper of the class

- Nominated for the Pierre Fauchard Academy UG Student Certificate of Merit Award 2012, from M.S. Ramaiah Dental College
- Nominated for the Indian Association of Public Health Dentistry (IAPHD)'s subject topper award for the year 2010 from the Department of Public Health Dentistry, M.S. Ramaiah Dental College

EXAMINATIONS

1. National Board of Dental Examination Part 1

Status- PASS 08/14/2013

2. TOEFL iBT

Score- 104 03/11/2016

READING 26

LISTENING 30

SPEAKING 24

WRITING 24

WORK EXPERIENCE

1. VIRGINIA COMMONWEALTH UNIVERSITY

Richmond, Virginia 2016-Present

Graduate research assistant, Dr, Iain Morgan Lab, Philips Institute of Oral Health Research, Virginia Commonwealth University

I have gained experience in techniques involved in molecular biology, protein chemistry and cell biology.

Lab Techniques Proficient in:

- i. Cell culture
- ii. Gel Electrophoresis
- iii. Ion Affinity Chromatography
- iv. Recombinant Protein Purification
- v. Western blot
- vi. Immunofluorescence and confocal microscope operation
- vii. Assays (including functional cell biology assays)
 - Immunoprecipitation assay
 - Replication assay
 - Luciferase based Transcription assay
 - Segregation assay
- viii. FACS analysis
- ix. siRNA protein knockdown
- x. DNA and RNA purification
- xi. Real time PCR
- xii. DNA gel electrophoresis
- xiii. Plasmid purification
- xiv. Basic molecular cloning

Proficient in the use of:

- Microsoft Word, Excel, Power Point, R- programming language, SPSS for data analysis

2. UNIVERSITY OF LOUISVILLE SCHOOL OF DENTISTRY

Louisville, Kentucky 2015 – 2016

Student Researcher, Dr. Potempa Lab, Department of Oral Immunology and Infectious Diseases

Lab Techniques Proficient in

- i. Gel Electrophoresis
- ii. Ion Affinity Chromatography Ni Sepharose High Performance
- iii. Protein Purification
- iv. BCA Analysis
- v. Gingipain Enzymatic Activity Assay
- vi. Acetone Precipitation
- vii. Western blot
- viii. Clone Manager 9 Program
- ix. Basic Molecular Biology Techniques, a few to mention:
 - Master plasmid construction
 - Primer design
 - Restriction Enzyme Digestion, Ligation
 - Plasmid Purification
 - Gel Purification
 - Transformation
 - Mutagenesis

Lab Safety Training Completed

Louisville, Kentucky 09/2015

- i. Blood Borne Pathogen Training
- ii. Laser Safety Training
- iii. Refresher Training for Radiation Users
- iv. Biosafety Training (BSL1/BSL2)
- v. NIH Guidelines
- vi. Select Agents
- vii. Formaldehyde Training
- viii. Lab Safety Training (09/11/2014)
- ix. Animal Training Level I, II, III

3. UNIVERSITY OF LOUISVILLE SCHOOL OF DENTISTRY

Louisville, Kentucky 01/2015 – 4/2015

Student Assistant, Simulation Lab

4. SMILE AVENUE

Bangalore, India 12/2011 – 06/2014

Dentist

Proficient in:

- Anterior and posterior teeth Root Canal treatment

- Class I, Class II, Class V cavity preparations Composite restorations, GIC and silver amalgam restorations
- Direct and indirect pulp-capping
- Fabrication of complete dentures and RPDs, Tooth preparation for FPDs
- Oral prophylaxis
- Coronoplasty
- Pit and fissure sealant placements
- Other preventive procedures
- Extraction of anterior and posterior primary and permanent teeth
- Fabrication of retainers
- Taking intra-oral periapical radiographs, ortho-pantamographs and bitewing radiographs

5. **MACULA HEALTHCARE PVT. LTD**

Bangalore, India 02/2014 –08/2014

Subject Expert- Prosthodontics, Entrance books, comprehensive self-study portal

Contributor for the development of the Dental Entrance Examination

Self-study portal, Entrance books

6. **M.S. RAMAIAH DENTAL COLLEGE**

Bangalore, India 08/2011 – 09/2012

Department Rotating Internship in following departments

- Oral Medicine & Radiology
- Public Health Dentistry
- Conservative Dentistry & Endodontics
- Periodontics
- Oral & Maxillofacial Surgery
- Prosthodontics
- Pedodontics
- Orthodontics
- Oral Pathology

7. **KAIWARA RURAL DENTAL HEALTH CENTRE**

Kolar District, India 03/2012 – 05/2012

Residential Posting

Dental care to people in the inaccessible areas.

I have also been part of screening and treatment camps.

8. **M.S. RAMAIAH MEMORIAL MEDICAL HOSPITAL**

Bangalore, India 02/2012 – 03/2012

Internship - Accident and Emergency Department

9. **M.S. RAMAIAH MEMORIAL MEDICAL HOSPITAL**

Bangalore, India 11/2011 – 12/2011

Basic Life Support (BLS) Training

10. **COMMUNITY OUTREACH PROGRAM**

Kolar District, India 01/2012 – 02/2012

Facilitator

Conducted treatment screening and treatment camps and oral survey

11. **MOCK FIRE DRILL RALLY BY GOVERNMENT OF KARNATAKA**

Bangalore, India 11/2011

Triage Supervisor